Oceanographic context for baseline characterization and future evaluation of MPAs along California's North Coast

Technical report to California Sea Grant for Projects R/MPA-31A, R/MPA-31B, and R/MPA-31C

10 July 2017

Eric P. Bjorkstedt[1,2], Marisol García-Reyes[3], Marcel Losekoot[4], William Sydeman[3], John Largier[4], Brian Tissot[5]

[1] NOAA Fisheries, Southwest Fisheries Science Center; [2] Department of Fisheries Biology, Humboldt State University; [3] Farallon Institute for Advanced Ecosystem Research; [4] Bodega Marine Laboratory, University of California, Davis; [5] Department of Biological Sciences, Humboldt State University

Cite as: Bjorkstedt, E. P., M. García-Reyes, M. Losekoot, W. Sydeman, J. Largier, B. Tissot. (2017) Oceanographic context for baseline characterization and future evaluation of MPAs along California's North Coast. Technical report to California Sea Grant for Projects R/MPA-31A, R/MPA-31B, and R/MPA-31C. 89 pp.

This page intentionally left blank.

Table of Contents

List of Figures (not including Appendices)

List of Tables

Executive Summary

Marine ecosystems along the North Coast of California exist in a highly energetic and variable oceanographic environment that strongly influences the dynamics and structure of the diverse marine populations that call this region home (Barth and Checkley 2009). Understanding the effect of marine protected areas (MPAs) implemented in this region therefore requires information on how oceanographic conditions vary over space and time. Baseline observations collected before or soon after implementation of MPAs depend in part on the oceanographic history of the region, and ongoing ocean observations can inform analysis of ecological and economic responses to MPAs over time (White et al. 2010). This report synthesizes a diverse suite of observations to provide this essential *oceanographic context* for baseline ecosystem studies (BES) in the North Coast Study Region (NCSR) and to establish a foundation for integrative studies, ongoing monitoring, and adaptive management of marine resources in the region. The primary intent of this work is to inform analysis of data collected during the BES and to the extent possible, to inform the design of future monitoring programs.

Our foremost purpose is to provide historical perspective on conditions occurring during the 2014-2016 Baseline Study Period (BSP). A great deal of this effort has been directed towards developing information specific to the NCSR that captures region-specific responses to the unprecedented, persistent 2014-2016 North Pacific marine heatwave (NPMHW) (Di Lorenzo and Mantua 2016) and associated ecosystem responses (including an equally unprecedented, massive, and persistent harmful algal bloom during 2015) (Leising et al. 2015, McClatchie et al. 2016).

Indeed, the warm ocean anomalies that affected the NSCR from mid-2014 through at least early 2016 as part of the NPMHW are central to the oceanographic context in which BES for the NCSR were conducted. This event has had strong effects on oceanographic conditions and substantial effects on marine ecosystems throughout the CCS, including NCSR and surrounding waters (Leising et al. 2015, Cavole et al. 2016, McClatchie et al. 2016). Fully understanding this event will take some time, as it differs in critical ways from the strong El Niño events that have in the past affected the California Current (McClatchie et al. 2016, Jacox et al. 2016). A key characteristic of the NPMHW is that the unusually warm waters observed during this period had not been a result of poleward transport by strong, coastwide currents, as had occurred during the strong 1997-98 El Niño, but rather originated offshore and followed large scale gyre currents in the North Pacific before impinging on the coast (Di Lorenzo and Mantua 2016, Jacox et al. 2016).

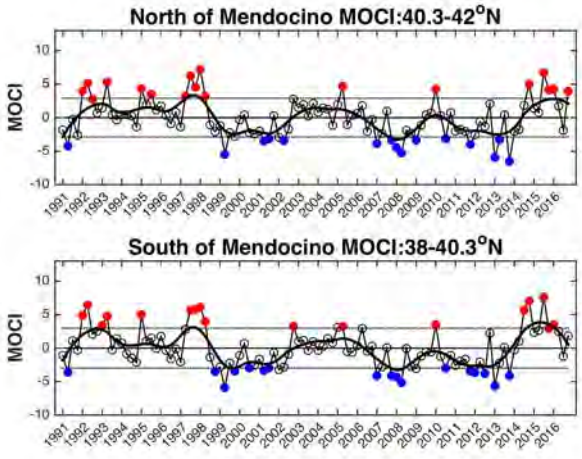

Figure ES1: Multivariate Ocean Climate Indicator (MOCI) for subregions within northern California. Red (blue) points indicate seasons that are unusually warm (cool) relative to the same season across years.

To support analysis of ecological data in light of the highly unusual oceanographic conditions that coincided with the BSP, we developed several data products that capture ecologically relevant variability and provide a basis for comparison to past conditions. Among these,

the Multivariate Ocean Climate Indicator (MOCI; Figure ES1) synthesizes local observations with climate indices to provide a simple index of whether the marine environment in a region of the California Current is tending towards warmer, presumably less productive conditions or towards cooler, more productive conditions. We also developed information on ocean currents measured by high-frequency radar and inferred from spatial variability in sea surface height (Figure ES2), and satellite observations of temperature and chlorophyll concentrations. These data provide a framework against which ecological data can be compared, in terms of raw values or anomalies from recent mean conditions.

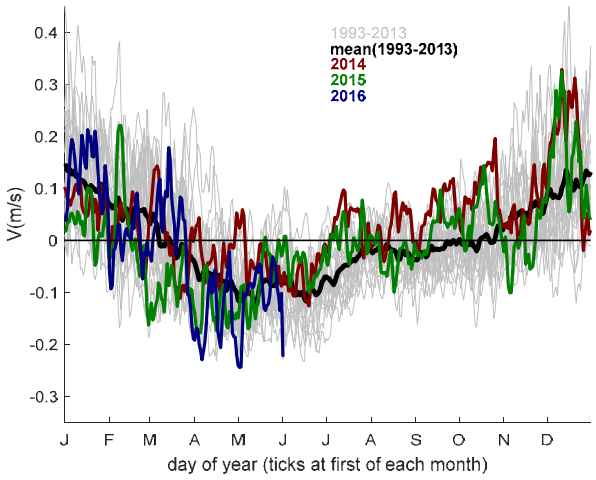

Figure ES2. Year-on-year comparison of mean daily meridional (north-south) flow along the coast, inferred from sea level anomaly measured by satellite altimeters and coastal tide gauges. Black line indicates day-of-year mean for historical observations shown in grey. Observations for the BSP are highlighted in color. See main text and Figure OC4 for additional detail. (Data courtesy C. Risien and P.T. Strub, Oregon State University).

We also quantify spatial oceanographic structure, with an eye both to putting BES in context and towards the design of ongoing monitoring programs. The MPA design process for the NCSR had at its disposal various datasets focused on coastal or benthic habitats (e.g., the distribution of rocky reefs, sandy beaches, kelp forests, etc.), but little more than a qualitative description of oceanographic structure in the region. Additional information on the region was developed over the course of the MPA design and siting process, but to a large degree, decisions regarding the selection of study sites within MPAs and reference sites for the BES were not informed by detailed analysis of oceanographic structure and pattern. Our spatial analysis yielded information on spatial and seasonal patterns in the occurrence of frontal structures within the NCSR (Figure ES3) and other measures of oceanographic conditions along the coast. Application of a statistical clustering algorithm (k-means clustering) to data on alongshore variability in several parameters (temperature, chlorophyll, currents, presence of fronts, and potential exposure to effects of freshwater discharge) revealed what appears to be consistent spatial structure and seasonal pattern—patterns that do not appear to have been disrupted by the spatially coherent fluctuations in temperature that occurred across the NCSR during the NPMHW. Although further work is required to establish links to ecosystem structure, the patterns emerging from this analysis appear to be sufficiently robust to warrant further analysis to delineate candidate 'oceanographic regions' within the NCSR that might structure in marine ecosystems at sub-regional scales (Figure ES4). These results connect to the growing appreciation that spatial structure has important ecological consequences (White 2008, Woodson et al 2012), and are

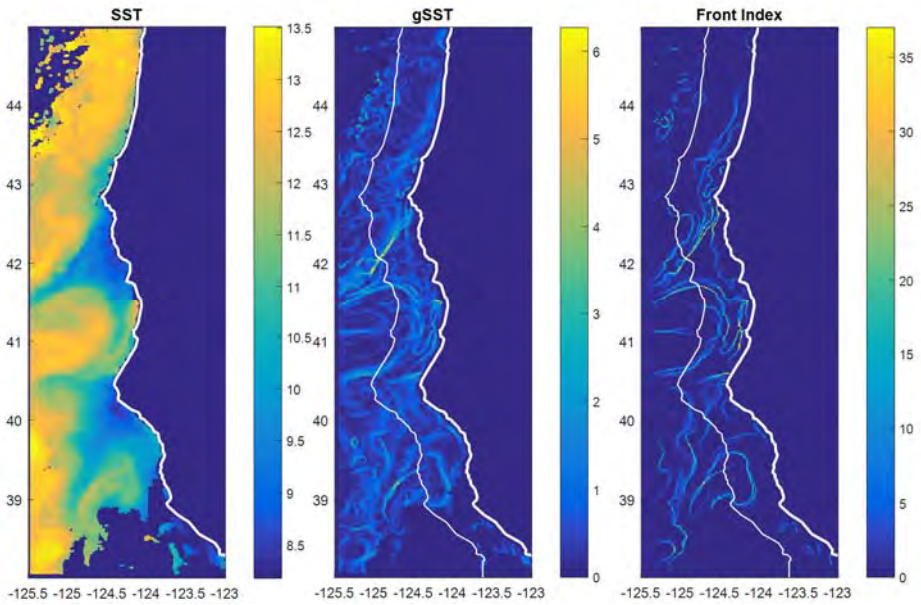

Figure ES3. Example analysis of spatial structure in coastal sea surface temperature (SST). Left panel: sea surface temperature (SST, °C). Middle panel: gradient (spatial change) in SST. Right panel: index of SST fronts that bound water masses of sharply different temperature based on modal analysis of SST. See main text and Figure SO1 for additional details on data and analysis.

intended to support more sophisticated analysis of baseline ecological data and evaluating links between ecosystem and oceanographic structure as a foundation for future monitoring.

To summarize, our analysis of ocean conditions documents that highly unusual oceanographic conditions that impacted the NCSR during the BSP. This event featured much warmer than usual temperatures, a harmful algal bloom, and an intense drought that no doubt impacted estuarine and nearshore ecosystems. Though it remains unclear how future conditions will unfold—specifically, whether the marine heatwave will yield to cooler conditions or heralds the onset of a warmer oceanographic regime—the anomalous conditions in place during the BSP are a critical element of the oceanographic context needed to interpret changes in ecosystem metrics going forward. Despite this unprecedented oceanographic event, average spatial oceanographic structure (e.g. fronts, temperature and chlorophyll gradients) appears to have remained relatively stable. For example, parts of the coast that are normally cooler than others appear to have remained so and fronts were more likely to be present off some areas than others, even as the whole coast warmed.

Moreover, the oceanographic information developed here, by explicitly placing recent observations in historical context, supports evaluation of what is consistent and what is variable about the structure and dynamics of the coastal ocean along the NCSR. Such insights might serve to inform the design and implementation of future monitoring and adaptive management of the MPA network, by helping to ensure that MPAs and reference sites are comparably situated with respect to oceanographic influence and to account for differences in ocean structure and dynamics that might contribute to variability among MPAs along the coast. Indeed, the breadth of contextual oceanographic information developed here for the NCSR might serve as a template or a nucleus for a statewide synthesis in support of broader, long-term monitoring and evaluation of California's MPA network.

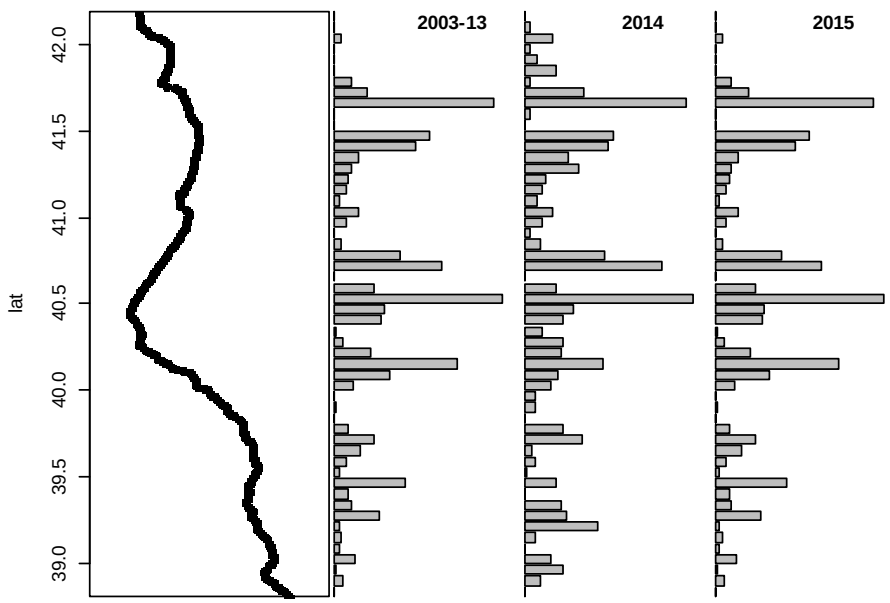

Figure ES4. Distribution of breaks demarcating groups identified by application of k-means clustering to monthly oceanographic data in the NSCR, by latitude. Length of the bar indicates the frequency at which a break was observed across all combinations of (a) k (the number of groups to be identified) ranging from 2 to 10, and (b) month of the year. Years included in each analysis are specified at the top of bar plot. To avoid inflating measures of likely structure, breaks bounding very short stretches of the coast separated from their group have been replaced with a break at the mid-point of the small section.

Introduction

Marine ecosystems along the North Coast of California exist in a highly energetic and variable oceanographic environment that plays a central role in the structure and dynamics of marine populations (Barth and Checkley 2009). Understanding the effect of marine protected areas (MPAs) implemented in this region (Figure I1) therefore requires information on the oceanographic context affecting MPAs and surrounding areas, both as it pertains to the nature of baseline observations collected before or soon after implementation of MPAs and the development of ecological and economic responses to MPAs over time (White et al. 2010). This report provides an overview of oceanographic information synthesized to provide this important context for baseline ecosystem studies (BES) in the North Coast Study Region (NCSR).

At the outset of this project, our goals were to 1) extract and assemble data relevant to the NCSR (including waters to the north, south, and offshore) from existing long-term oceanographic and climatic data sets and to augment these data through development of recently emerging sources of oceanographic observations and synthesis, (2) derive oceanographic products (e.g., indices or regional ocean conditions and oceanographic structure) on multiple spatial and temporal scales relevant to evaluating MPA performance, and (3) serve the NCSR baseline monitoring community directly by making these results available and interpretable to colleagues conducting ecological field surveys. Over the course of this work, we were compelled to expand our efforts to characterize the dynamic response of the NCSR to the unprecedented, persistent 2014-2016 North Pacific marine heatwave (NPMHW) (Di Lorenzo and Mantua 2016) in the course of developing historical perspective on conditions occurring during the 2014-2016 Baseline Study Period (BSP).

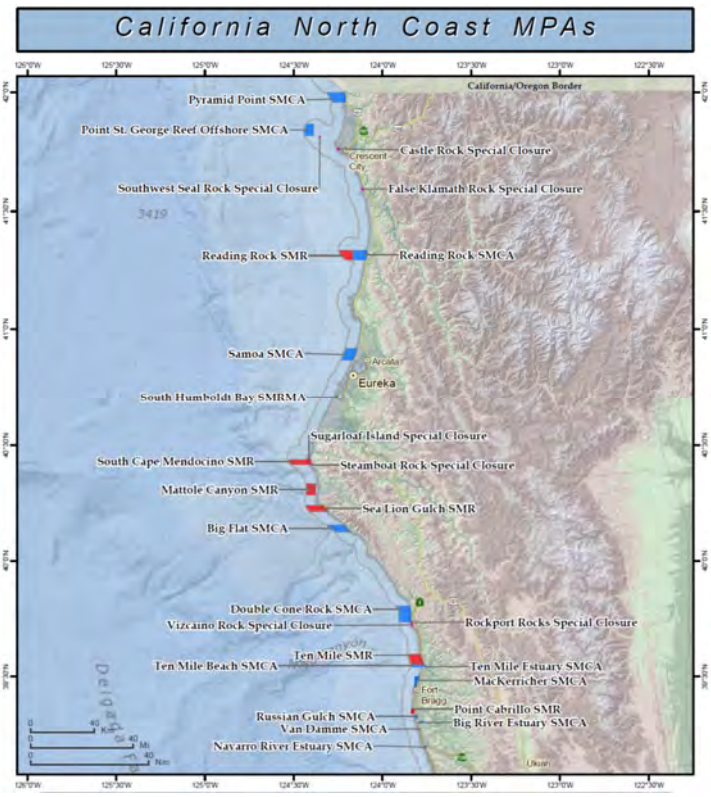

Figure I1. Location of Marine Protected Areas (all designations) in the North Coast Study Region. Excerpted from a chart prepared by CDFW, Marine Region GIS Lab (15 September 2013) and available at https://www.wildlife.ca.gov/conservation/marine/mpas/network/northern-california.

Indeed, the importance of the NPMHW to understanding the oceanographic context in which BES for the NCSR were conducted cannot be understated, as this event has had strong effects on oceanographic conditions and substantial effects on marine ecosystems throughout the CCS, including NCSR and surrounding waters (Leising et al. 2015, Cavole et al. 2016, McClatchie et al. 2016). A key characteristic

of the NPMHW is that the unusual water masses and warm conditions observed during this period had not been, at least for the most part, carried to the NCSR by strong, coastwide poleward transport, as had occurred during the strong 1997-98 El Niño, but were rather a consequence of offshore and southerly water masses impinging on the coast (Di Lorenzo and Mantua 2016).

We also build on our historical temporal analysis to extend our understanding of spatial pattern in oceanographic conditions across the NCSR. Thus, results presented in this report go beyond documenting historical forcing of nearshore ecosystems and how conditions during the BSP compare to the past, to support comparisons between MPAs and reference sites sampled during the BES and potentially to inform the design of ongoing monitoring plans and adaptive management of the MPA network. This effort was motivated by the relative lack of information on spatial oceanography available during the MPA design process (especially relative to the scope and resolution of information on habitat and ecosystem distributions), coupled with the growing appreciation that spatial structure has important ecological consequences (White 2008, Woodson et al 2012).

Connecting oceanographic context to ecological data

Oceanographic information has an inherently hierarchical structure, ranging from time series of measurements taken at a single location up to statistical indices that distill pattern from the dynamic state of the ocean over large spatial scales. In this report, we take advantage of this structure to develop oceanographic context for the NCSR suitable for interpreting the response of coastal ecosystems to spatial management at scales ranging from the MPA network down to individual MPAs and reference sites. This context reflects our best understanding of how oceanographic information informs analysis of ecological data, with particular attention to the scales over which oceanographic information is aggregated.

For some questions, oceanographic information at relatively fine spatial scales is of critical importance, particularly when considering alongshore variability in habitat conditions or the role of oceanographic structure in shaping populations and assemblages (Woodson et al 2012). However, in many cases, indices that capture dominant modes of variability over large spatial scales turn out to have greater power to explain ecological variability in marine systems than do time series of observations at a more local scale (Di Lorenzo et al. 2008, Kiester et al. 2011, Sydeman et al 2014, García-Reyes and Sydeman 2017). Why this is so, particularly in the CCS, boils down to two factors. First, even if based on analysis of spatial and temporal variability of a single parameter (e.g., sea surface temperature), large-scale indices effectively capture coherent, correlated patterns in temperature, salinity, vertical structure, circulation, etc., that collectively influence the ecosystem. Second, the response of the CCS to remote forcing is (typically) so strong or persistent that the effects of local forcing manifest as fluctuations imposed on slower changes in ocean structure driven by large scale climate events or trends. Moreover, the dynamics of populations and ecosystems in any individual MPA depend strongly on larval transport and survival and thus, on oceanographic processes operating at scales far beyond the bounds of the MPA (as well as fishing outside of MPAs; White et al. 2013), yet such dynamics are not necessarily well captured by local environmental observations. In this report, therefore, we present a suite of data products and analyses that are relevant to this broad range of questions.

Organization of the report

The report is organized as follows. First, we establish a broader historical and spatial context for the BSP within the NCSR, grounded in an overview of the oceanographic setting of the NCSR followed by a brief review of recent oceanographic conditions and dynamics in the broader California Current and North Pacific. Next, we present a broad suite of data products specifically focused on the NCSR that capture oceanographic conditions prior to and during the BSP. The diversity of data products and analyses presented here does not readily lend itself to a more traditional structure that collates "Methods" and "Results" that comprehensively address all products simultaneously. Instead, presentation of data sources, analysis, and interpretation is organized around distinct data products so that relevant methods and results are co-located and more readily available to the reader. Finally, we present a general synthesis of oceanographic conditions affecting the NCSR during the BSP and recommendations for future work to link oceanographic and ecological data in evaluating MPA performance.

Within the main body of the report, we present several sorts of oceanographic information and analyses expected to be relevant to present and future monitoring of ecosystems in the NCSR. First, we present a Multivariate Ocean Climate Index (MOCI)—a compact, holistic synthesis of information compiled from commonly reported regional oceanographic indices and *in situ* observational time series—focused on the NCSR (building on Sydeman et al. 2014 and García-Reyes and Sydeman 2017). Next, results from analysis of several remote sensing data sets are presented to provide information on spatial and temporal variability in ocean currents, temperature, and chlorophyll concentrations in the NCSR, and how conditions observed during the BSP compare to historical patterns. Finally, we analyze information from remote sensing data sets to quantify spatial structure in the coastal oceanography of the NCSR as a source of insight to patterns that structure marine ecosystems and that may inform comparisons between MPAs and reference sites based on data collected during BES as well as design of future monitoring efforts. This information is intended to complement the various datasets focused on coastal or benthic habitats (e.g., the distribution of rocky reefs, sandy beaches, kelp forests, etc.) available to (or developed during) the MPA design process for the NCSR.

As initially conceived, this group of projects was intended to support the BES through development of broadly applicable oceanographic information by oceanographers, thus sparing investigators leading ecological projects the burden of developing this information independently. Accordingly, the main body of the report includes illustrative examples of the sort of results or data products available (or possible to derive) from the data we have compiled in support of the BES, and discusses general patterns apparent in the data. For many of the data sets, particularly those that are spatially explicit, we include appendices of figures that illustrate variation in spatial pattern in oceanographic conditions or anomalies over time. In general, these coarsely resolve the evolution of oceanographic conditions over the BSP, which is intended to serve as a foundation for ecological investigators' consideration of conditions in place during a particular survey or changes in conditions between surveys, and to drive more focused queries of the underlying data specific to particular ecological questions.

Oceanographic setting of the North Coast Study Region

The NCSR is embedded in the California Current System, which itself is part of the larger North Pacific. Ecosystem productivity in the CCS (and NCSR) is highly dependent on seasonal wind-driven upwelling

that supplies nutrient-rich water to coastal habitats (Smith and Barber 1981; Checkley and Barth 2009). However, much of the physical and biological variability in the CCS is linked to large scale climate processes. This includes the effects of El Niño/La Niña events that originate in the Equatorial Pacific and (sometimes) propagate into the CCS from the south through oceanic signals (coastally trapped Kelvin waves) or more rapidly through atmospheric teleconnections that alter the structure and intensity of winds that drive upwelling in the CCS (Di Lorenzo et al. 2013). Variability in the strength the major oceanic gyres of the North Pacific—as captured in, e.g., the Pacific Decadal Oscillation (PDO; Mantua and Hare 2002) and the North Pacific Gyre Oscillation (NPGO; Di Lorenzo et al. 2008)—affects the strength and source of flow into the California Current, which in turn influences the structure of the CCS and how the CCS will respond to variability in winds and other forcing at local scales (Chaak and Di Lorenzo 2007).

Our analysis goes beyond examination of patterns in annual mean conditions to resolve oceanographic conditions at monthly or seasonal scales to ensure that potentially important patterns are not obscured in annual means. This is motivated in part by recent studies have identified the importance of variability in late winter conditions that, when favorable, can "pre-condition" the ecosystem to respond robustly to upwelling in the spring (Black et al. 2010,2011, Sydeman and Bograd 2009, Schroeder et al. 2013), and more generally the need to consider the timing of critical physical and biological transitions with respect to species' reproductive phenology as part of understanding how climate affects marine ecosystems (e.g., Sydeman et al. 2006).

The NSCR lies in a transitional region of the dynamic and spatially variable California Current System (CCS) (Checkley and Barth 2009). To the north of the NCSR, upwelling is highly seasonal (April-September). Upwelling increases in maximum intensity as one moves south, reaching peak strength in the region between Cape Blanco and Cape Mendocino, and the seasonal range of upwelling also increases. South of the NCSR, upwelling declines in average strength as it gradually extends throughout the year (Bograd et al., 2009, García-Reyes and Largier, 2012). Major bathymetric features (Hecata Bank) and coastal headlands (e.g. Cape Blanco, Cape Mendocino, and Point Arena) in southern Oregon and northern California favor the development of complex offshore circulation patterns and mesoscale oceanographic structures (e.g., upwelling jets, squirts, eddies, and retention zones) that impact the NCSR (Largier et al. 1993; Barth et al. 2000; Keister et al. 2008) and can have important influence on the transport and retention of plankton in coastal waters (e.g., Keister et al. 2010; Morgan et al. 2011, 2012). The direction and intensity of dominant shelf currents in this region fluctuates seasonally, with equatorward flow during the spring and summer (at least in areas away from the coast; Largier et al 1993) and tendency for poleward flow in the winter (i.e., the Davidson Current), although latitudinal and interannual variations in northerly coastal flows have not been well characterized to date.

The NCSR is also influenced by riverine outputs from major coastal rivers such as the Eel and Klamath rivers, as well as numerous other coastal rivers, particularly in areas north of Cape Mendocino. Although the scale of their influence depends on size, geology, and other watershed characteristics, coastal rivers can be an important source of freshwater and sediment that alter oceanographic conditions in nearshore environments and benthic habitats further offshore (Geyer et al. 2000, Wheatcroft and Borgeld 2000). Typically, freshwater discharge in the NCSR will have relatively localized effects (in contrast to, for example, how the Columbia River plume influences circulation patterns off the coast of Oregon and Washington), but some of these effects—especially those related to sediment delivery—can have lasting effects on marine habitats.

Recent climate events in the California Current

The BSP spanned a sequence of highly unusual climate events that have been collectively described as the 2014-16 North Pacific Marine Heatwave. The MHW had its beginning in winter 2013, when persistent and unusual high pressure over western North America redirected winter storms, leading to reduced mixing of surface waters (reduced entrainment of deep, cold waters) and reduced southward transport of cold water from the Bering Sea and Gulf of Alaska. As a consequence, surface waters over a massive region of the North Pacific were much warmer than average for a given location and time of year. This widespread temperature anomaly is known as the "warm blob" (Bond et al 2015). These warmer (less cooled) than usual waters drifted east with the prevailing ocean currents, with initial effects of warming becoming apparent in mid 2014 and culminating in warm waters impinging on the coast with the seasonal collapse of upwelling in late summer/early fall 2014. The high pressure ridge sitting over western North America also contributed to the strong drought affecting California (Swain et al 2014). Strong upwelling in early 2015 cooled the coast, but warm conditions were quickly restored as upwelling abated in mid-2015 and coastal waters again warmed significantly.

In near concert, conditions along the equator began to evolve in a manner suggesting the onset of a potentially strong El Niño in 2014, but this event stalled out and did not fully develop (Leising et al. 2015). In 2015, a strong El Niño did develop along the equator and subsequently reinforced warming throughout much of the California Current beginning in late-2015 (Jacox et al. 2016). In this case, however, oceanic signals (e.g., Kelvin waves propagating north along the coast), appear to have been relatively weak, and much of the warming observed in the CCS has been attributed to changes in winds triggered by atmospheric teleconnection (i.e., long-distance effects attributed to the ocean's influence on atmospheric structure) to the tropics (Di Lorenzo and Mantua 2016, Jacox et al 2016, Frischknecht et al 2017). Poleward shifts in species distributions indicate that unusual poleward flow did occur during the El Niño, but there is not clear evidence that unusually strong poleward currents developed throughout the CCS (McClatchie et al. 2016, Rudnick et al. 2017). Rather it appears that conditions during the height of the El Niño event in the CCS might be as much or more a consequence of the preceding warm anomalies than a direct and immediate consequence of the El Niño event itself.

Bond et al. (2015), Di Lorenzo and Mantua (2016), Jacox et al (2016), and recent State of the California Current reports (Leising et al 2015, McClatchie et al. 2016) provide additional detail regarding the genesis, evolution, and consequences of the 2014-2016 'marine heatwave' throughout the Northeast Pacific and the California Current. Biological oceanographic responses to these events relevant to the NSCR include shifts in plankton community structure during the BSP and an unprecedented harmful algal bloom (HAB) in 2015 (Leising et al 2015, McCabe et al. 2016, McClatchie et al. 2016; see the review of observations from the Trinidad Head Line below for additional detail). Overall, conditions experienced during the marine heatwave contrast starkly with conditions observed in 2013, which was marked by strong upwelling and cold temperatures, and much of the preceding decade during which, save for the moderate 2009-2010 El Niño, cooler conditions tended to prevail; see previous 'State of the California Current' Reports for deeper historical information (available at http://calcofi.org/ccpublications/ ccreports.html).

Oceanographic context for the NCSR

In general, there is a robust understanding of the contrast between relatively cool, productive periods and warmer, less productive conditions in the CCS related to climate variability, but it is also well known that there can be strong regional variability in how the CCS responds to particular events. Despite growing insight from developing observational time series in the NCSR, it is not yet well documented how changes associated with these climate modes specifically manifest in the region, especially with respect to ecosystem responses.

The following sections lay out several products that will support ongoing analysis of ecological data from MPAs in the NCSR, both directly and in terms of suggesting future development of new indices. Table 1 summarizes the types of data included or considered in analyses presented in this report, many of which are brought into our analysis as components of the Multivariate Ocean Climate Indicator (MOCI) developed for the NCSR.

Multivariate Ocean Climate Indicator (MOCI): a synthetic index for the NCSR

The Multivariate Ocean Climate Indicator (MOCI; Sydeman et al 2014, García-Reyes and Sydeman 2017) synthesizes several oceanic and atmospheric observational time series local to a region of interest with indices of large scale modes of climate variability that strongly influence the CCS. By bringing this suite of measurements together into a single index, MOCI effectively captures the blended effect of local forcing overlain on the underlying structure and dynamics of the CCS that is captured in the climate indices, thereby providing a more focused perspective on oceanic variability at a regional scale.

Comparison of MOCI to various ecological time series demonstrates that region-specific MOCI represent environmental conditions relevant to ecological processes in the NCSR and throughout the CCS (García-Reyes and Sydeman 2017). Long time series of biological data in the NCSR are sparse, but in the central and southern California regions, MOCI has shown skill relating to biological variability across trophic levels (Sydeman et al. 2014). Within the NCSR, MOCI shows good correlations with indices of copepod community structure off northern California and Oregon (García-Reyes and Sydeman 2017). As more biological data becomes available in the NCSR, we will evaluate the skill of MOCI in describing ecological patterns, including responses to the NPMHW of 2014-2016.

Data sets included in MOCI are selected to satisfy several criteria. Each must have continuous seasonal values since 1991, be updated frequently, and be publicly available via the Internet. Moreover, each of the data sets included in MOCI must be a direct measure or robust index of physical processes known to influence the marine ecosystem, which in this region includes regional climate as well as local oceanic processes. Data included in MOCI is described below, as well as the methodology to calculate it and its interpretation. For a more detailed description, see García-Reyes and Sydeman (2017). MOCI for the NCSR (and other regions) is updated quarterly (http://www.faralloninstitute.org/moci).

Indices of basin scale climate variability

Indices representative of several modes of basin-scale climate variability are commonly considered in evaluating variability in the CCS (Di Lorenzo 2012, Messié and Chavez 2011). Of these four are included in MOCI: the Pacific Decadal Oscillation (PDO, Mantua and Hare 2002), the North Pacific Gyre Oscillation (NPGO, Di Lorenzo et al. 2008), the Multivariate El Niño-Southern Oscillation [ENSO] Index (MEI, Wolter

and Timlin 1998), and the Northern Oscillation Index (NOI, Schwing et al 2002) (Table 1). Each captures a major mode of variability in oceanic or atmospheric variability that influence flow and vertical structure in the CCS (Chhak and Di Lorenzo 2007).

Table 1: Datasets integrated into assessment of oceanographic context for baseline ecological studies in the North Coast Study Region. Note that some are not included in results presented, but were consulted in the course of analysis to corroborate findings presented.

	Dataset	Definition	Source	URL (as of January 2017)
Climate Indices	Multivariate ENSO Index (MEI)	see Wolter and Timlin (1998)	NOAA, ESRL	www.esrl.noaa.gov/psd/enso/mei
	Pacific Decadal Oscillation (PDO)	see Mantua and Hare (2002)	U Washington, JISAO	research.jisao.washington.edu/pdo/PDO.latest
	North Pacific Gyre Oscillation (NPGO)	see Di Lorenzo et al. (2008)	E. Di Lorenzo	www.o3d.org/npgo/npgo.php
	Northern Oscillation Index (NOI)	see Schwing et al (2002)	NOAA, SWFSC/ERD	www.pfel.noaa.gov/products/PFEL/modeled/indices/NOIx/data/noix.txt
	Bakun Upwelling Index	volume of water upwelled per unit coastline	NOAA, SWFSC/ERD	www.pfeg.noaa.gov/products/PFELData/upwell/monthly/upindex.mon
In situ sensors	Buoy Data	SST	NOAA, NDBC	www.ndbc.noaa.gov
		surface air temperature		
		alongshore wind stress (from wind speed and heading)		
		sea level pressure		
	Sea Level Stations	sea level anomaly	NOAA,CO-OPS	www.co-ops.nos.noaa.gov
Remotely sensed data and derived products	AVISO+TG	sea level anomaly; components of geostrophic flow	OSU	Craig Risien and P. Ted Strub (OSU, pers. comm.)
	HF Radar	components of surface currents	SIO	hfrnet.ucsd.edu/thredds/ncss/grid/HFR/USWC/6km/hourly/RTV/HFRADAR,_US_West_Coast,_6km_Resolution,_Hourly_RTV_best.ncd
	MODIS-Aqua	3 day composite of daytime SST		coastwatch.pfeg.noaa.gov/erddap/files/erdMWsstd3day/
		3 day composite chl a concentrations	NOAA, SWFSC/ERD	coastwatch.pfeg.noaa.gov/erddap/files/erdMWchla3day/
	The California Current merged satellite-derived 4-km dataset	5 day composite chl a concentrations blended observations, 2X interpolated	SIO/SPG	spg.ucsd.edu/Satellite_data/CC4km/Chla_5day_interpolated_2x.zip
		5 day SST derived from Optimally Interpolated SST fields		spg.ucsd.edu/Satellite_data/CC4km/SSTOI_5day.zip; original data at podaac.jpl.nasa.gov/dataset/NCDC-L4LRblend-GLOB-AVHRR_OI
	MUR SST	daily SST; blended observations from multiple sensors	JPL PODAAC	podaac.jpl.nasa.gov/Multi-scale_Ultra-high_Resolution_MUR-SST
	River Discharge	monthly flow for gauged rivers	USGS	waterdata.usgs.gov/nwis/monthly

In the several years leading up to the BSP, these indices reflected generally cooler, productive conditions across the CCS, yet during much of the BSP, all three indices indicated persistently warmer (presumably less productive) conditions and reduced equatorward transport in the California Current. The NPMHW that marked this period has no analog in the historical record

In situ observations

Several sources of *in situ* observations of ocean conditions are available throughout the NCSR, including observations of various parameters at buoys maintained by NOAA and coastal shore stations supported

by NOAA through CeNCOOS. Four NOAA/NDBC buoys (www.ndbc.noaa.gov) located over the continental shelf within the NCSR provide high frequency (at least hourly) observations of wind speed and direction, sea and air surface temperature, and sea level pressure since 1981. The quasi-real time access to the data and its length in time, make these data ideal for developing updated indices of environmental variability that can be put in historical context to evaluate current observations. NOAA/Co-Ops (www.co-ops.nos.noaa.gov) serves observations from sea level gauges from four locations within the NCSR (Figure MAP).

Direct *in situ* observations capture local variability in conditions known to influence ecosystems. For example, temperature has a direct influence on organisms' physiology at very local scales, and (especially coupled with information on local winds) provides additional information on how effectively upwelling is bringing cool, nutrient rich waters to the surface. Such observations are essential for evaluating the strength of coupling between local conditions and processes operating at larger scales as part of understanding oceanographic conditions affecting marine ecosystems and the MPAs and MPA networks embedded therein.

MOCI for the NCSR

MOCI for the NCSR blends four climate indices (MEI, PDO, NPGO, NOI) described above that capture important basin-scale dynamics impinging on the CCS (and thus, the NCSR) with a suite of local observational time series (sea surface and air temperature, wind stress, and sea level pressure from buoys, sea level from coastal gauges, and the Bakun upwelling index) (Table 1). In all cases, regardless of temporal resolution in the underlying data set, data are brought into the MOCI calculation after being averaged across seasons (i.e., Winter [January-March], Spring [April-June], Summer [July-September], and Fall [October-December]) to yield four seasonal values per calendar year. Differences in season delineation do not strongly influence patterns in the resulting MOCI values.

MOCI is calculated by first parsing each time series into separate season-specific time series, normalizing each (seasonal) time series, aligning the time series by year, and applying a principal component analysis to the resulting matrix. The leading mode of variability emerging from the analysis (PC1) is retained as the MOCI for that particular season (Sydeman et al 2014, García-Reyes and Sydeman 2017; these references also provide additional detail on the calculation and interpretation of MOCI as an oceanographic and ecological index). Note that a separate calculation is performed each season (e.g., the series of winter observations, of spring observations, etc.) so that comparisons are among seasons across years. Seasonal components of MOCI are subsequently collated to generate a year-round MOCI that represents variability around the 'expected' seasonal cycle. By construction, MOCI ranges from positive values that indicate warm temperatures and weaker upwelling, (conditions typically associated with reduced productivity) to negative values that indicate stronger upwelling and cooler temperatures (conditions commonly thought to be conducive to elevated productivity) (Sydeman et al. 2014, García-Reyes and Sydeman 2017). High absolute values indicate substantially warmer or cooler season-specific conditions.

Figure M1 shows MOCI for sub-regions within the NSCR, nested within a broader northern California region delineated in a recent coastwide application of MOCI (García-Reyes and Sydeman, 2017). Note that the spatial domain of MOCI for northern California includes portions of the coast south of the NCSR (to 38°N), a decision motivated in part by our present conceptual understanding of regional

oceanography and by constraints imposed by the spatial distribution of buoy observations and the desire to include replicate time series within the southern sub-domain of the NCSR.

MOCI for the NCSR capture generally coherent patterns across the region, including several ENSO events (El Niño in 1992-1993, 1997-1998, end of 2015, and la Niña in 1999) as well as the intensity and phasing of the 2014-2016 marine heatwave that has affected the Northeast Pacific (Gentemann et al 2017). Focusing on more recent years, the second half of both 2014 and 2015 were characterized by strongly positive MOCI values, driven by coincident warm temperatures, weak upwelling (in the summer), and several climate indices attaining values associated with a broader warming in the California Current. MOCI also captured the temporary cooling in coastal waters driven by springtime upwelling in 2015 and 2016. Overall, conditions experienced during the marine heatwave contrast starkly with conditions observed in 2013, which was marked by strong upwelling and cold temperatures, and much of the preceding decade during which, save for the moderate 2009-2010 El Niño, cooler conditions tended to prevail.

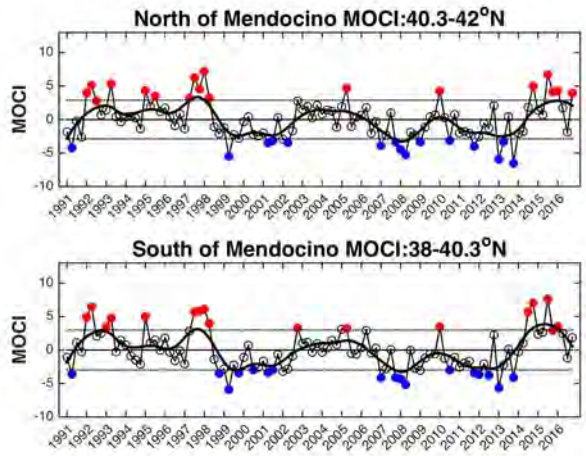

Figure M1: Multivariate Ocean Climate Index (MOCI) for subregions within northern California. Red (blue) points indicate seasons that are unusually warm (cool) relative to the same season across years.

Ocean currents

Ocean currents influence the dynamics and structure of marine populations through, e.g., larval transport, and are thus a critical element of the oceanographic context in which MPAs are situated. To examine circulation patterns in the NCSR, we analyzed information from two data sources: 1) surface currents based on observations from a coastal network of high-frequency radar stations, and 2) flows inferred from spatial structure in sea surface height measured with satellite-borne altimeters and coastal tide gauges.

Although the underlying data are resolved at finer spatial and temporal scales, and provide a rich basis for additional analysis, we focus here on resolving variability in zonal (north-south) and meridional (east-west) components of currents at a relatively coarse resolution across the NCSR. Indices of alongshore flow (and sea level anomaly), especially, serve as an indicator of physical mechanisms that influence ecosystem productivity (e.g., upwelling v. downwelling and the related slope and depth of the thermos- and nutricline).

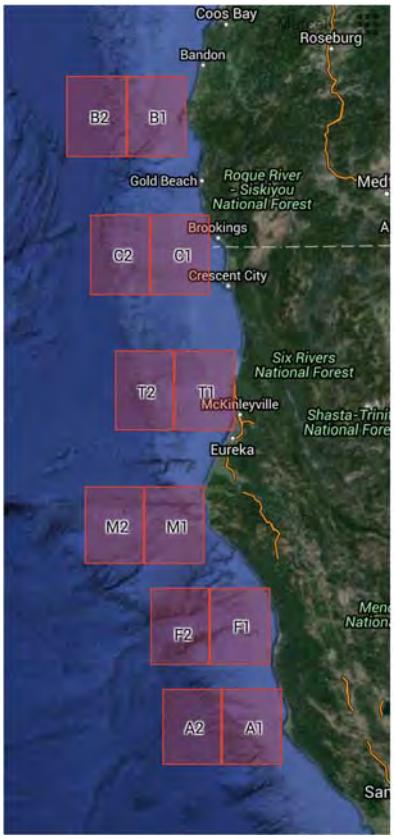

Figure OC1. Boxes delineated for extraction of current data measured by HF radar and inferred from AVISO+TG.

High-frequency (HF) radar

Over the past decade and more, a developing network of HF radars has been used to measure surface currents at hourly or greater resolution along extensive swaths of the US West Coast (Kim et al 2011). We obtained HF radar data compiled and curated by the Scripps Institute of Oceanography that provides hourly surface current measurements for the entire US West Coast, in the form of *u* (easterly or zonal) and *v* (northerly or meridional) components on a 6 km grid (Table 1). From these data, we calculated simple spatial and temporal averages of *u* and *v* (treating each component separately) for the boxes delineated in Figure OC1 and 7-day non-overlapping periods spanning the available time series. Boxes were designated to highlight particular regions of interest, guided by preliminary analysis indicating that observational coverage was reasonably good and consistent over the time series, thereby minimizing the risk that artefacts affecting the estimation of current vectors from radial observations would influence the spatially averaged results. Data gridded to 0.10° were used to prepare maps of mean monthly flow as the basis for descriptions of flow structure in the NCSR.

Variability in alongshore and cross-shelf flow from HF Radar

Figure OC2 presents time series of monthly mean zonal (*u*, nominally cross-shelf) and meridional (*v*, nominally alongshore) flows for nearshore and offshore regions indicated in Figure OC1. Interpretation of zonal flows in terms of cross-shelf transport requires caution, because (1) cross-shelf currents tend to be weaker than alongshore flow in this region, and (2) resolution of east-west components of flow is sensitive to the orientation of the coast (i.e., an equatorward current flowing parallel to the coast south of Cape Mendocino will have a positive zonal component, simply because the alongshore current is

directed to the southeast). In general, alongshore circulation patterns are coherent across the shelf and into outer waters, with generally stronger variability (more extreme average current speeds) occurring further from the coast. In part, attenuation of average flow nearshore reflects the influence of coastal counter-currents that develop in response to strengthening flow in regions away from the coast.

Meridional (north-south) flow measured by HF radar is generally coherent across the NCSR, at least at seasonal scales, although similarly broad coherence in zonal flows is not apparent (Figure OC2). Flow in the region off Trinidad Head tends to be weaker (in general) than elsewhere in the NCSR, which is consistent with more sluggish circulation in this region (Largier 1993). This area around Trinidad Head also appears to mark a break between coherent patterns in both cross-shelf and along shore flow in the north and reduced coherence to the south, particularly with respect to cross-shelf flow, but we caution that this may be an artifact of placement of boxes relative to oceanographic features rather than a robust and spatially coherent change in the structure of coastal currents.

The available time series of HF radar observations off the NCSR is relatively short (2006-2016), which limits our ability to compare flows during the BSP to a robust climatology of seasonal flow patterns (Figure OC3). Nevertheless, comparing meridional flows for the BSP to flows during previous years, there is some evidence that flow off the NCSR was more poleward (less equatorward) from mid-summer through early winter during the BSP, particularly in 2014 (Figure OC3), even though the net direction of (spatially averaged) flows did not turn consistently poleward throughout the NCSR until September/October 2014. In contrast, off Cape Blanco (to the north of the NCSR) alongshore flow tended to remain robustly equatorward until September/October of 2014. Comparisons of zonal currents across years also provide evidence that currents were stronger and more consistent to the north of the NCSR (off Cape Blanco) during the BSP.

Satellite altimetry and coastal tide gauges

Variability in the elevation of the sea surface, although subtle (typically on the order of changes in centimeters in mean sea surface height [SSH] over horizontal distances of hundreds of kilometers), belie

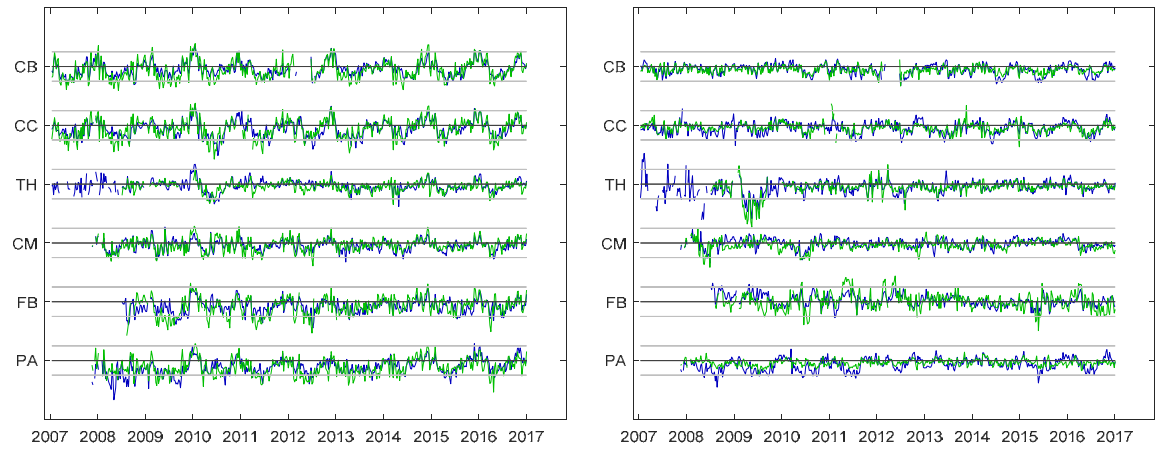

Figure OC2. Weekly mean meridional (left panel) and zonal (right panel) flows measured by HF radar in the NCSR and neighboring regions. Blue and green lines indicate flows measured in nearshore and offshore boxes, respectively (see Figure OC1 for box designations).

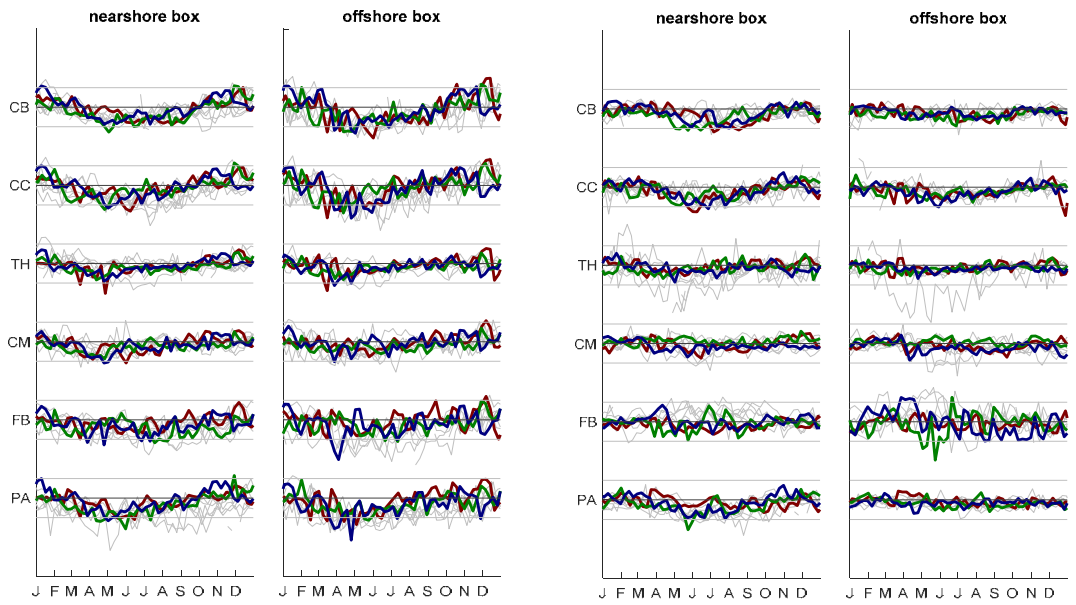

Figure OC3. Year-on-year comparison of weekly mean meridional (left two panels) and zonal (right two panels) currents measured by HF radar in the NCSR, extracted from boxes delineated in Figure OC1. Grey lines indicate observations from 2006 to 2013. Observations spanning the baseline period are highlighted in red (2014), green (2015), and blue (2016). Grey lines above and below reference lines indicate flows of ±0.25 m s^{-1}.

much more dramatic subsurface structure (e.g., changes in the depth of a particular isotherm by tens of meters or more over similar horizontal scales). This structure in the ocean is associated with geostrophic currents, directly analogous to the winds that flow around high and low pressure centers in the atmosphere (Stewart 2008, Pond and Pickard 2013). Thus, patterns in SSH measured from space (satellite altimetry) can be used to infer currents in the upper portion of water column.

Risien and Strub (2016) applied methods developed by Saraceno et al. (2008) to combine observations from satellite altimeters that measure variability in sea surface height (processed and served by AVISO; www.aviso.altimetry.fr) with observations at coastal tide gauges (obtained from NOAA CO-OPS (tidesandcurrents.noaa.gov) to produce a data set of sea level anomaly (SLa) and components of (inferred) geostrophic flow. The combination of satellite and coastal observations overcomes the (present) inability of satellite altimeters to observe sea surface height near the coast, and improves the skill of altimetry-based sea level measurements (and by extension, estimates of circulation patterns) within this coastal band (Saraceno et al. 2008, Risien and Strub 2016). We obtained a version of this data set updated through mid-2016 (C. Risien and P.T. Strub, OSU, *pers. comm.*), from which we retained results from the AVISO+TG analysis and extracted information for the NCSR and surrounding waters.

Variability in alongshore and cross-shelf flow inferred from sea surface height data

Inferred meridional flows averaged along the NCSR coast show clear seasonality consistent with the development of a coastal upwelling jet during the spring, and subsequent development of weaker circulation inshore as the coastal jet migrates offshore and dissipates in the late summer and fall. Zonal flows also show a clear seasonal pattern and spatial correlation with coastline orientation, suggesting that this variability is dominated by east-west components of flow along a curving coastline.

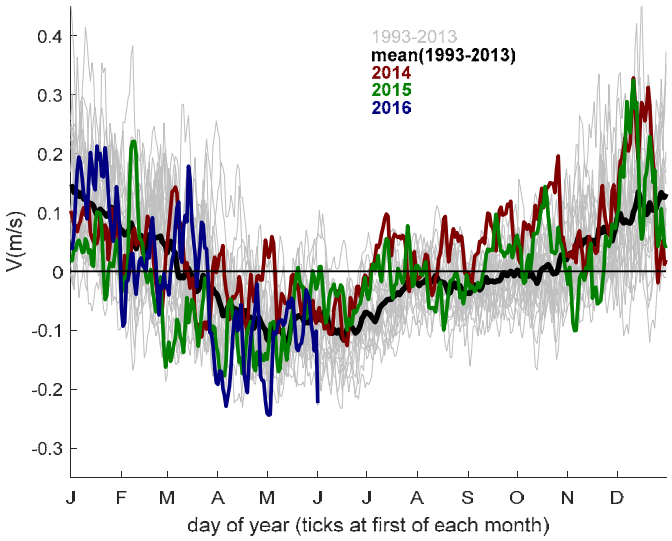

Figure OC4. Year-on-year comparison of mean daily meridional flow from AVISO+TG across a 0.75° wide coastal band spanning the NCSR. Black line indicates day-of-year mean for historical observations shown in grey. Observations for the BSP are highlighted in color.

During 2014, anomalously poleward flows developed (i.e., equatorward flows weakened) early in the year, and tipped over to absolute poleward flow much earlier than usual (July) (Figures OC4 and OC5). Poleward flow dominated during the lead up to the arrival of "Warm Blob" waters in September/October 2014, and subsequently persisted throughout the rest of 2014 and into early 2015. In spring 2015, upwelling was associated with weaker equatorward flow than usual, yet, especially in the northern part of the NCSR, sufficed to generate cooler conditions along the coast. Anomalously high sea level along the coast persisted through much of the 2015-2016 winter, in conjunction with El Niño, but rapidly recovered towards average values in spring 2016 (Figures OC4, OC5, Appendix OC). Note that the presence of anomalously high sea levels at the coast in conjunction with equatorward flow is consistent with the presence of stronger SSH anomalies offshore (i.e., a downward slope in the sea surface towards the coast despite broadly elevated SSH).

Comparison between HF Radar and Altimetry-derived alongshore flow

Meridional (north-south) flows inferred from AVISO+TG and HF radar show strong agreement off the NCSR, with stronger agreement in regions away from the coast (Figure OC6). The disparity between AVISO+TG and HF radar measurements of alongshore flow in summer and fall 2014 are likely to reflect the competing influences of large scale transport and local upwelling on how the effects of the warm blob manifested along the coast: even as the blob was arriving in the area (as resolved by the geostrophic signal captured in the sea level data), local upwelling (resolved by HF radar) was holding the warm waters at bay. Correlations in cross-shelf flow estimates based on HF radar and satellite altimetry are essentially non-existent.

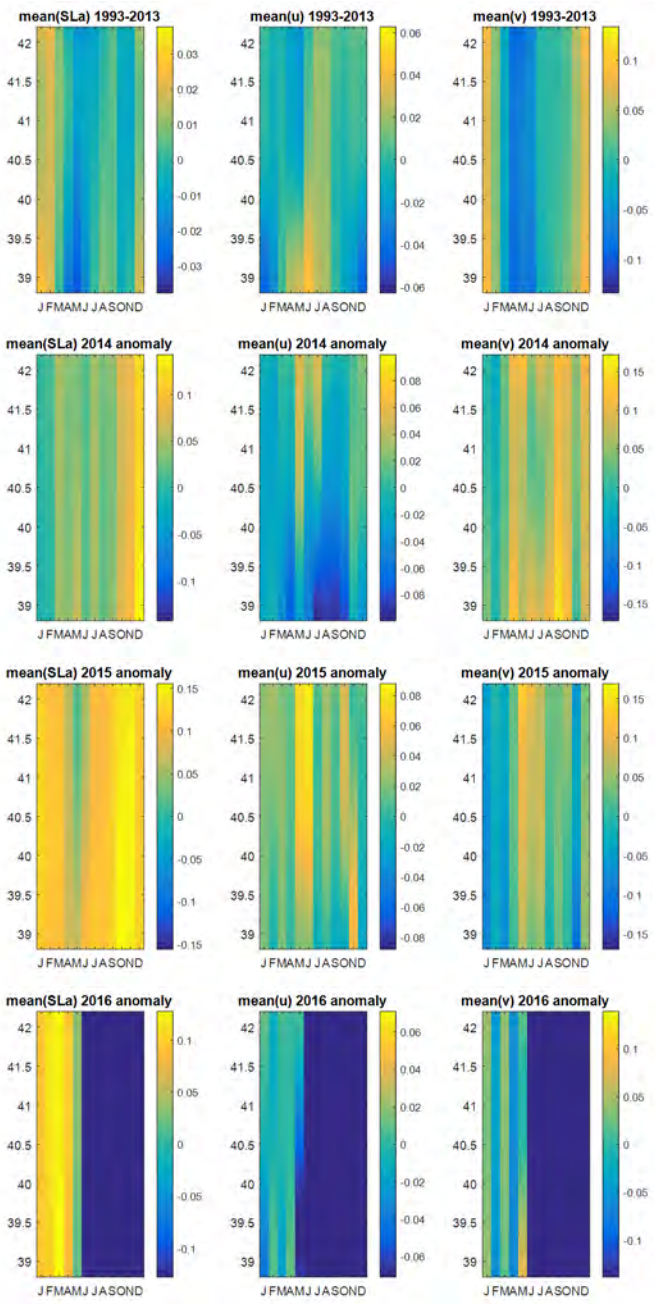

Figure OC5. Top row: climatological (1993-2013) seasonal cycle in monthly mean SLa, *u*, and *v* from AVISO+TG observations (Risien and Strub 2016) for the NCSR. Second through fourth rows: anomaly in monthly mean SLa, *u*, and *v*, for the years of the BSP.

Neither the cross-shelf pattern in correlations of alongshore flow nor the lack of correlation in cross-shelf flow are unexpected. There are several reasons that this is so. First, in the nearshore region, indices based on the altimetry/sea-level data set are strongly determined by interpolation linking oceanic structure and (point) observations of sea level taken at shore-based tide gauges, and so have reduced resolution relative to the HF radar observations. Moreover, the sparse distribution of tide gauge stations that anchor the inshore boundary of the SSH fields limits the ability of this analysis to resolve alongshore gradients in SSH which would underpin estimates of cross-shelf flow. Second, the seafloor can influence currents extending deeper into the water column more strongly than those at the surface. Third, HF radar, focused as it is on very near-surface currents rather than vertically integrated

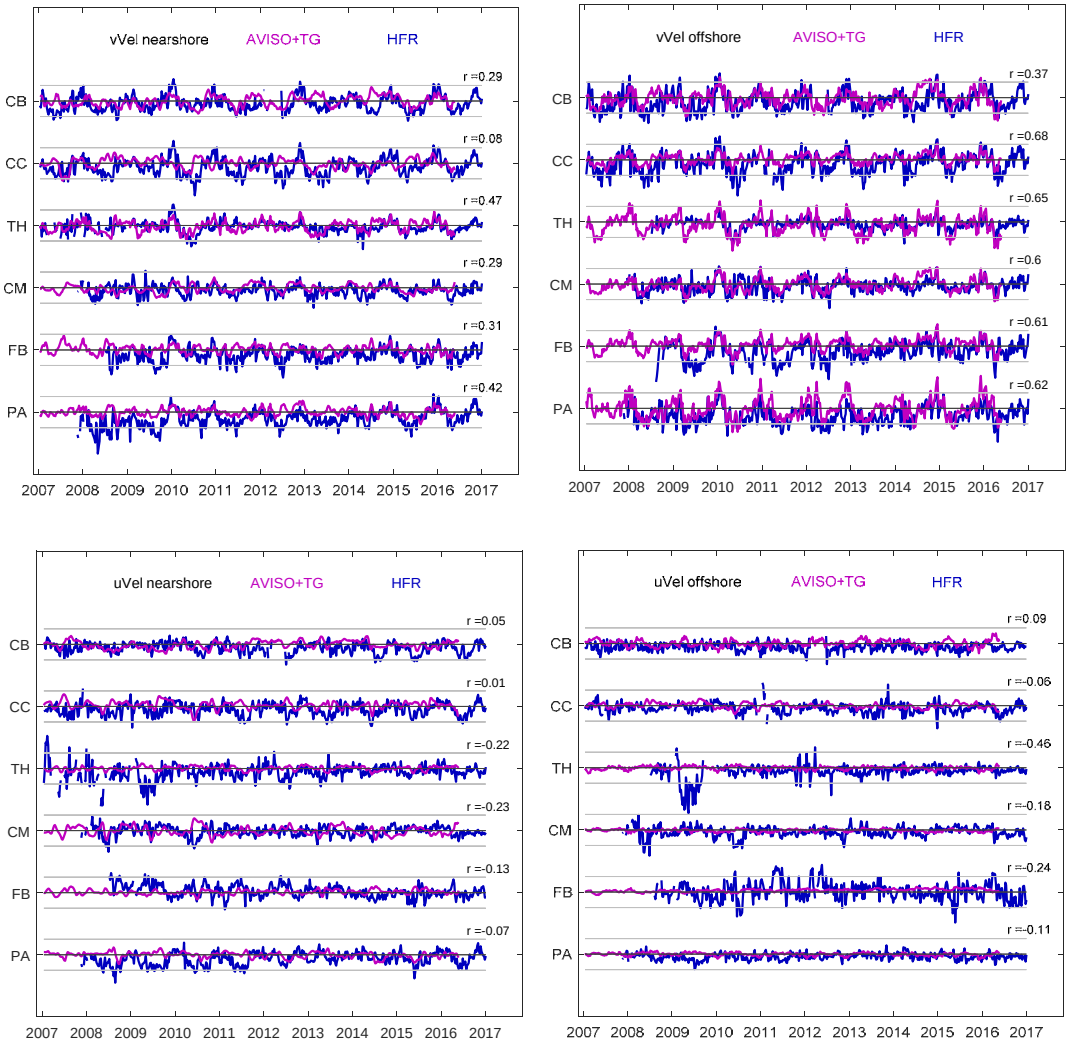

Figure OC6. Comparison of currents measured by HF radar (HFR, blue) and inferred from sea surface height structure derived from satellite altimetry and coastal tide gauges (AVISO+TG, magenta) for regions corresponding to boxes in Figure OC1. Upper and lower panels are for meridional and zonal currents, respectively. Left and right panels are for nearshore and offshore boxes, respectively. Grey lines above and below reference lines indicate flows of ±0.25 m s^{-1}.

flow of a substantially thicker slab of water, is likely to better capture cross-shelf flows driven by wind-forced Ekman transport and finer-scale effects of spatial variability in winds than can be detected in geostrophic currents driven by broader (and more slowly changing) structure in the coastal ocean.

Evolution of spatial circulation patterns during BSP

Mean flows provide insight to coherent, regional responses to climate forcing, yet also tend to obscure variability over space and time that might influence observations during a particular survey or series of surveys in an important way. Thus, for some purposes, it may be useful to examine sequential maps of currents to characterize the evolution of flow patterns over time. Appendix OC provides such maps of monthly mean flows for the period immediately preceding and spanning the BSP. These maps are intended to support preliminary analysis and hypothesis development; if warranted, variability can be explored at higher temporal resolution. (Note that these figures are best viewed on-screen, with some magnification.)

In conjunction with indices of net transport (and, of course, other environmental conditions), mapped current data has the potential to be useful as descriptive context for ecological surveys. An example of this is illustrated in Figure OC7, which shows that spatial signatures of the temporal patterns described above are readily apparent in mapped currents. Offshore, equatorward currents (i.e., flows typical of ongoing upwelling) begin to breakdown during summer 2014, beginning with the onset of poleward flow in July 2014 in regions south of Cape Mendocino, extension of these currents across the NCSR by October 2014, and the occurrence of peak poleward flow in December 2014. As this pattern evolved, the region off Cape Blanco was consistently marked by offshore transport typical of upwelling (better resolved by HF radar). Note that, broadly speaking, the patterns apparent in HF radar are also apparent in currents estimated from SSH fields, with the strongest similarities being observed in alongshore flow patterns (Appendix OC). Similar examples from periods of stronger upwelling (e.g., in 2013, or in Spring 2015) or any period of interest can be drawn from the time series.

Figure OC7. Maps of monthly average currents for August, September, and October 2014 illustrating transition from upwelling to poleward flow. Top row: HF Radar observations with current heading indicated by orientation of arrow head and speed (m/s) indicated by shading. Bottom row: Currents inferred from sea surface height based on interpolated observations from satellite altimeters (AVISO) and coastal tide gauges. Current direction and speed (m/s) indicated by vector. See Appendix OC for larger versions of these plots in broader temporal context.

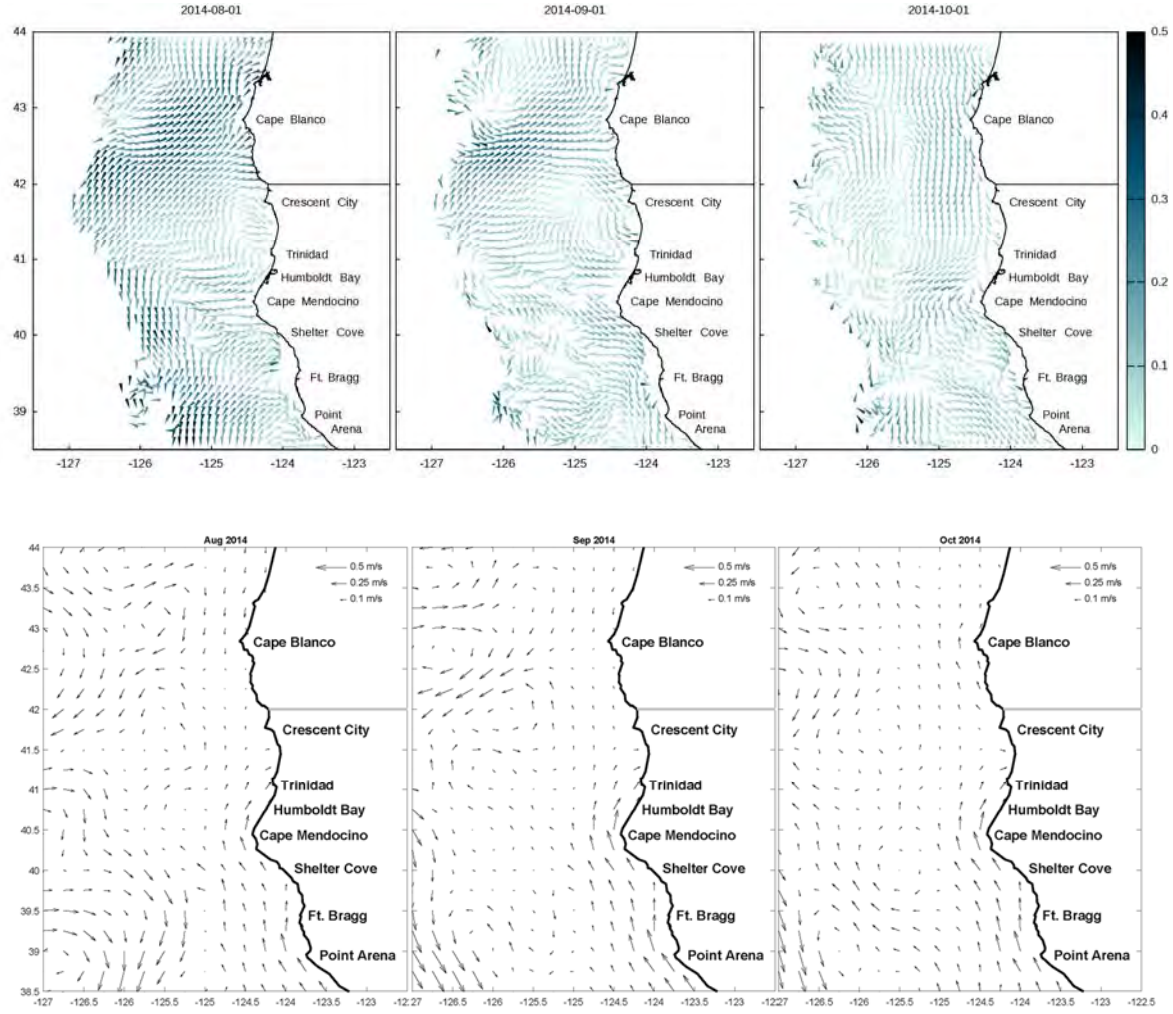

Freshwater discharge to coastal habitats in the NCSR

The NCSR lies along a coast that receives considerable amounts of rainfall, much of which falls from the late fall through spring. Watersheds draining directly to the NCSR coast vary in size from small, short run catchments along the Lost Coast to major river systems such as the Klamath/Trinity and the Eel rivers that drain extensive inland basins. The largest watersheds drain into the Pacific north of Cape Mendocino. South of Cape Mendocino, smaller basins drain the coastal mountains that separate coastal watersheds from inland tributaries to the Sacramento River. These watersheds supply freshwater, sediment (Geyer et al. 2000, Wheatcroft and Borgeld 2000), organic detritus, nutrients (especially

micronutrients such as iron [Chase et al. 2007]), driftwood, and other material to coastal and estuarine habitats. As a consequence, a coastal site's proximity to rivers is expected to influence stratification and nearshore circulation in coastal waters, the structure of benthic habitats (especially with respect to sediment), energy and nutrient fluxes, and disturbance.

Temporal variability in freshwater discharge

We obtained monthly mean flow data for rivers draining to the NCSR coast from the USGS (https://waterdata.usgs.gov/nwis/monthly), and summarized these data into annual (August-July) climatologies of monthly mean flows and cumulative monthly mean flows (a proxy for total annual flow). Against these climatologies, we highlight flow data for the BSP (2014 through 2016) and the preceding 13 years (2000-2013), to illustrate recent intensity of freshwater river discharge into coastal waters of the NCSR (examples shown in Figure FW1; see Appendix FW for additional watersheds). Discharge data are available only for a limited number of rivers, typically those that drain larger watersheds. Several of the larger rivers are affected by major impoundments in the upper watershed. Information on the numerous small watersheds is not available, though discharge from these streams may also have important effects on more local scales.

As a consequence of persistent atmospheric ridging that diverted storm tracks to the north (Swain et al 2014), the seasonal increase in freshwater discharge typically observed in the fall was substantially delayed in 2013-2014 across the NCSR, with substantial flows only beginning to occur in February, rather than in November or December of the preceding year (Figure FW1). In contrast, flows in 2014-2015 and 2015-2016 followed a more typical seasonal pattern, despite starting from extremely low summer levels.

Spatial variability in exposure of coastal habitats to freshwater discharge

We are not aware of high-resolution, broadly distributed time series of direct observations how river discharge affects coastal habitats in the NCSR. Nevertheless, it is well-known that different regions in the NCSR vary in their exposure to freshwater inputs. To account for this variability, we calculated a simple index of potential exposure to freshwater in which proximity to river mouths is scaled by a measure of potential discharge from coastal watersheds. In doing so, we focused on rivers likely to discharge sufficient freshwater to influence conditions beyond the immediate surf zone and potentially affect local circulation patterns (i.e., to suffice in forming a reasonably persistent freshwater lens or riverine plume) as well as to deliver substantial sediment to coastal habitats, and ignore the local effects of small coastal rivulets.

This index is based on watershed location (latitude and longitude of mouth), watershed area, and climatological annual precipitation over the watershed synthesized in GIS by the Fisheries Ecology Division of NMFS in the course of technical recovery planning for listed salmon and steelhead populations in northern California and southern Oregon (Agrawal et al 2005). Watersheds draining into Humboldt Bay are considered as a single aggregate source to the coastal ocean. Information on watershed area and mean precipitation together serve as a proxy for relative discharge (aggregated over the course of a year), though we note that important factors such as evapotranspiration, snow storage, the effects of impoundments, diversions, and the like are ignored in this metric, as are seasonal and

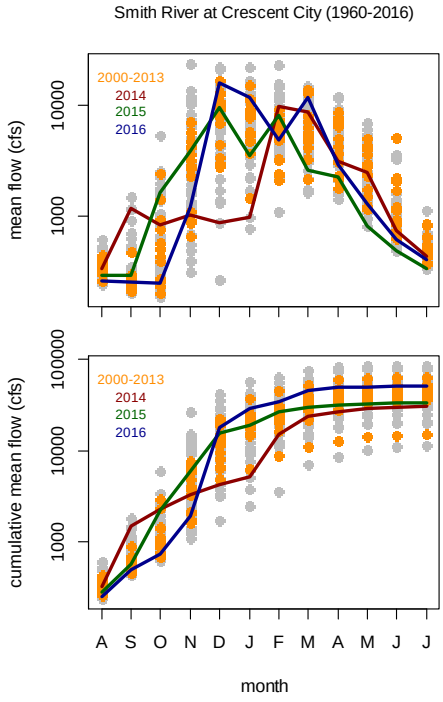

Figure FW1: Year-on-year (August [y-1] to July [y]) comparison of monthly mean flow (upper panel) and cumulative monthly mean flow (lower panel) for the Smith River. Note that the timing differs from water year definitions (Oct-Sep) to capture important variability in early fall more clearly.

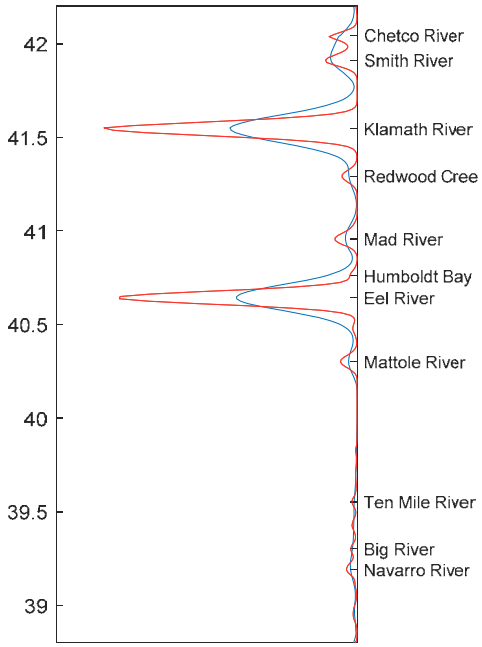

Figure FW2. Index of relative exposure of coastal habitats to freshwater discharge as a function of watershed size, mean annual precipitation, and distance along the coast. Color indicates patterns of relative exposure for arbitrary assumptions of narrow (red) and broad (blue) alongshore extent of freshwater influence along coast.

interannual variability in discharge, such as is captured in the climatology summary described above. Interannual variability in discharge is largely coherent across the NCSR, so this index should adequately capture relative exposure to freshwater among coastal habitats in any given year, although any interaction between precipitation and watershed characteristics is not necessarily captured.

The resulting index of freshwater discharge is used to weight the exposure of coastal locations to freshwater from each river as a function of distance from the river mouth. We subsequently aggregate exposure (to all sources of riverine input) for each coastal location across the NCSR to form an index of total exposure to freshwater (Figure FW2). Note that the scale and resolution of this analysis does not account for small-scale local effects, whether due to small coastal rivulets draining directly to a beach or due to variability in coastal topography that influences dispersal or retention of freshwater along the

coast. This index also does not account for the poleward displacement of buoyancy plumes expected under calm conditions or during downwelling conditions typical of the winter rainy season.

Remotely sensed sea surface temperature and chlorophyll a

Several sources of remote sensing data for sea surface temperature (SST) and chlorophyll a (chl a) concentration that span the NCSR are available online through aggregating servers, e.g., CoastWatch (http://coastwatch.pfeg.noaa.gov/erddap/index.html), or by direct download from primary source programs' websites. Available data sets range from relatively lightly processed data sets to data products in which multiple observational data sets are rationalized and combined, sometimes with additional interpolation to fill in spatial or temporal gaps in coverage. For this project we selected as a "lightly processed" data set the 3-day composited SST and chl a data sets based on concurrent observations by the MODIS-Aqua sensor for available dates from late 2002 through 2016, as an example of a data set with a useful balance of high spatial resolution (0.0125° grid spacing) and good temporal resolution in the face of pixel-scale variability in coverage for much of the NCSR. To corroborate these analyses, we conducted complementary (though more cursory) analysis on data extracted for the NCSR from (a) the Multi-scale Ultra-high Resolution Sea Surface Temperature (MUR-SST) data set, in which observations from several sensors are combined to produce a daily, high-resolution SST product (mapped to 0.01° resolution), (b) a blended and merged chl a data product with 5 day and 4 km (approximately 0.036°) resolution produced by the Scripps Photobiology Group (SPG; Kahru et al 2012, 2015), and (c) an interpolated SST data product with identical resolution derived by SPG from the coarser (0.25° resolution) Optimally Interpolated SST (OISST v2) data product.

Estimates of chlorophyll concentrations in the upper (visible) water column are based on ratios of reflectance at specified wavelengths in the green-to-blue range of the visible spectrum, and in contrast to SST, which is based on radiation from the ocean surface, are based on observations integrated over the portion of the upper water column through which light penetrates (and returns). How these spectra are observed varies demonstrably among the sensors that have been deployed over time. Kahru et al (2012), in developing the SPG chl a data set, have compared these several sensors against extensive *in situ* observations and among themselves to construct statistical adjustments that improve correspondence between each sensor's measurements and field measurements and to improve agreement among sensors (Kahru et al 2015). The adjusted data sets are then merged (and in the case of the data used here) double interpolated to offset coverage gaps due to clouds.

We have focused on the MODIS-Aqua data set to retain its spatial and temporal resolution (at a cost of some coverage). However, as noted in the metadata for the MODIS-Aqua data set, the algorithm used to convert spectral observations to estimates of chl a concentration has not yet been fully vetted as 'science quality'. Cursory comparisons between the MODIS-Aqua and SPG blended data confirm that the MODIS-Aqua appears to underestimate chl a concentrations at the higher end of the range (Kahru 2012). Therefore, to bring the MODIS-Aqua data into better agreement with the SPG blended chl a data, we backcalculated reflectance ratios from the original MODIS-Aqua data (using the OC3 algorithm and published coefficients) and re-calculated chl a concentrations from these ratios using the improved algorithm presented in Kahru et al (2015) specific to the MODIS-Aqua sensor. Note that this does not mean that the results presented here are 'science quality' as commonly understood within the remote sensing research community. Nevertheless, this quick re-analysis appears to have improved the

resolution of patterns in phytoplankton blooms along the coast by better capturing the full range of chlorophyll concentrations.

Temporal patterns and spatial structure in coastal SST and chlorophyll a

Ocean fronts—relatively sharp transitions between water masses with different characteristics—have been observed to influence transport of planktonic organisms and form regions of enhanced productivity in diverse oceanographic settings (Bakun 2006, Woodson et al. 2012). In the NCSR, as for much of the CCS, most fronts occur at boundaries between cooler, saltier upwelled water and warmer, fresher waters. Freshwater plume fronts also occur in the vicinity of river mouths, and can become more extensive and contiguous during periods of continued, heavy rainfall and concurrent freshwater discharge.

We use the high-resolution MODIS-Aqua 3-day composite SST record and coincident estimates of chlorophyll-a (chl a) concentrations as the basis for examining spatial patterns in ocean structure. Again, a primary motivation for selecting this data set was the high spatial resolution afforded by this sensor and the lack of *a priori* smoothing via interpolation and blending of asynchronous observations from different instruments; application of the gradient- and especially the distribution-based algorithms below yielded more diffuse patterns when applied to interpolated data sets. Prior to analysis, we applied a 7x7 (centered) median filter to reduce pixel-scale noise in each 3 day composite image; this is standard practice in image analysis (Nieto et al 2014), and had minimal effect on the structure resolved in the image. We then calculated two indices of oceanographic structure from each filtered SST field.

Gradient indices

We calculated the gradient (and the heading of maximum gradient) in SST (∇SST and h∇SST) by applying a 3×3 Sobel operator to each SST field. Strong gradients occur in regions where SST is changing rapidly over space and indicate frontal structures. From the gradient field, it is possible to identify candidate frontal regions by screening for regions exceeding a critical threshold for ∇SST. For our purposes, however, we implemented a different algorithm for identifying fronts (see below), and instead restrict our use of temperature gradient information to using averaged ∇SST over space as a general index of structure in the coastal ocean, whether due to consistently occurring, sharp, well defined fronts or due to more diffuse, mobile, or ephemeral features.

SST front index

To identify frontal structure more rigorously, we adapted a method for identifying temperature fronts developed by Nieto et al (2014) as an improvement on foundational work by Cayula and Cornillon (1992, 1995) and Diehl et al (2002). The Neito et al. (2014) algorithm (and those on which it is based) use statistical decomposition of SST distributions to identify fronts as boundaries between water masses that exhibit distinctly different temperature distributions. Neito et al. (2014) advanced this method by applying the algorithm over a series of overlapping 'tiles' to identify repeatedly detected features and to ensure that features are not missed as a consequence of where they fall relative to the grid over which the calculations are performed. In brief, our implementation of this approach proceeds as follows:

1. SST values from a (spatial) observation window are binned into 0.05 °C intervals. The resulting histogram is smoothed, and subsequently used to identify local maxima corresponding to modes in temperature distribution.

2. Hasselblad's (1966) algorithm for fitting multiple (normal) distributions is applied to the subset of SST values. Temperatures corresponding to local maxima in the smoothed temperature distribution are used as initial guesses for the fitting algorithm. This calculation returns means and standard deviations for component distributions as well as the proportion of the composite distribution represented in each component. Note that this step differs from the strict constraint on fitting only bimodal distributions implemented in Nieto et al (2014) and Cayula and Cornillon (1992, 1995), and allows for multiple features to be detected in each tile.
3. Relatively uninformative component distributions (i.e., those representing a trivial fraction of the population of pixels included in the analysis or having high standard deviation), if any, are discarded from the inputs to the fitting algorithm. Likewise, modes with means that differ by less than a critical threshold are combined in a new set of initial values. If a decremented set of initial values is produced during this step, it is used to initialize a new fit to the SST distribution. This step may be repeated.
4. Boundaries between component distributions are identified as temperatures (between means) where each contributing distribution has equal weight. Contours of frontal isotherms are calculated, and a frontal index is developed by incrementing counts for pixels crossed these contours. Note that a pixel may be crossed by multiple isotherms in regions of sharp gradients.

For the analysis here, this algorithm has been applied to a set of overlapping 30x30 pixel tiles that are systematically offset at 5 pixel intervals along both north-south and east-west directions so that each

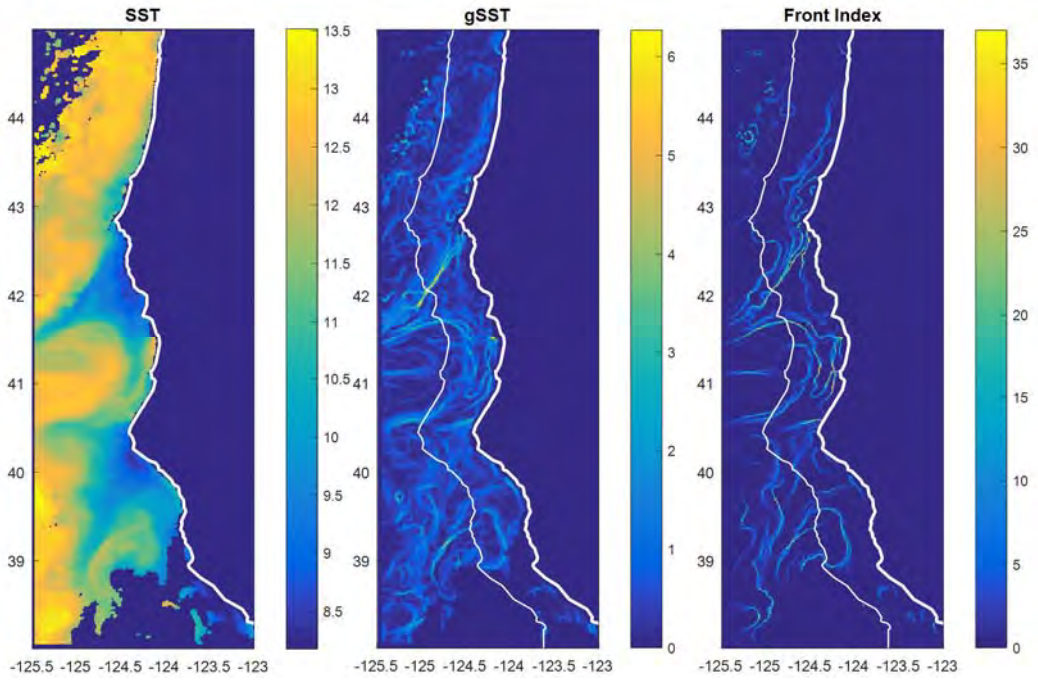

Figure SO1. Illustration of spatial structure metrics derived from remotely sensed SST observations. Left panel: SST (°C) for 1-3 June 2013 (3-day composite) from MODIS-Aqua sensor (daytime passes). Middle panel: ∇SST (Δ°C/0.0125°) based on application of 3x3 Sobel operator to SST in left panel. Right panel: Front Index based on application of algorithm adapted from Nieto et al. (2014) to SST field in left panel. Front Index is the average number of times a pixel is crossed by a contoured isotherm that has been identified as a frontal boundary, scaled for coverage.

(interior) pixel is part of 36 distinct, overlapping tiles. This arrangement of tiles results in a boundary buffer of 25 pixels along the edges of the field where data are less frequently included in sampling tiles for analysis. To avoid having spurious results in the boundary region confound our results, we implemented this algorithm over a spatial domain that extended well beyond the bounds of the NCSR and excluded these boundary regions from subsequent analysis. Figure SO1 illustrates an example SST field and associated fields of ∇SST and Frontal Index based on analysis of SST from the 3-day composited MODIS-Aqua data set.

In contrast to the algorithm developed by Nieto et al. (2014), our analysis does not include an algorithm to combine nearly contiguous front segments into longer coherent structures. Rather, the composited Front Index reflects both where fronts consistently appear and how sharply these features are defined (multiple isotherms can intersect a given pixel in regions of very sharp gradients). The latter element, especially, recognizes that the placement of fronts, in terms of selecting which isotherms represent the boundary between water masses, is less certain in regions where such boundaries lie in regions of weaker gradients due to greater sensitivity in the mode-fitting step to the collection of SST values where modes in the SST distribution are less distinct. This approach also places greater priority on a statistical description (including uncertainty) of where fronts are likely to exist rather than quantitative identification of specific features at a particular instant in time.

Nearshore oceanography: spatial pattern, seasonal climatology, and BSP anomalies

For the satellite measurements and structural indices derived therefrom, we extracted data for a coastal band defined lying within 0.625° to 0.75° longitude (up to 50 pixels for the highest resolution data sets, 3 for coarsest) due west of the coastline (e.g., see region demarcated by thin white line in Figure SO1). This band suffices to spans conditions along transects normal to the coastline out to an approximate minimum of approximately 30 km for post hoc analysis—the narrowest part of this band in the NCSR

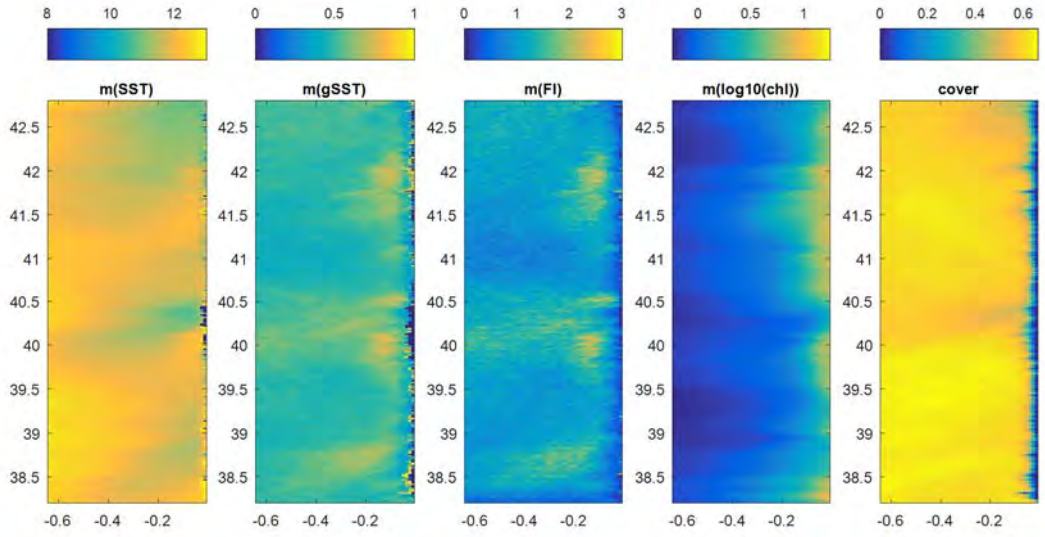

Figure SO2 From left to right: annual mean SST (°C) by latitude (y-axis) and cross-shelf distance (in degrees longitude, x-axis; annual mean gradient in SST (Δ°C/0.0125°); annual mean Front Index; annual mean $\log_{10}$(chl a) (mg/m^3); and SST pixel coverage (%) for the MODIS-Aqua sensors off the NCSR from 2003 through 2015.

extends southwest off the region near Punta Gorda (Figure SO2). From the resulting deck of temporally distinct coastal bands, we extract a climatology over the period of observation, monthly climatologies, and, for the BSP, monthly means and anomalies.

Full year (Figure SO3) and monthly (Appendix SO) mean SST, SST-related metrics, and chl a, compiled across a coastal band illustrate persistent or consistently repeated oceanographic patterns across the NCSR. Visual inspection of these plots reveals alongshore structure in nearshore oceanographic conditions across the NCSR. For example, the short stretch between Cape Mendocino and Punta Gorda (roughly 40.3-40.5°N) appears to be consistently exposed to cooler, likely saltier, chlorophyll-poor water, while coastal habitats just to the north and south of this region appear to be more consistently affected by frontal structures that approach the shore. Likewise, cooler and relatively low chl a conditions are more consistently observed in the lee of Cape Blanco, off Point St. George and in the vicinity of Point Arena. Coastal regions between (and particularly in the lee of) headlands are marked by generally warmer water and higher chl a concentrations inshore of areas of elevated frontal structure. These general patterns are corroborated by similar analysis of blended and smoothed data sets (results not shown).

Similar averages calculated for each month of the year (i.e., all Januarys across years) reveals the annual cycle of variability in SST, SST-based structure, and chl a, and suggests that spatial patterns observed in the annual mean are consistently apparent throughout much of the year. These patterns generally persist even though the overall values of temperature and other parameters, and how strongly these parameters differ alongshore varies in intensity over the annual cycle (Figure S03, Appendix SO). Figure SO4 shows anomalies in monthly mean conditions within the coastal band observed during the BSP

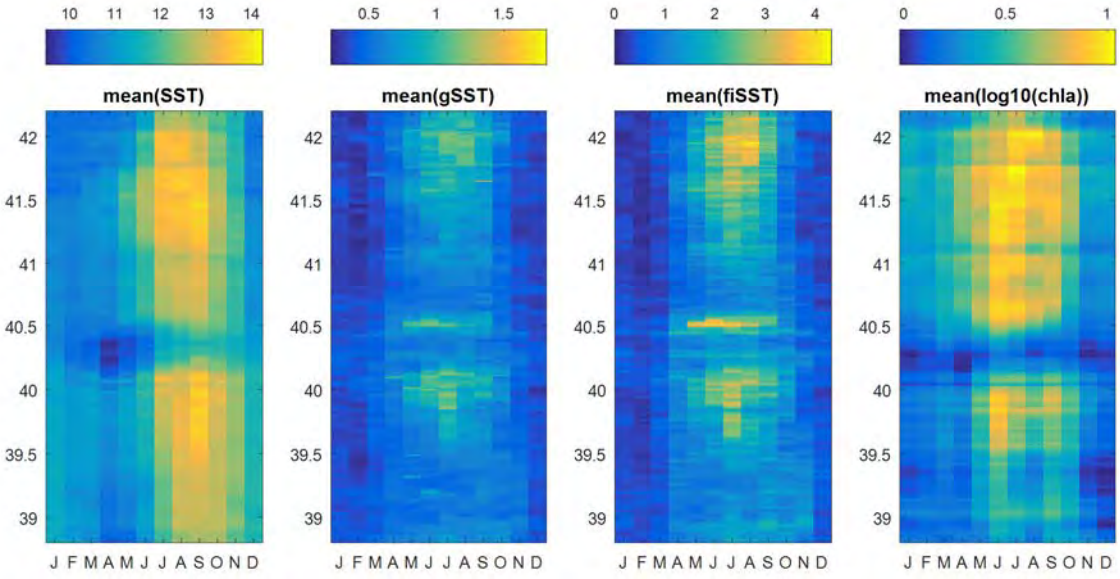

Figure SO3. Left panel: monthly mean SST (°C) for 2003-2015 from MODIS-Aqua. Second panel: monthly mean ∇SST (Δ°C/0.0125°) compiled from gradient fields calculated for individual 3 day composite SST fields. Third panel: mean monthly Front Index compiled from results of application of algorithm adapted from Nieto et al. (2014) to individual 3 day composite SST fields. Right panel: monthly mean $\log_{10}$(chl a) (mg/m^3) for 2003-2015 from MODIS-Aqua. All values are averaged over a coastal band within 0.125° (due west) of the coast.

(2014-2016) relative to a 2003-2013 climatology of monthly mean conditions. The regionwide influence of major climate events (e.g., the Warm Blob and El Niño) is clearly apparent as coherent warming and cooling patterns along the coast. Note that there appears to be relatively little effect of these major climate events on the two measures of spatial variability in SST, suggesting that the spatial pattern of variability in temperature was not dramatically disrupted by the warming events. Gradients in SST in the vicinity of Cape Mendocino, however, appear to have been weaker in late summer 2015. Similar anomalies and spatiotemporal patterns are observed in blended and interpolated data sets (results not shown).

Alongshore structure of coastal oceanographic conditions

The MPA design process for the NCSR had at its disposal various datasets focused on coastal or benthic habitats (e.g., the distribution of rocky reefs, sandy beaches, kelp forests, etc.), but relatively little oceanographic information beyond a qualitative description of oceanographic structure in the region. Additional information on the region was developed over the course of the MPA design and siting process, but to a large degree, decisions regarding the selection of study sites within MPAs and reference sites were not informed by detailed analysis of oceanographic structure and pattern. As a next step towards enhancing oceanographic perspectives for study of MPAs in the NCSR, we applied statistical grouping analysis to oceanographic conditions mapped onto narrow band representative of the placement of MPAs along the coast. Results from this analysis are intended to serve two complementary functions: to place baseline studies in context, particularly with respect to evaluating comparability between MPAs and reference sites, and to support design of ongoing monitoring plans.

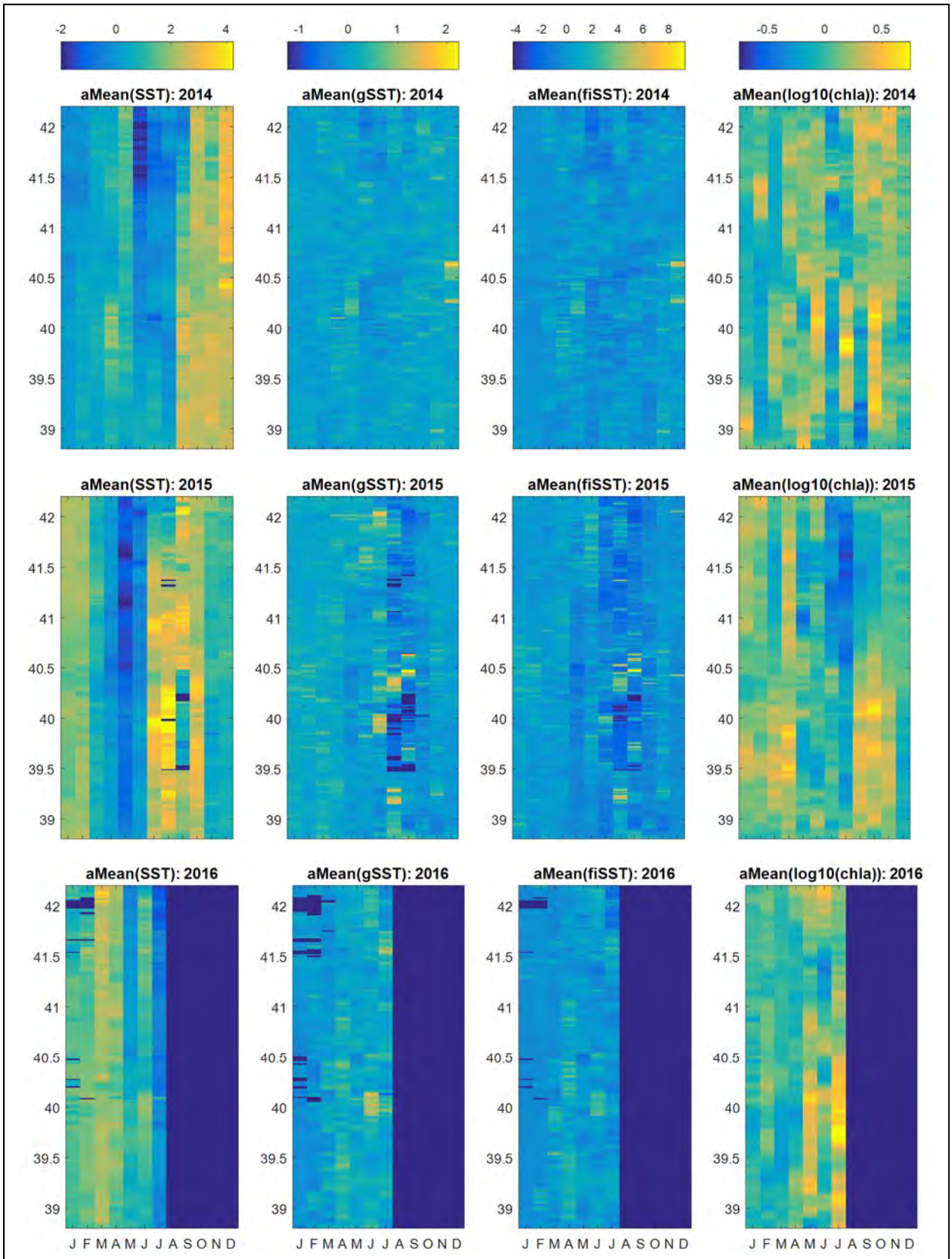

Figure SO4. As in Figure SO3: monthly anomalies for 2014-2016 based on a climatology for 2003-2013.

For this analysis, we constructed a matrix of oceanic conditions based on remote sensing observations of SST, chlorophyll concentrations, and sea level anomaly and geostrophic currents inferred from spatial structure in SSH. For SST and chl a, we extracted monthly mean values based on the MODIS-Aqua data set at its native grid resolution of 0.0125° over the range of the NCSR. Gaps arising in shorter term records (e.g., for individual years or months) due to persistently poor observation coverage were filled by interpolation. Sea level anomaly, inferred meridional and zonal flows from AVISO+TG were interpolated (by spline) to the resolution of the SST data and projected on to a smoothed coastline to estimate monthly mean alongshore and cross-shelf (as opposed to strictly north-south and east-west) components of (geostrophic) nearshore flow. This set of observations was combined with (a) indices of frontal structure derived from remotely sensed SST fields and (b) an index of potential freshwater influence based on proximity to river mouths, scaled by an aggregate function of watershed size and precipitation (for a description of this index, please refer to the section on Freshwater Influence above).

Having constructed matrices of both annual and month-specific mean conditions, we applied a statistical technique known as 'k-means clustering' (Hartigan and Wong 1979, implemented as function 'kmeans' in R) that is designed to discriminate among regions (groups) with similar characteristics. This technique seeks to assign each location to one of a user-specified number of regions in a way that minimizes the differences among sites within that region[1]. We conducted this analysis for datasets that included or excluded latitude as a proxy for the structuring effect of distance. In general, latitude was found to have limited influence, presumably because much of the variability related to alongshore distance was captured in the spatial patterns of other parameters (e.g., SST and freshwater exposure). Including latitude in the analysis, however, served to ensure that cases of small numbers of points being assigned as discontinuous members of groups situated elsewhere along the coast were exceedingly rare.

We conducted a range of analyses based on specifying that the NSCR be partitioned into 2 to 10 regions (Figure KM1). The proportion of the total variance captured by differences between regions (rather than as variability within regions) typically leveled off around 75-80% for cases where the NCSR was partitioned into 6 to 8 regions. This result was consistently observed for both analyses conducted on annual and monthly climatological mean conditions. Likewise, regional boundaries were consistently delineated in several locations, regardless of whether the analysis was based on annual or monthly climatological data: Cape Mendocino, the region between Punta Gorda and Shelter Cove, and the region near Caspar, CA (Figure SO6; see Appendix SO for monthly groupings). To the north of Cape Mendocino, the analysis consistently differentiated between regions near the mouths of the Klamath and Eel Rivers and the stretches of coast between these rivers (Figure KM2, and see Appendix: 'k-means clustering'). Several regional boundaries along the coast appear to be robust to the number of regions specified for the analysis and, based on analysis of climatological monthly means, over the course of the year (Figure KM2). Not surprisingly, breaks in the vicinity of Cape Mendocino are among the most consistently observed throughout the annual cycle.

[1] More specifically, the analysis uses permutation to seek groupings that minimize the aggregate (sum-of-squares) differences between the mean characteristics across all locations within a region and the characteristics of each location within that region. Repeated (n = 150) random initial assignments were used to ensure that robust groupings were achieved, which were then examined for consistent spatial pattern.

Analysis based on annual mean and monthly mean conditions for 2014 and 2015 do not show substantial or systematic departures from the patterns observed for 2003-2013 (Figure KM2). This suggests that typical (normalized) spatial structure in the nearshore oceanography of the NCSR is reasonably robust over time, even though mean conditions across the NCSR may change. Such consistency in structure is not unexpected, given our understanding of how winds and topography interact to structure circulation in the coastal ocean (Marchesiello, et al. 2003). These results, therefore, suggest a possible avenue for incorporating oceanographic information into the geographical design of MPA monitoring plans.

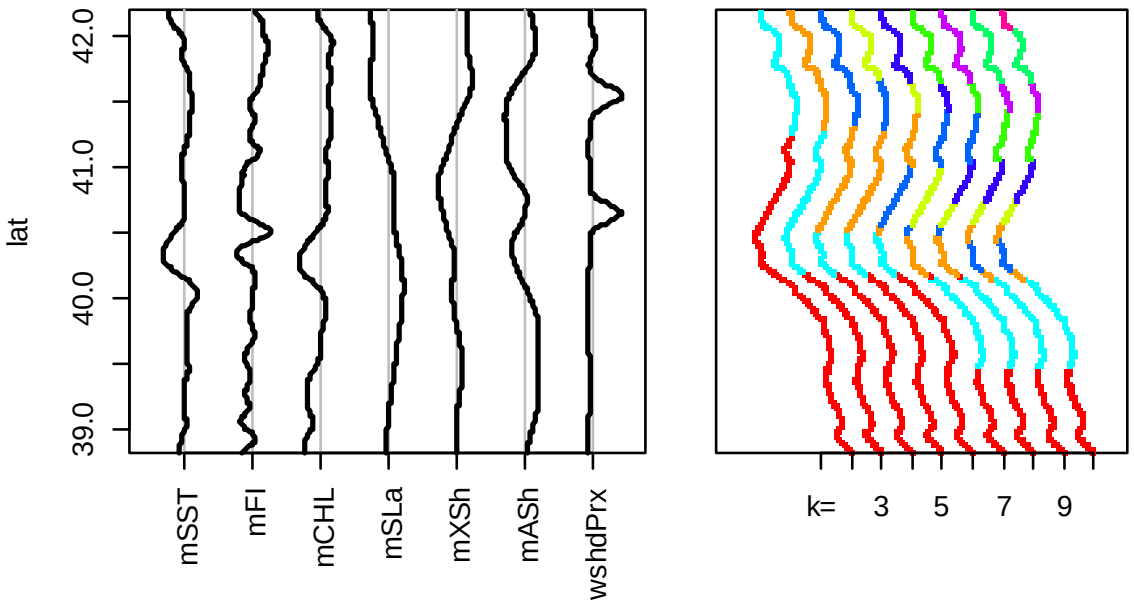

Figure KM1. Left panel: non-dimensional (normalized) variability in annual mean coastal oceanographic conditions (2003-2013) along the NCSR. Right panel: groupings identified by k-means clustering applied to the data shown in left panel for k = 2-10 clusters. Colors delineate groupings within each analysis, but do not carry meaning from one analysis to the next.

Parallel analysis using non-metric multidimensional scaling (NMDS) analysis confirms the suspicion that the boundaries identified here are, in general not stark, but rather emerge as breaks in more continuous—but certainly variable—characteristics of coastal habitats (results not shown). Nevertheless, results from this analysis of geographic provide a basis for focusing additional evaluation on similarities and differences among particular locations along the coast.

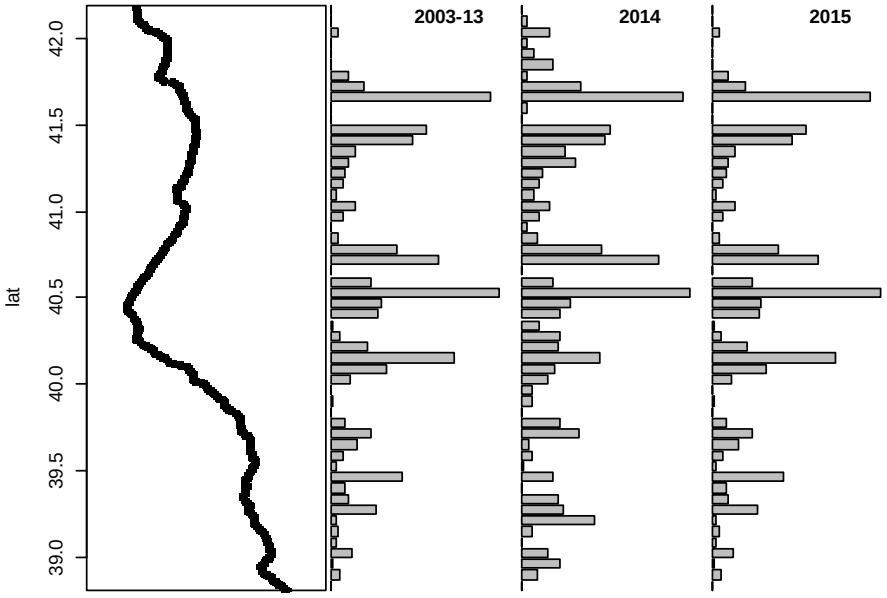

Figure KM2. Distribution of breaks demarcating groups identified by application of k-means clustering to monthly oceanographic data in the NSCR, by latitude. Length of the bar indicates the frequency at which a break was observed across all combinations of (a) k (the number of groups to be identified) ranging from 2 to 10, and (b) month of the year. Years included in each analysis are specified at the top of bar plot. To avoid inflating measures of likely structure, any (rare) breaks bounding very short stretches of the coast separated from their group have been replaced with a break at the mid-point of the small section.

Ocean observations and ecosystem productivity indicators from the Trinidad Head Line

The Trinidad Head Line (THL; 41.05° N) is one of the few year-round, high-frequency data sets that combine time series biological and physical observations in the CCS (Bjorkstedt and Peterson 2016). Oceanographic and ecosystem effects of the 2014-2016 marine heatwave throughout the CCS, including observations along the THL, have been summarized in recent "State of the California Current" reports (Leising et al. 2015, McClatchie et al. 2016) and elsewhere (e.g., Cavote et al 2016). Here we highlight some results from the THL as a source of offshore biological information relevant to BES in the NCSR.

Physical observations along the THL corroborate observations based on other *in situ* and remote sensors, and clearly capture the effects of the NPMHW off the NCSR (Leising et al. 2015, McClatchie et al. 2016). Some of the biological observations from the Trinidad Head Line that are potentially relevant to interpreting data from BES in the NCSR include:

- A marked and persistent shift in the structure of the copepod assemblage has from seasonally consistent representation of northern species during the spring and summer to consistent dominance by species with warm-water and oceanic affinities. Concurrently, numerous species

with southern and offshore distributions were recorded during periods dominated by the NPMWH.
- Concurrent shifts in the euphausiid community marked by declines in the abundance of cold-water species, increases in the abundance of warm-water species, and the novel observation of species typically associated with warmer waters to the south or offshore.
- Declines in the mean size of adult euphausiids (specifically *Euphausia pacifica*) during warm conditions associated with the NPMHW, suggesting the potential for krill to have reduced quality as prey for higher trophic levels.
- A general trend in the composition of plankton samples to be increasingly dominated by taxa, such as pyrosomes, commonly associated with warmer, offshore waters rather than cool, upwelled waters.

In addition, the BSP was impacted by an unprecedentedly massive harmful algal bloom (HAB) of domoic acid-producing *Pseudo-nitchzia* that developed and persisted throughout much of spring and summer 2015. Causes of this bloom appear to have been increased stratification (due to warm surface waters) and changes in nutrient fluxes that favored, yet stressed, *Pseudo-nitchzia* over other phytoplankton. Coastal surveys of this event, coupled with repeated sampling along the THL, and the persistence of high domoic acid concentrations in Dungeness crab off Trinidad, all point to the region off Humboldt Bay being a potential a hotspot for such blooms (McCabe et al. 2016, McClatchie et al. 2016). (Non-quantitative assays for domoic acid in archived samples the THL suggest that elevated concentrations of domoic acid also occurred off the northern NCSR in 2014 and into 2016 (Kudela, Anderson, Bjorkstedt, unpublished data).)

In summary, coastal pelagic and planktonic ecosystems off the NCSR clearly responded to the NPMHW in ways consistent with the shifts in large-scale transport and ecosystem productivity observed in the physical data. Such responses have important implications for interpreting the status and trajectory of coastal and benthic ecosystems in the NCSR.

Synthesis

This report brings together a diverse suite of oceanographic information as a resource for placing ecological information collected during the BSP into historical and spatial context. Integrating ecological and oceanographic data will require additional effort to identify relevant variables and to extract information tailored to specific ecological questions. This report establishes a strong foundation for integrative analysis of data from BES and ongoing assessment of MPAs and ecosystem dynamics in the NCSR, and importantly, establishes a sense of what might be possible to extract from available oceanographic data to inform our understanding of ecological pattern.

The major conclusion to be drawn from our analysis of historical and recent oceanographic data is that the BSP for the NCSR was strongly influenced by highly unusual oceanographic conditions associated with the widespread, persistent 2014-2016 North Pacific marine heatwave (Di Lorenzo and Mantua 2016). Substantially warmer-than-usual temperatures and somewhat stronger poleward flow (or weakened equatorward flow) were recurrent features during the BSP—conditions that have important consequences for larval transport, nutrient supply to coastal habitats, productivity in the coastal ocean, and ecosystem structure in the NCSR and the CCS in general. It is important to note that the unusual water masses observed during the NPMHW were not due to extensive, coastwide poleward transport,

as had occurred during the strong 1997-98 El Niño, but were rather a consequence of changes in upwelling dynamics, unusual ocean-atmosphere heat fluxes, and offshore and southerly water masses impinging on the coast (Di Lorenzo and Mantua 2016). Observations and analysis of pelagic and planktonic ecosystems across the CCS, including observations along the Trinidad Head Line (41.05° N), clearly show the effects of changes in transport and water mass characteristics on plankton communities and indicators of ecosystem productivity (Leising et al 2015, McClatchie et al 2016, Cavotte et al. 2016). Analogous effects on ecosystems that were the focus of BES are to be expected, with poleward shifts of species' distributions, increased or novel observations of southern species, and declines of cold-preferring species among the most likely patterns to be observed (Cavotte et al. 2016). That said, for some species, the marine heatwave appears to have had surprisingly beneficial effects: recruitment in rockfishes appears not to have declined, at least for all species, during this period, despite expectations that cooler, productive ocean conditions tend to favor these species (Leising et al 2015, McClatchie et al 2016, Cavotte et al. 2016). The causes of these counterintuitive patterns is under investigation.

One implication of these findings is that oceanographic conditions concurrent with much of the ecological sampling conducted during the BES were not representative of conditions affecting the region during the planning processes that culminated in implementation of MPAs in the NCSR or that were in place while BES were being designed. What is not yet clear is whether these highly unusual events will yield to more "normal" conditions in the CCS or mark a transition to a new climate regime. Regardless, contextual oceanographic information will be essential to interpreting analysis of future data, particularly given the potential for climate change to alter the oceanography of the California Current (e.g., Rykaczewski et al. 2015).

Another useful result emerging from this analysis is that spatial structure in the coastal ocean appears to be relatively robust to large scale climate variability. In other words, regardless of whether it is warmer or cooler than normal, some places along the coast will, on average be cooler or be exposed to higher chlorophyll concentrations or be in closer proximity to frontal features than others. Note that these patterns emerge in averages over time—these structures can be highly variable on short (e.g., daily) time scales—and should be interpreted in terms of the probability that a given location will be exposed to particular conditions relative to another location. These patterns are linked to coastal topography (headlands in particular), which affect nearshore wind fields in predictable ways, and in turn generate patterns like upwelling plumes and retention zones in the coastal ocean. Based on previous research (e.g., Woodson et al, 2012) it is likely that ecosystems across the NCSR will exhibit patterns related to persistent oceanographic structure, but further analysis is required to establish whether this is indeed the case.

In summary, the body of oceanographic data collated here for the NCSR and analysis products based on these data provide a strong foundation for enhancing our understanding of patterns emerging from baseline ecological studies. Moreover, the oceanographic information developed here, by explicitly placing recent observations in an historical context, supports evaluation of what is consistent and what is variable about the structure and dynamics of the coastal ocean along the NCSR. Such insights have strong potential to inform the design and implementation of future monitoring and adaptive management of the MPA network, by helping to ensure that MPAs and reference sites are comparably situated and differences in how oceanographic dynamics affect MPAs along the coast.

As a final note, we have presented much of the data and analysis in this report at seasonal or monthly resolution, which is generally adequate for characterizing environmental conditions relevant to MPA monitoring at a similar temporal scale, and for characterizing the scope and magnitude of the unprecedented perturbations related to the NPMHW. The underlying datasets are a rich resource, however, for exploring variability at shorter "event" time scales, and we intend to support integrative analyses of BES data through extraction and analysis of higher resolution time series as warranted. To complement this historical perspective, we also have focused substantial attention on developing contextual oceanographic information at spatial resolutions that better connect to scales of MPA networks and possibly even individual MPAs across the NCSR. The hierarchical synthesis of ocean data—ranging from integrated regional conditions within the context of broader climate variability to indices of spatial structure in oceanographic conditions along the coast—that emerged from this work seems well suited to supporting research in the context of spatial processes that, integrated over time, connect ocean dynamics to coastal habitats in structuring marine ecosystems (e.g., Woodson et al. 2012). Future efforts to update and enhance ocean data in support of MPA monitoring and research are likely to benefit from maintaining a similar perspective.

Long-term monitoring recommendations

Oceanographic information is essential for understanding changes in marine ecosystems and elucidating the effects of MPAs in proper context. To support continued efforts to integrate oceanographic information in MPA evaluations, we offer several recommendations regarding future work.

Perhaps our strongest recommendation is that future monitoring be *preceded* by an effort to refine and (to the degree possible) to automate the development and provision of oceanographic context in the vein of what has been developed here. An appropriate suite of products will include indices such as MOCI that provide information on regional trends in productivity and transport that speak most clearly to network-wide pattern, but will also have a specific focus on resolving (and assessing variability in) spatial structure in coastal oceanographic conditions in a manner that complements characterizations of benthic and intertidal habitats. Had such context been available in advance of BES, we suspect that it would have proven useful in the design of ecological sampling programs, particularly with respect to the selection of reference sites.

Taking this a step further, we recommend that a statewide 'ocean context' product be developed as a foundational resource to support effective, well-designed ecological assessment of individual MPAs and of the statewide MPA network as a whole in the years and decades to come. This seems essential, regardless of whether oceanographic conditions revert towards climatological means or the NPMHW marked a transition to a persistent "warm regime". Partnering with the appropriate Regional Associations of the national Integrated Ocean Observing System (IOOS), i.e., CeNCOOS and SCCOOS, should be considered as a way to leverage support and to take advantage of existing platforms for developing analysis and serving data to users.

With this in mind, we offer several additional recommendations. First, given the importance of large scale climate variability as a driver of ecosystem dynamics in the California Current, coupled with the need to tie these climate indices to local observations, it is essential that the existing observation and analysis systems continue to be supported. This recommendation clearly goes beyond the scope of direct support through programs or agencies likely to fund future monitoring of MPAs. Nevertheless,

the value of these time series for developing oceanographic context as a basis for interpreting ecological dynamics is clear. Interested parties should encourage and support continuation of robust *in situ* observation programs, such as the array of coastal moorings and the HF radar network, and remote sensing platforms that provide observations specific to the NCSR. These data sources are essential for characterizing local pattern and variability and for anchoring larger scale climate dynamics at a regional scale (as per integration in NSCR-specific indices such as the MOCI).

Second, we recommend that collection of *in situ* measurements—at a minimum temperature, ideally measured at the inshore and offshore bounds of a study area where practical—should be a nearly universal requirement for future monitoring. Such environmental data should be collected as a time series, not only as snapshots coincident with ecological sampling, as ecological dynamics integrate of environmental variability over time. Resolving the local signature of oceanographic events provide a basis for evaluating the strength of links (or lack of links) between local environmental conditions and larger-scale indices of ocean conditions, and thus support analysis of local responses in terms of local conditions within a broader context. That such data were not routinely collected during the BSP, represents a lost opportunity to more rigorously link ecological observations to oceanographic conditions during the BSP, and to evaluate whether dynamics in study sites selected for ongoing monitoring are more or less idiosyncratic with respect to ocean conditions.

That said, we do not expect substantial near-term benefits from directly integrating local, *in situ* time series into locally-specific indices analogous to MOCI, as indices like MOCI require long, continuous, coincident time series of input variables for their construction. Environmental time series established within individual MPAs as part of long-term monitoring will not meet these criteria for several years or decades.

Third, we recommend that ongoing development of contextual oceanographic information continue to emphasize large-scale dynamics, yet also focus on enhancing the resolution of information available at scales relevant to individual MPAs and reference sites. To this end, we recommend that future monitoring programs explicitly support collaborations between oceanographers and ecologists, as it will require substantial effort to identify and evaluate links between oceanographic structure and ecosystem pattern. Such collaborations represent an efficient approach to dealing with challenges in accessing and interpreting oceanographic information in a way that is informative and relevant to ecological patterns. Based on the feasibility of developing spatial oceanographic information for the NSCR, and the finding that spatial patterns appeared to be consistent from year to year, we recommend further development of information on spatial structure as a basis for evaluation of ecological data and design of future monitoring programs. Based on past research, we expect that the information and indices developed in this report are likely to have some bearing on temporal and spatial patterns observed in marine ecosystems, but the nature of these relationships has yet to be established for the NSCR and especially for the BSP given the highly anomalous conditions that coincided with the baseline studies.

Acknowledgements

We gratefully acknowledge the efforts of the many scientists and technicians who have contributed to the observational time series summarized in this report, and the diverse agencies and programs who have supported this work. We thank Craig Risien and Ted Strub (OSU, CEOAS) for making available an updated version of their AVISO+TG data set. We also thank Roxanne Robertson, the Captain and Crew of the R/V Coral Sea, and the numerous members of the scientific crew who make possible the oceanographic observations along the Trinidad Head Line.

Literature Cited

Agrawal, A., R. S. Schick, E. P. Bjorkstedt, B. G. Szerlong, M. N. Goslin, B. C. Spence, T. H. Williams, K. M. Burnett. (2005). Predicting the potential for historical coho, Chinook, and steelhead habitat in northern California. U.S. Department of Commerce, NOAA Technical Memorandum NMFS, NOAA-TM-NMFS-SWFSC-379, 25 p.

Bakun, A., (2006). Fronts and eddies as key structures in the habitat of marine fish larvae: opportunity, adaptive response and competitive advantage. Scientia Marina, 70(S2), pp.105-122.

Black, B. A., I. D. Schroeder, W. J. Sydeman, S. J. Bograd, and P. W. Lawson (2010), Wintertime ocean conditions synchronize rockfish growth and seabird reproduction in the central California Current Ecosystem, Canadian Journal of Fisheries and Aquatic Sciences, 67, 1149-1158.

Black, B. A., I. D. Schroeder, W. J. Sydeman, S. J. Bograd, B. K. Wells, and F. B. Schwing (2011), Winter and summer upwelling modes and their biological importance in the California Current Ecosystem, Global Change Biology, 17, 2536-2545.

Bond, N. A., Cronin, M. F., Freeland, H., & Mantua, N. (2015). Causes and impacts of the 2014 warm anomaly in the NE Pacific. Geophysical Research Letters, 42(9), 3414-3420.

Botsford, L. W., Moloney, C. L., Hastings, A., Largier, J. L., Powell, T. M., Higgins, K., & Quinn, J. F. (1994). The influence of spatially and temporally varying oceanographic conditions on meroplanktonic metapopulations. Deep Sea Research Part II: Topical Studies in Oceanography, 41(1), 107-145.

Cavole, L.C.M., Demko, A.M., Diner, R.E., Giddings, A., Koester, I., Pagniello, C.M., Paulsen, M.L., Ramirez-Valdez, A., Schwenck, S.M., Yen, N.K. Zill, M.E., and Franks, P.J.S., 2016. Biological Impacts of the 2013-2015 Warm-Water Anomaly in the Northeast Pacific. Oceanography, 29(2), pp.273-285.

Cayula, J. F., & Cornillon, P. (1992). Edge detection algorithm for SST images. Journal of Atmospheric and Oceanic Technology, 9(1), 67-80.

Cayula, J. F., & Cornillon, P. (1995). Multi-image edge detection for SST images. Journal of Atmospheric and Oceanic Technology, 12(4), 821-829.

Chase, Z., Strutton, P. G., & Hales, B. (2007). Iron links river runoff and shelf width to phytoplankton biomass along the US West Coast. Geophysical Research Letters, 34(4).

Chhak, K., & Di Lorenzo, E. (2007). Decadal variations in the California Current upwelling cells. Geophysical Research Letters, 34(14).

Diehl, S. F., Budd, J. W., Ullman, D., & Cayula, J. F. (2002). Geographic window sizes applied to remote sensing sea surface temperature front detection. Journal of Atmospheric and Oceanic Technology, 19(7), 1105–1113.

Di Lorenzo, E., Schneider, N., Cobb, K. M., Franks, P. J. S., Chhak, K., Miller, A. J., McWilliams, J.C., Bograd, S.J., Arango, H., Curchitser, E., & Powell, T. M. (2008). North Pacific Gyre Oscillation links ocean climate and ecosystem change. Geophysical Research Letters, 35(8).

Di Lorenzo, E., Combes, V., Keister, J.E., Strub, P.T., Thomas, A.C., Franks, P.J., Ohman, M.D., Furtado, J.C., Bracco, A., Bograd, S.J. and Peterson, W.T., 2013. Synthesis of Pacific Ocean climate and ecosystem dynamics. Oceanography, 26(4), pp.68-81.

Di Lorenzo, E., & Mantua, N. (2016). Multi-year persistence of the 2014/15 North Pacific marine heatwave. Nature Climate Change, 6, 1042-1047.

Ebert, T. A., & Russell, M. P. (1988). Latitudinal variation in size structure of the west coast purple sea urchin: a correlation with headlands. Limnology and Oceanography, 33(2), 286-294.

Fan, S., Swift, D. J., Traykovski, P., Bentley, S., Borgeld, J. C., Reed, C. W., & Niedoroda, A. W. (2004). River flooding, storm resuspension, and event stratigraphy on the northern California shelf: observations compared with simulations. Marine Geology, 210(1), 17-41.

Fisher, J. L., W. T. Peterson, and R. R. Rykaczewski (2015), The impact of El Niño events on the pelagic food chain in the northern California Current, Global Change Biology, 21(12), 4401-4414, doi:10.1111/gcb.13054.

Frischknecht, M., Münnich, M. and Gruber, N., 2017. Local atmospheric forcing driving an unexpected California Current System response during the 2015–2016 El Niño. Geophysical Research Letters, 44, 304–311, doi:10.1002/ 2016GL071316.

García-Reyes, M., & Sydeman, W. J. (2017). California Multivariate Ocean Climate Indicator (MOCI) and marine ecosystem dynamics. Ecological Indicators, 72, 521-529.

Gentemann, C. L., Fewings, M. R., & García-Reyes, M. (2017). Satellite sea surface temperatures along the West Coast of the United States during the 2014–2016 northeast Pacific marine heat wave. Geophysical Research Letters 44, 312-319.

Geyer, W. R., Hill, P., Milligan, T., & Traykovski, P. (2000). The structure of the Eel River plume during floods. Continental Shelf Research, 20(16), 2067-2093.

Hartigan, J. A. and Wong, M. A. (1979). A K-means clustering algorithm. Applied Statistics 28, 100–108.

Jacox, M. G., Hazen, E. L., Zaba, K. D., Rudnick, D. L., Edwards, C. A., Moore, A. M., & Bograd, S. J. (2016). Impacts of the 2015–2016 El Niño on the California Current System: Early assessment and comparison to past events. Geophysical Research Letters, 43(13), 7072-7080.

Kahru, M., Jacox, M. G., Lee, Z., Kudela, R. M., Manzano-Sarabia, M., & Mitchell, B. G. (2015). Optimized multi-satellite merger of primary production estimates in the California Current using inherent optical properties. Journal of Marine Systems, 147, 94-102.

Kahru, M., Kudela, R. M., Manzano-Sarabia, M., & Mitchell, B. G. (2012). Trends in the surface chlorophyll of the California Current: Merging data from multiple ocean color satellites. Deep Sea Research Part II: Topical Studies in Oceanography, 77, 89-98.

Keister, J. E., Peterson, W. T., & Pierce, S. D. (2009). Zooplankton distribution and cross-shelf transfer of carbon in an area of complex mesoscale circulation in the northern California Current. Deep Sea Research Part I: Oceanographic Research Papers, 56(2), 212-231.

Keister, J. E., E. Di Lorenzo, C. A. Morgan, V. Combes, and W. T. Peterson (2011), Zooplankton species composition is linked to ocean transport in the Northern California Current, Global Change Biology, 17, 2498-2511.

Kim, S. Y., Terrill, E. J., Cornuelle, B. D., Jones, B., Washburn, L., Moline, M. A., Paduan, J.D., Garfield, N., Largier, J.L., Crawford, G. & Kosro, P. M. (2011). Mapping the US West Coast surface circulation: A

multiyear analysis of high-frequency radar observations. Journal of Geophysical Research: Oceans, 116(C3).

Leising, A. W., et al. (2015). State of the California Current 2014-15: Impacts of the Warm-Water" Blob". Mantua, N. J., & Hare, S. R. (2002). The Pacific decadal oscillation. Journal of oceanography, 58(1), 35-44.

Marchesiello, P., McWilliams, J. C., & Shchepetkin, A. (2003). Equilibrium structure and dynamics of the California Current System. Journal of Physical Oceanography, 33(4), 753-783.

McCabe, R. M., Hickey, B. M., Kudela, R. M., Lefebvre, K. A., Adams, N. G., Bill, B. D., Gulland, F., Thomson, R.E., Cochlan, W.P, and Trainer, V. L. (2016). An unprecedented coastwide toxic algal bloom linked to anomalous ocean conditions. Geophysical Research Letters, 43(19).

McClatchie, S., et al. (2016). State of the California Current 2015-16: Comparisons with the 1997–98 El Niño. CalCOFI Reports 57: 5-61.

Messié, M., & Chavez, F. (2011). Global modes of sea surface temperature variability in relation to regional climate indices. Journal of Climate, 24(16), 4314-4331.

Nieto, K., Demarcq, H., & McClatchie, S. (2012). Mesoscale frontal structures in the Canary Upwelling System: New front and filament detection algorithms applied to spatial and temporal patterns. Remote Sensing of Environment, 123, 339-346.

Pond, S. and Pickard, G.L., (2013). Introductory dynamical oceanography. Elsevier.

Risien, C. M., & Strub, P. T. (2016). Blended sea level anomaly fields with enhanced coastal coverage along the US West Coast. Scientific data, 3.

Rudnick, D.L., et al. A climatology of the California Current System from a network of underwater gliders. Prog. Oceanogr. (2017), http://dx.doi.org/10.1016/j.pocean.2017.03.002

Rykaczewski, R. R., Dunne, J. P., Sydeman, W. J., García-Reyes, M., Black, B. A., & Bograd, S. J. (2015). Poleward displacement of coastal upwelling-favorable winds in the ocean's eastern boundary currents through the 21st century. Geophysical Research Letters, 42(15), 6424-6431.

Sakuma, K. M., Bjorkstedt, E. P., & Ralston, S. (2013). Distribution of pelagic juvenile rockfish (Sebastes spp.) in relation to temperature and fronts off central California. California Cooperative Oceanic Fisheries Investigations Reports, 54, 167-179.

Schroeder, I. D., Black, B. A., Sydeman, W. J., Bograd, S. J., Hazen, E. L., Santora, J. A., & Wells, B. K. (2013). The North Pacific High and wintertime pre-conditioning of California current productivity. Geophysical Research Letters, 40(3), 541-546.

Schwing, F. B., Murphree, T., & Green, P. M. (2002). The Northern Oscillation Index (NOI): a new climate index for the northeast Pacific. Progress in Oceanography, 53(2), 115-139.

Stewart (2008). Introduction to Physical Oceanography. Available at https://oceanography.tamu.edu/academics/camps-and-outreach/ocean-world/resources/Stewart_PObook.pdf

Swain, D. L., Tsiang, M., Haugen, M., Singh, D., Charland, A., Rajaratnam, B., & Diffenbaugh, N. S. (2014). The extraordinary California drought of 2013/2014: Character, context, and the role of climate change. Bulletin of the American Meteorological Society, 95(9), S3.

Sydeman, W. J., R. W. Bradley, P. Warzybok, C. L. Abraham, J. Jahncke, K. D. Hyrenbach, V. Kousky, J. M. Hipfner, and M. D. Ohman (2006), Planktivorous auklet *Ptychoramphus aleuticus* responses to ocean climate, 2005: Unusual atmospheric blocking? Geophys. Res. Lett., 33, L22S09, doi:10.1029/2006GL026736.

Sydeman, W. J., Thompson, S. A., García-Reyes, M., Kahru, M., Peterson, W. T., & Largier, J. L. (2014). Multivariate ocean-climate indicators (MOCI) for the central California Current: Environmental change, 1990–2010. Progress in Oceanography, 120, 352-369.

Wheatcroft, R. A., & Borgeld, J. C. (2000). Oceanic flood deposits on the northern California shelf: large-scale distribution and small-scale physical properties. Continental Shelf Research, 20(16), 2163-2190.

White, J. W. (2008). Spatially coupled larval supply of marine predators and their prey alters the predictions of metapopulation models. The American Naturalist, 171(5), E179-E194.

White, J. W., Botsford, L. W., Hastings, A., & Largier, J. L. (2010). Population persistence in marine reserve networks: incorporating spatial heterogeneities in larval dispersal. Marine Ecology Progress Series, 398, 49-67.

Wing, S. R., Botsford, L. W., Largier, J. L., & Morgan, L. E. (1995). Spatial structure of relaxation events and crab settlement in the northern California upwelling system. Marine Ecology Progress Series, 128, 199-211.

Wolter, K., & Timlin, M. S. (1998). Measuring the strength of ENSO events: how does 1997/98 rank?. Weather, 53(9), 315-324.

Woodson, C. B., McManus, M. A., Tyburczy, J. A., Barth, J. A., Washburn, L., Caselle, J. E., Carr, M.H., Malone, D.P., Raimondi, P.T., Menge, B.A. & Palumbi, S. R. (2012). Coastal fronts set recruitment and connectivity patterns across multiple taxa. Limnology and Oceanography, 57(2), 582-596.

Financial Report

The following report on expenditures related to this project integrates independent reports across the collaborating institutions: Humboldt State University (HSU), UC Davis/Bodega Marine Lab (BML), and Farallon Institute for Advanced Ecosystem Research (FAIER) as summarized in Table FR1. This project was not field-based, so major reallocations within budgets are driven primarily from differences between proposed and realized staffing and changes in benefits packages that affected calculations based on salary:fringe ratios and from slight disparity in estimates of needed effort and effort actually required to support completion of the proposed work.

Humboldt State University

Changes in wage and fringe allocations reflected a shift in personnel engaged in this project; we elected to support an existing full-time technician (Roxanne Robertson) who assisted with data assembly and analysis, rather than hire a part-time technician as originally proposed. Minor budget categories (Travel and Other) were reallocated to cover the additional Fringe Benefit expenses so incurred; necessary travel was covered by other (Federal) support. Grantee share of Total wages and salaries remains in deficit at current time of accounting, but paperwork for final accounting of matching effort (Tissot) is in process. Effort contributed by PI Eric Bjorkstedt (NOAA/NMFS) and use of Federal IT resources in support of this project represent substantial, though inadmissible, matching contributions.

UC Davis/Bodega Marine Lab

Increased expenditure on Fringe allocated to CASG due to post-proposal changes in fringe calculation. These additional expenses were offset from Travel (not used) and Other Expenses (underspent) categories. Travel expenses were not required as colleagues traveled to BML in conjunction with other supported travel, rather than requiring BML personnel to travel to HSU.

Farallon Institute

Changes in both Sea Grant and Grantee Share allocations to Total Salaries and Wages were required to match unanticipated additional effort required by this project, but were offset by reduced Fringe expenses and greater coverage of Fringe expenses by Grantee. Travel expenses in support of presenting results from this work exceeded budgeted expenses due to cost of travel, but were offset by additional grantee share in support of this travel. Reduction in Grantee Share due to forgone IDC is offset by direct accounting of expenses related to travel and expendable supplies covered by the Grantee.

Table FR1: Summary comparison of budgeted and actual expenses by institution related to projects R/MPA-31(A,B,C) “Oceanographic context for baseline characterization and future evaluation of MPAs along California's North Coast”

PI	Bjorkstedt	R/MPA-31A							
Institution	HSU		SGF = "Sea Grant Funds"						
Agency	CASG		GS = "Grantee Share"						
Title	Oceanographic Context								
Start date	2/1/2014 - 3/31/2017		**Budget**		**Actual**		**Variance**		**Explanation of Variances > 10%**
Year	ALL		SGF	GS	SGF	GS	SGF	GS	NOTES
		Total salaries & wages	$ 16,014	$ 11,180	**$ 15,859**	**$ 11,409**	-1%	2%	Final accounting of match time in process
		Fringe	$ 3,931	$ -	**$ 4,936**		26%	0%	
		Total permanent equip	$ -	$ -			0%	0%	
		Expendable supplies and equip	$ -	$ -			0%	0%	
		Total (domestic) travel	$ 660	$ -	**$ -**		-100%	0%	
		Pubs & Comms	$ -	$ -			0%	0%	
		Total Other	$ 190	$ -	**$ -**		-100%	0%	
		TOTAL DIRECT	$ 20,795	$ -	**$ 20,795**		0%	0%	
		IDC	$ 5,199	$ -	**$ 5,199**		0%	0%	
		IDC (foregone) waived as match		$ 4,159	**$ -**	**$ 4,159**	0%	0%	
		TOTAL COSTS	$ 25,994	$ 15,339	**$ 25,994**	**$ 15,568**	0%	1%	
PI	Largier	R/MPA-31B							
Institution	UC DAVIS								
Agency	CASG								
Title	Oceanographic Context								
Start date	2/1/2014 - 3/31/2017		**Budget**		**Actual**		**Variance**		**Explanation of Variances > 10%**
Year	ALL		SGF	GS	SGF	GS	SGF	GS	NOTES
		Total salaries & wages	$ 14,173	$ 5,083	**$ 13,984**	**$ 5,083**	-1%	0%	
		Fringe	$ 5,939	$ 1,884	**$ 8,172**	$ 1,884	38%	0%	Additional effort directed to project
		Total permanent equip	$ -	$ -	**$ -**	$ -	0%	0%	
		Expendable supplies and equip	$ -	$ -	**$ -**	$ -	0%	0%	
		Total (domestic) travel	$ 1,000	$ -	**$ -**	**$ -**	-100%	0%	Anticipated travel not required
		Pubs & Comms	$ -	$ -	**$ -**	$ -	0%	0%	
		Total Other	$ 1,287	$ -	**$ 243**	$ -	-81%	0%	Anticipated expenses
		TOTAL DIRECT	$ 22,399	$ 6,967	**$ 22,400**	**$ 6,967**	0%	0%	
		IDC	$ 5,601	$ 5,831	**$ 5,600**	**$ 5,831**	0%	0%	
		IDC (foregone) waived as match		$ 6,889	**$ -**	**$ 6,889**	0%	0%	
		TOTAL COSTS	$ 28,000	$ 19,687	**$ 28,000**	**$ 19,687**	0%	0%	
PI	Sydeman	R/MPA-31C							
Institution	Farallon Institute								
Agency	CASG								
Title	Oceanographic Context								
Start date	2/1/2014 - 3/31/2017		**Budget**		**Actual**		**Variance**		**Explanation of Variances > 10%**
Year	ALL		SGF	GS	SGF	GS	SGF	GS	NOTES
		Total salaries & wages	$ 36,763	$ 11,215	**$ 40,656**	**$ 12,252**	11%	9%	Required more effort than anticipated
		Fringe	$ 11,029	$ 1,526	**$ 7,318**	$ 2,531	-34%	66%	Charged more to grantee share
		Total permanent equip	$ -	$ -	**$ -**	$ -	0%	0%	
		Expendable supplies and equip	$ 300	$ -	**$ -**	$ 354	-100%	0%	Charged to grantee share
		Total (domestic) travel	$ 1,000	$ -	**$ 1,118**	**$ 520**	12%	0%	More than anticipated; offset by grantee share
		Pubs & Comms	$ -	$ -	**$ -**	$ -	0%	0%	
		Total Other		$ -	**$ 243**	$ -	0%	0%	
		TOTAL DIRECT	$ 49,092	$ 12,741	**$ 49,335**	**$ 15,657**	0%	23%	
		IDC	$ 4,909		**$ 4,909**		0%	0%	
		IDC (foregone) waived as match		$ 11,167	**$ -**	**$ 8,040**	0%	-28%	Offset by increased grantee share in named categories
		TOTAL COSTS	$ 54,001	$ 23,908	**$ 54,244**	**$ 23,697**	0%	-1%	
		Please note that these amounts are only through 2/27/17.							
		The final financials will be provided after 3/31/17 (the final day to post expenses).							

Appendix OC: Monthly mean ocean currents January 2013 to May 2016.

This appendix presents a series of maps for the North Coast Study Region Baseline Study Period showing (left-hand panels) monthly mean surface currents derived from observations made with HF radar, paired with (right-hand panels) concurrent estimates of monthly mean geostrophic currents inferred from variation in sea surface height derived from satellite altimetry (AVISO) and interpolated to coastal tide gauges following Risien and Strub (2016). In HF radar current plots, arrow indicates direction of flow and shading indicates speed in m/s. In plots of geostrophic currents, current speed (m/s) is indicated by vector length (scale in upper right-hand corner). These maps are intended to provide broad context in terms of conditions leading up to and during observations made during ecological surveys, and as a resource for formulating more specific queries of the underlying data sets as part of analyses designed to explore connections between oceanographic and ecological data. Note that these maps are best viewed on-screen under some magnification.

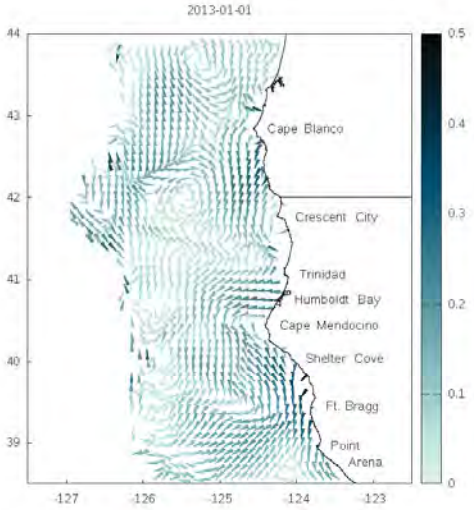
2013-01-01
Cape Blanco
Crescent City
Trinidad
Humboldt Bay
Cape Mendocino
Shelter Cove
Ft. Bragg
Point Arena

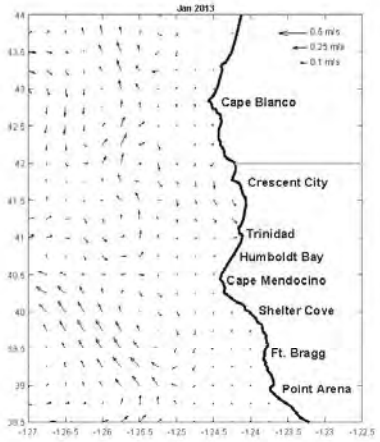
Jan 2013
0.5 m/s
0.25 m/s
0.1 m/s
Cape Blanco
Crescent City
Trinidad
Humboldt Bay
Cape Mendocino
Shelter Cove
Ft. Bragg
Point Arena

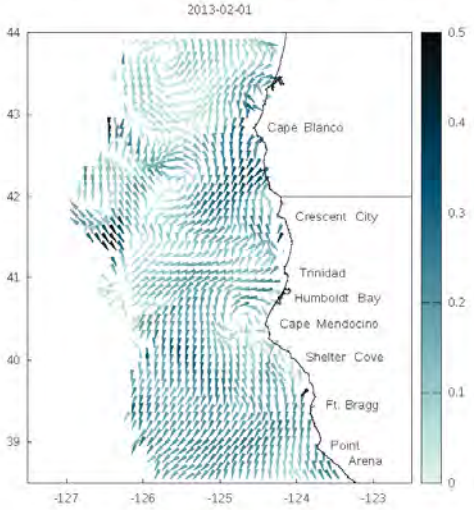
2013-02-01
Cape Blanco
Crescent City
Trinidad
Humboldt Bay
Cape Mendocino
Shelter Cove
Ft. Bragg
Point Arena

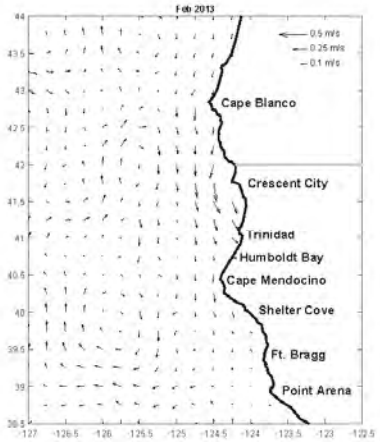
Feb 2013
0.5 m/s
0.25 m/s
0.1 m/s
Cape Blanco
Crescent City
Trinidad
Humboldt Bay
Cape Mendocino
Shelter Cove
Ft. Bragg
Point Arena

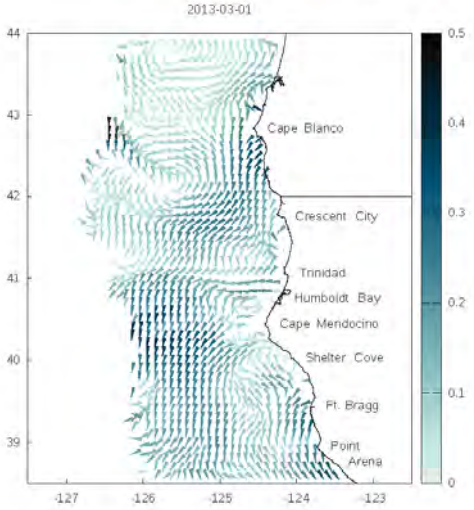
2013-03-01
Cape Blanco
Crescent City
Trinidad
Humboldt Bay
Cape Mendocino
Shelter Cove
Ft. Bragg
Point Arena

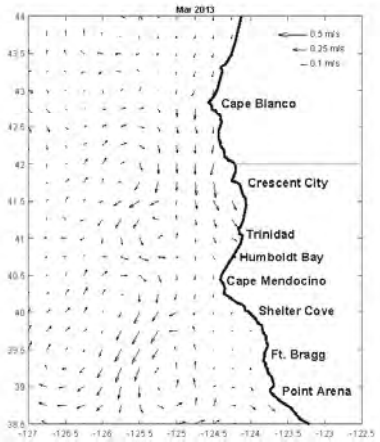
Mar 2013
0.5 m/s
0.25 m/s
0.1 m/s
Cape Blanco
Crescent City
Trinidad
Humboldt Bay
Cape Mendocino
Shelter Cove
Ft. Bragg
Point Arena

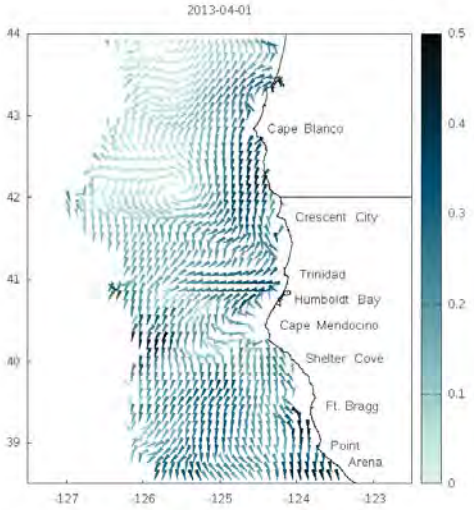
2013-04-01
Cape Blanco
Crescent City
Trinidad
Humboldt Bay
Cape Mendocino
Shelter Cove
Ft. Bragg
Point Arena

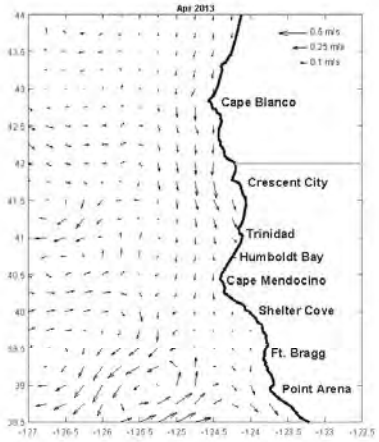
Apr 2013
0.5 m/s
0.25 m/s
0.1 m/s
Cape Blanco
Crescent City
Trinidad
Humboldt Bay
Cape Mendocino
Shelter Cove
Ft. Bragg
Point Arena

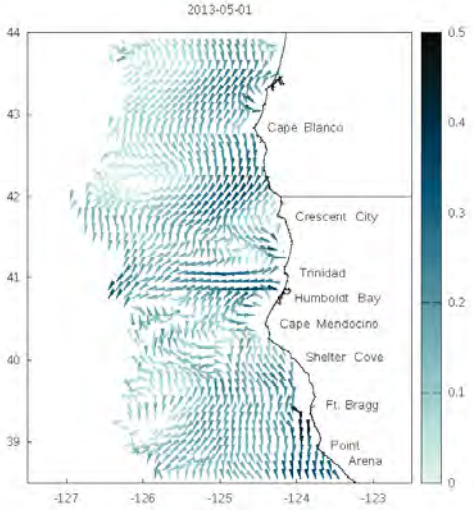
2013-05-01
Cape Blanco
Crescent City
Trinidad
Humboldt Bay
Cape Mendocino
Shelter Cove
Ft. Bragg
Point Arena

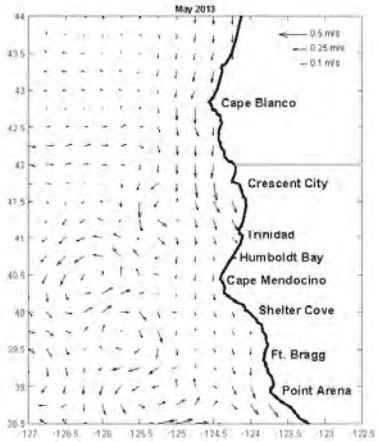
May 2013
0.5 m/s
0.25 m/s
0.1 m/s
Cape Blanco
Crescent City
Trinidad
Humboldt Bay
Cape Mendocino
Shelter Cove
Ft. Bragg
Point Arena

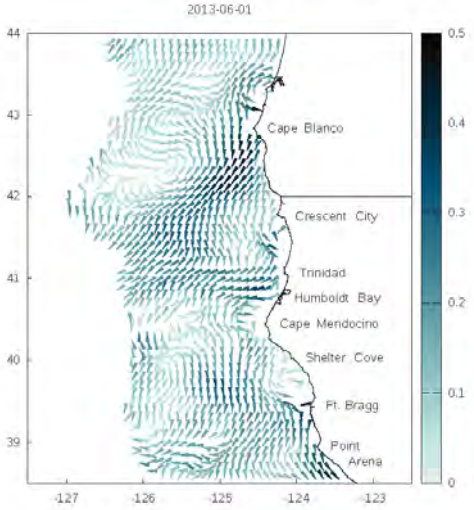
2013-06-01
Cape Blanco
Crescent City
Trinidad
Humboldt Bay
Cape Mendocino
Shelter Cove
Ft. Bragg
Point Arena

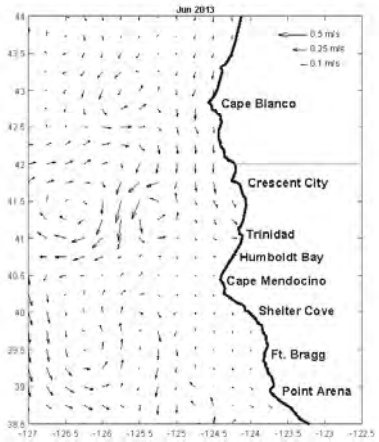
Jun 2013
0.5 m/s
0.25 m/s
0.1 m/s
Cape Blanco
Crescent City
Trinidad
Humboldt Bay
Cape Mendocino
Shelter Cove
Ft. Bragg
Point Arena

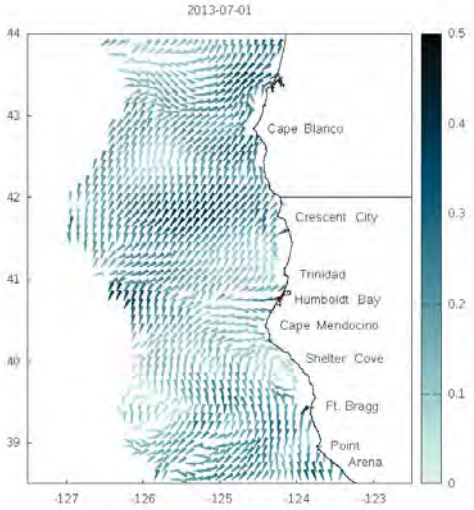
2013-07-01
Cape Blanco
Crescent City
Trinidad
Humboldt Bay
Cape Mendocino
Shelter Cove
Ft. Bragg
Point Arena

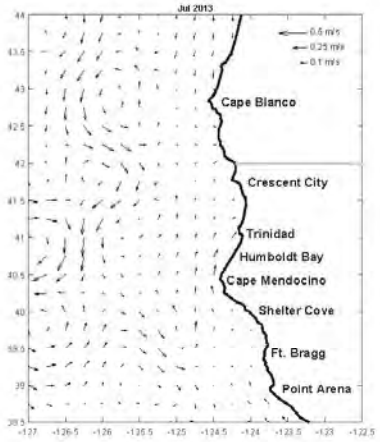
Jul 2013
0.5 m/s
0.25 m/s
0.1 m/s
Cape Blanco
Crescent City
Trinidad
Humboldt Bay
Cape Mendocino
Shelter Cove
Ft. Bragg
Point Arena

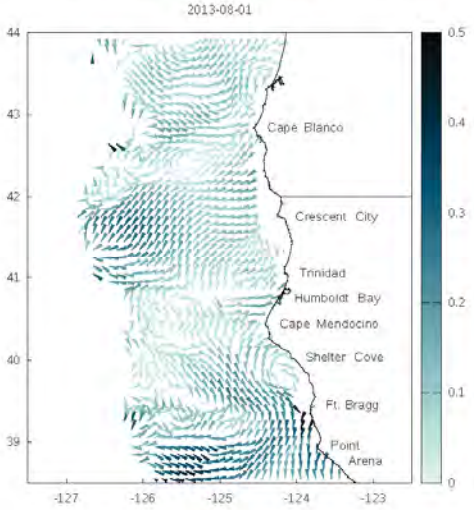
2013-08-01
Cape Blanco
Crescent City
Trinidad
Humboldt Bay
Cape Mendocino
Shelter Cove
Ft. Bragg
Point Arena

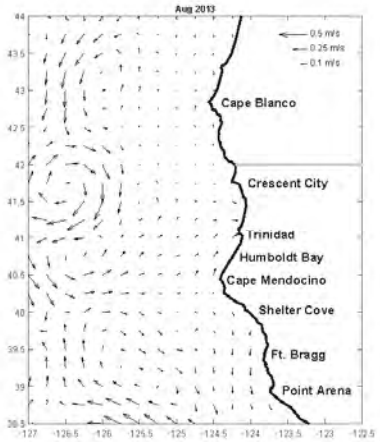
Aug 2013
0.5 m/s
0.25 m/s
0.1 m/s
Cape Blanco
Crescent City
Trinidad
Humboldt Bay
Cape Mendocino
Shelter Cove
Ft. Bragg
Point Arena

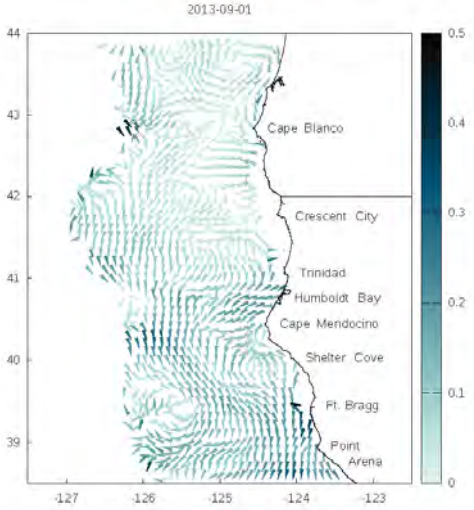
2013-09-01
Cape Blanco
Crescent City
Trinidad
Humboldt Bay
Cape Mendocino
Shelter Cove
Ft. Bragg
Point Arena

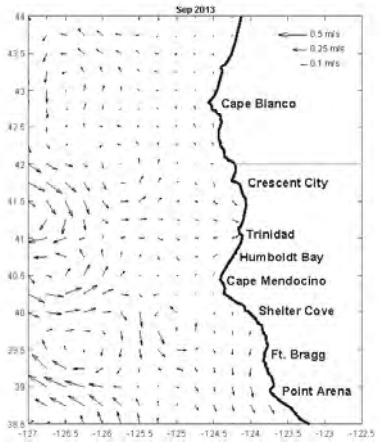
Sep 2013
0.5 m/s
0.25 m/s
0.1 m/s
Cape Blanco
Crescent City
Trinidad
Humboldt Bay
Cape Mendocino
Shelter Cove
Ft. Bragg
Point Arena

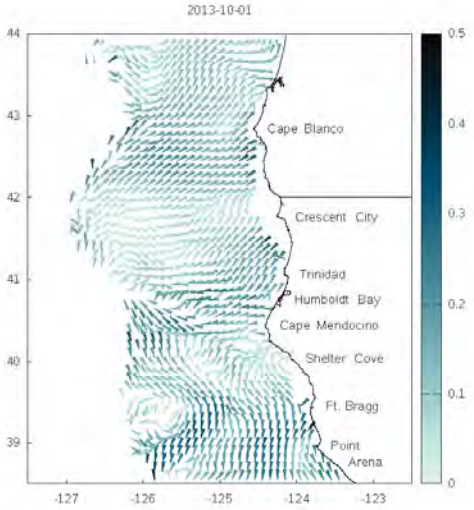
2013-10-01
Cape Blanco
Crescent City
Trinidad
Humboldt Bay
Cape Mendocino
Shelter Cove
Ft. Bragg
Point Arena

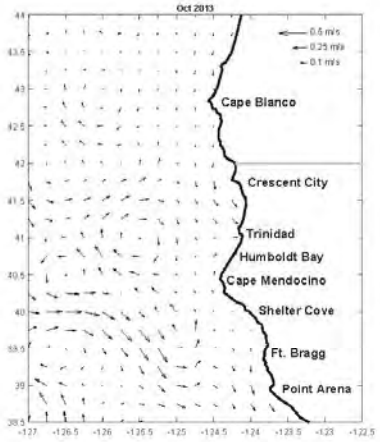
Oct 2013
0.5 m/s
0.25 m/s
0.1 m/s
Cape Blanco
Crescent City
Trinidad
Humboldt Bay
Cape Mendocino
Shelter Cove
Ft. Bragg
Point Arena

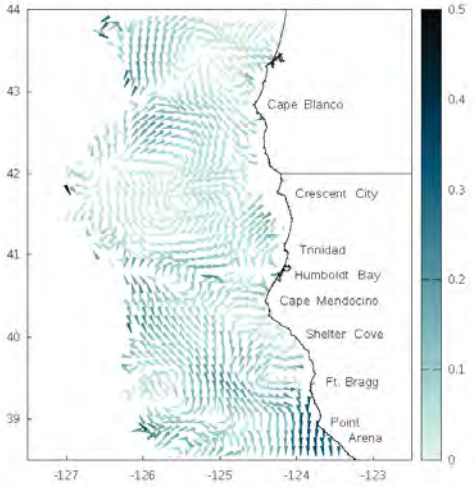
2013-11-01
Cape Blanco
Crescent City
Trinidad
Humboldt Bay
Cape Mendocino
Shelter Cove
Ft. Bragg
Point Arena

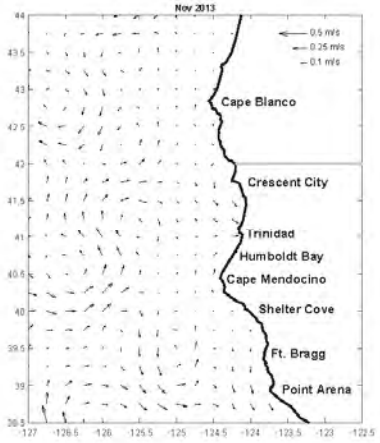
Nov 2013
0.5 m/s
0.25 m/s
0.1 m/s
Cape Blanco
Crescent City
Trinidad
Humboldt Bay
Cape Mendocino
Shelter Cove
Ft. Bragg
Point Arena

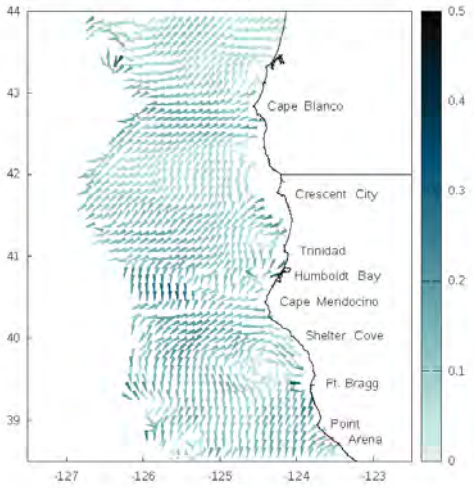
2013-12-01
Cape Blanco
Crescent City
Trinidad
Humboldt Bay
Cape Mendocino
Shelter Cove
Ft. Bragg
Point Arena

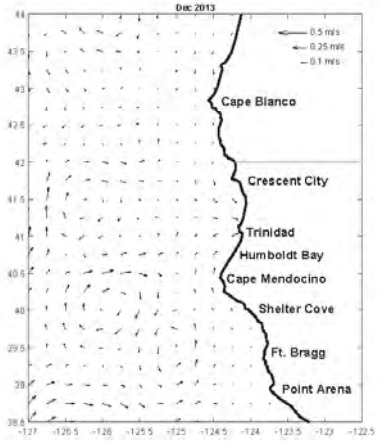
Dec 2013
0.5 m/s
0.25 m/s
0.1 m/s
Cape Blanco
Crescent City
Trinidad
Humboldt Bay
Cape Mendocino
Shelter Cove
Ft. Bragg
Point Arena

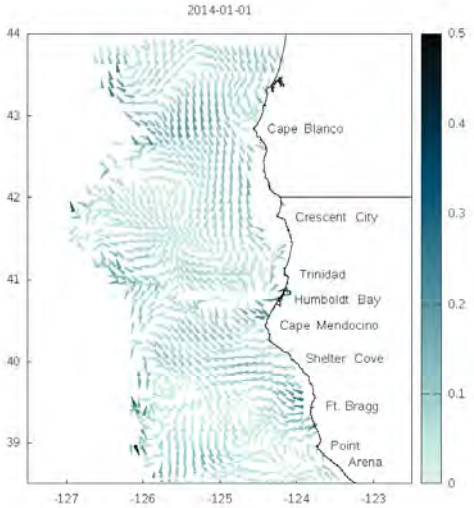
2014-01-01
Cape Blanco
Crescent City
Trinidad
Humboldt Bay
Cape Mendocino
Shelter Cove
Ft. Bragg
Point Arena

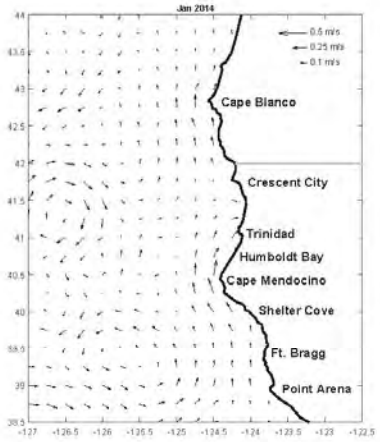
Jan 2014
0.5 m/s
0.25 m/s
0.1 m/s
Cape Blanco
Crescent City
Trinidad
Humboldt Bay
Cape Mendocino
Shelter Cove
Ft. Bragg
Point Arena

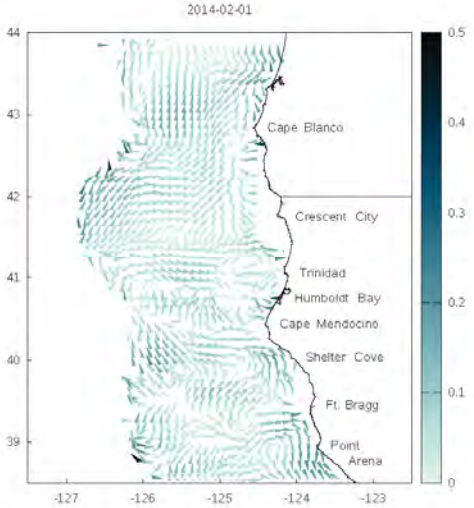
2014-02-01
Cape Blanco
Crescent City
Trinidad
Humboldt Bay
Cape Mendocino
Shelter Cove
Ft. Bragg
Point Arena

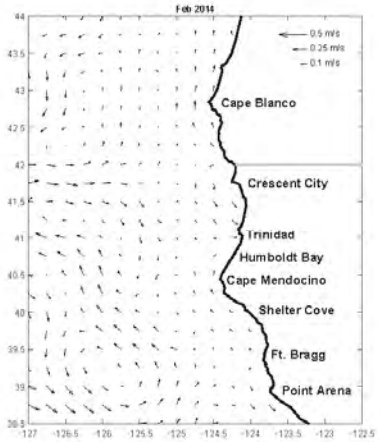
Feb 2014
0.5 m/s
0.25 m/s
0.1 m/s
Cape Blanco
Crescent City
Trinidad
Humboldt Bay
Cape Mendocino
Shelter Cove
Ft. Bragg
Point Arena

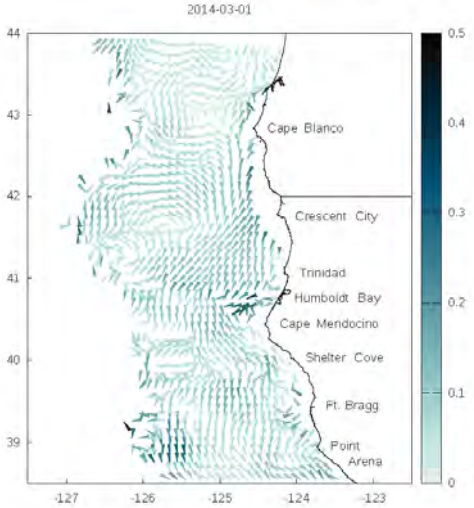
2014-03-01
Cape Blanco
Crescent City
Trinidad
Humboldt Bay
Cape Mendocino
Shelter Cove
Ft. Bragg
Point Arena

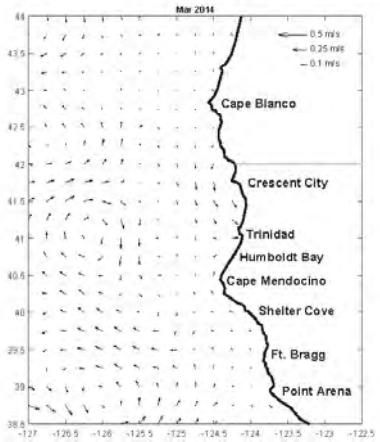
Mar 2014
0.5 m/s
0.25 m/s
0.1 m/s
Cape Blanco
Crescent City
Trinidad
Humboldt Bay
Cape Mendocino
Shelter Cove
Ft. Bragg
Point Arena

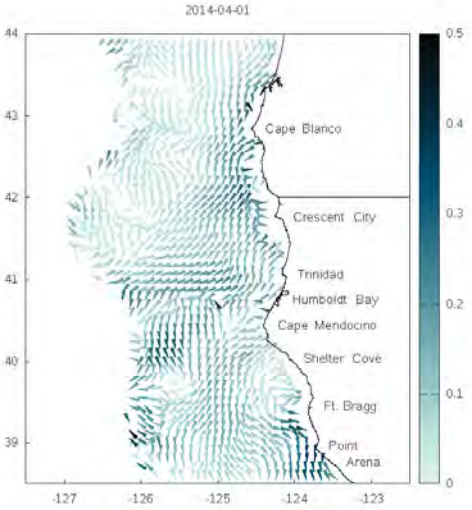
2014-04-01
Cape Blanco
Crescent City
Trinidad
Humboldt Bay
Cape Mendocino
Shelter Cove
Ft. Bragg
Point Arena

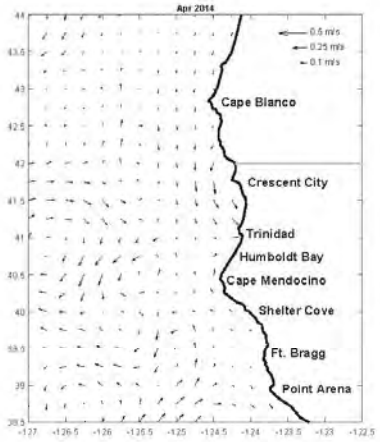
Apr 2014
0.5 m/s
0.25 m/s
0.1 m/s
Cape Blanco
Crescent City
Trinidad
Humboldt Bay
Cape Mendocino
Shelter Cove
Ft. Bragg
Point Arena

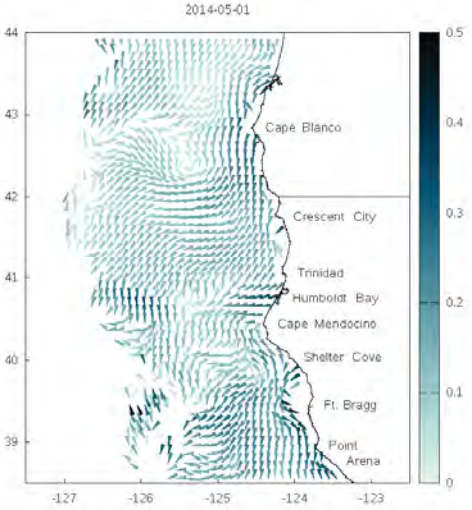
2014-05-01
Cape Blanco
Crescent City
Trinidad
Humboldt Bay
Cape Mendocino
Shelter Cove
Ft. Bragg
Point Arena

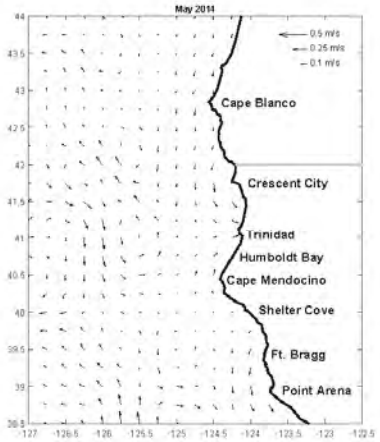
May 2014
0.5 m/s
0.25 m/s
0.1 m/s
Cape Blanco
Crescent City
Trinidad
Humboldt Bay
Cape Mendocino
Shelter Cove
Ft. Bragg
Point Arena

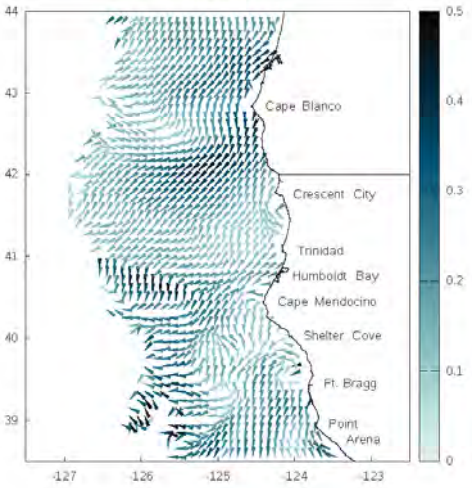
2014-06-01
Cape Blanco
Crescent City
Trinidad
Humboldt Bay
Cape Mendocino
Shelter Cove
Ft. Bragg
Point Arena

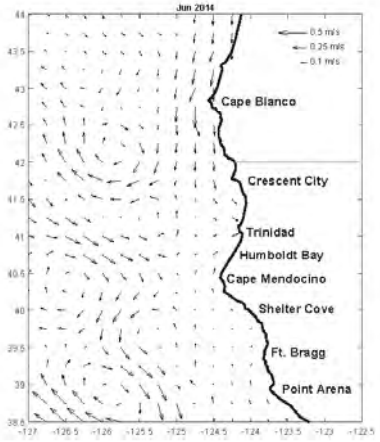
Jun 2014
0.5 m/s
0.25 m/s
0.1 m/s
Cape Blanco
Crescent City
Trinidad
Humboldt Bay
Cape Mendocino
Shelter Cove
Ft. Bragg
Point Arena

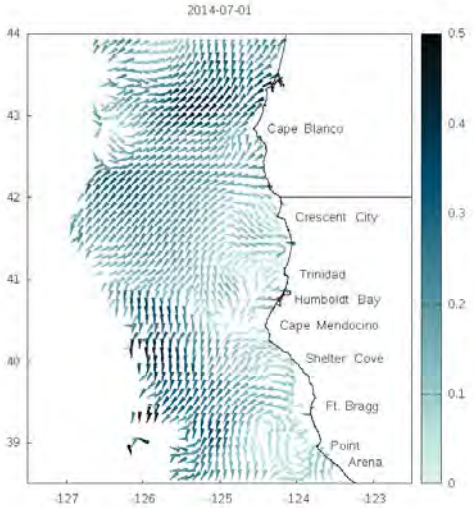
2014-07-01
Cape Blanco
Crescent City
Trinidad
Humboldt Bay
Cape Mendocino
Shelter Cove
Ft. Bragg
Point Arena

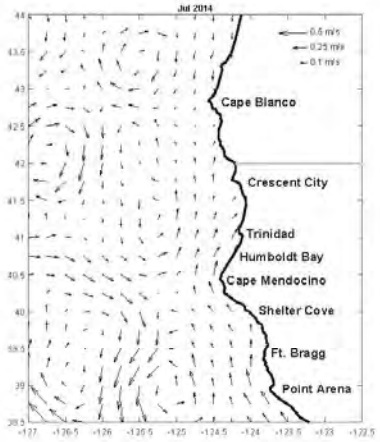
Jul 2014
0.5 m/s
0.25 m/s
0.1 m/s
Cape Blanco
Crescent City
Trinidad
Humboldt Bay
Cape Mendocino
Shelter Cove
Ft. Bragg
Point Arena

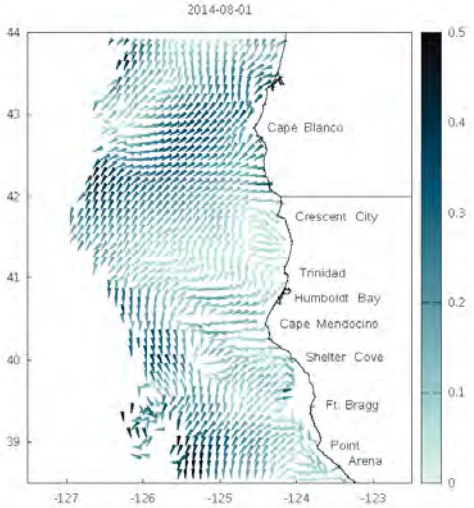
2014-08-01
Cape Blanco
Crescent City
Trinidad
Humboldt Bay
Cape Mendocino
Shelter Cove
Ft. Bragg
Point Arena

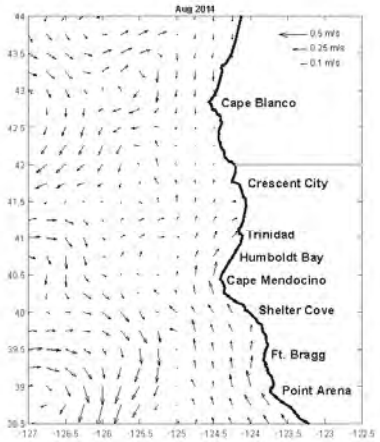
Aug 2014
0.5 m/s
0.25 m/s
0.1 m/s
Cape Blanco
Crescent City
Trinidad
Humboldt Bay
Cape Mendocino
Shelter Cove
Ft. Bragg
Point Arena

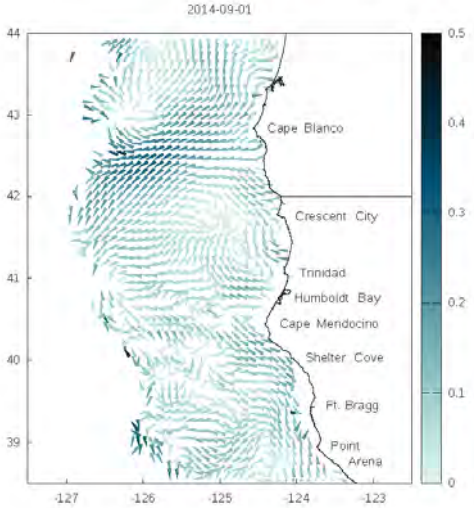
2014-09-01
Cape Blanco
Crescent City
Trinidad
Humboldt Bay
Cape Mendocino
Shelter Cove
Ft. Bragg
Point Arena

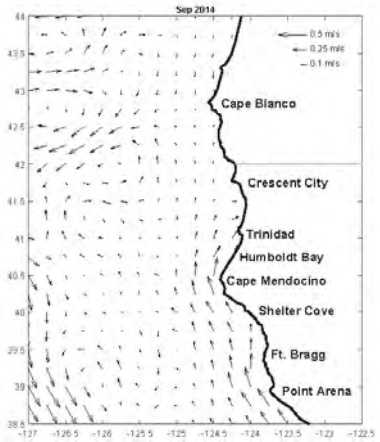
Sep 2014
0.5 m/s
0.25 m/s
0.1 m/s
Cape Blanco
Crescent City
Trinidad
Humboldt Bay
Cape Mendocino
Shelter Cove
Ft. Bragg
Point Arena

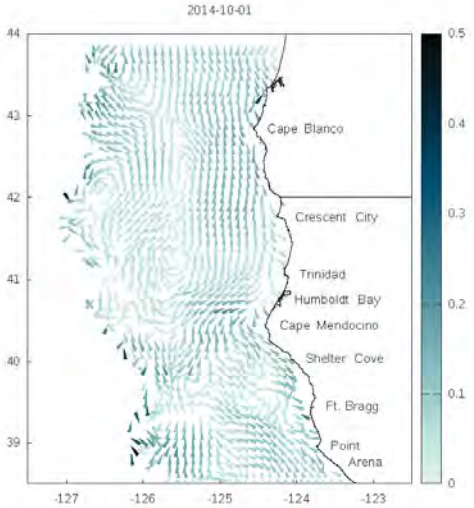
2014-10-01
Cape Blanco
Crescent City
Trinidad
Humboldt Bay
Cape Mendocino
Shelter Cove
Ft. Bragg
Point Arena

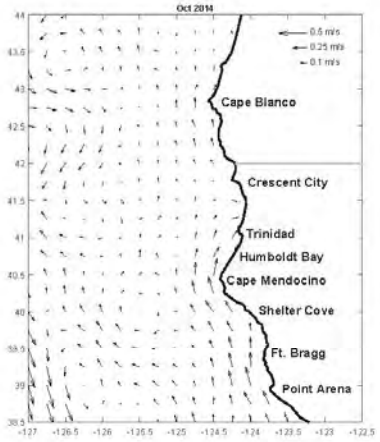
Oct 2014
0.5 m/s
0.25 m/s
0.1 m/s
Cape Blanco
Crescent City
Trinidad
Humboldt Bay
Cape Mendocino
Shelter Cove
Ft. Bragg
Point Arena

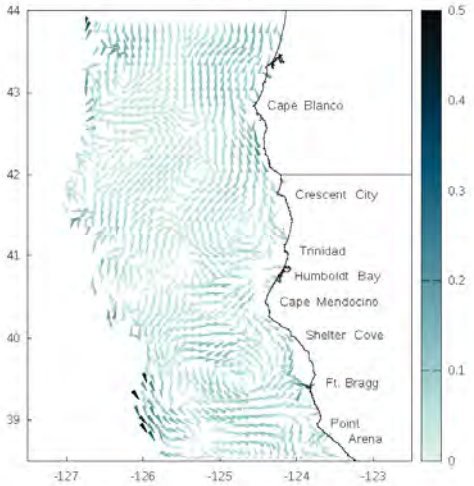
2014-11-01
Cape Blanco
Crescent City
Trinidad
Humboldt Bay
Cape Mendocino
Shelter Cove
Ft. Bragg
Point Arena

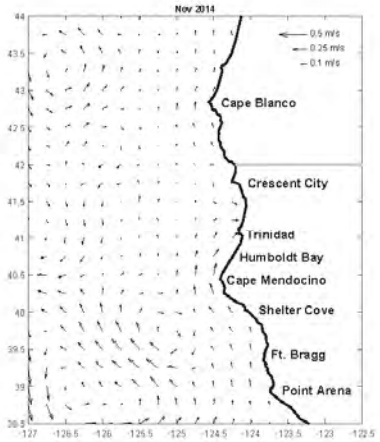
Nov 2014
0.5 m/s
0.25 m/s
0.1 m/s
Cape Blanco
Crescent City
Trinidad
Humboldt Bay
Cape Mendocino
Shelter Cove
Ft. Bragg
Point Arena

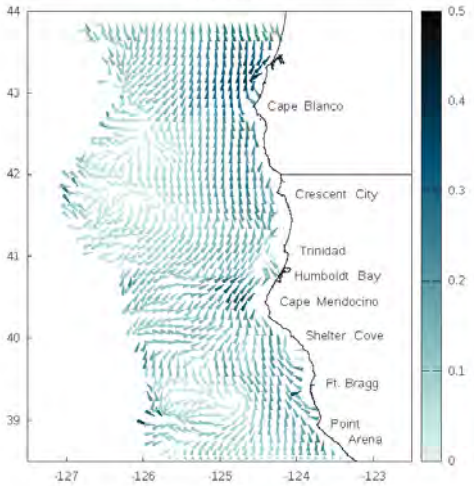
2014-12-01
Cape Blanco
Crescent City
Trinidad
Humboldt Bay
Cape Mendocino
Shelter Cove
Ft. Bragg
Point Arena

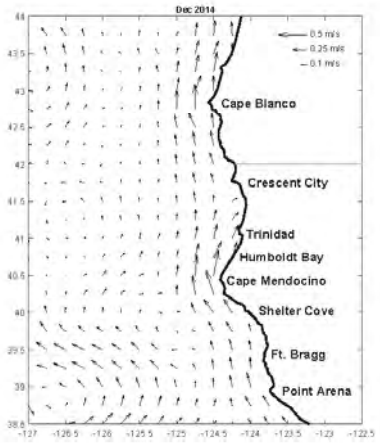
Dec 2014
0.5 m/s
0.25 m/s
0.1 m/s
Cape Blanco
Crescent City
Trinidad
Humboldt Bay
Cape Mendocino
Shelter Cove
Ft. Bragg
Point Arena

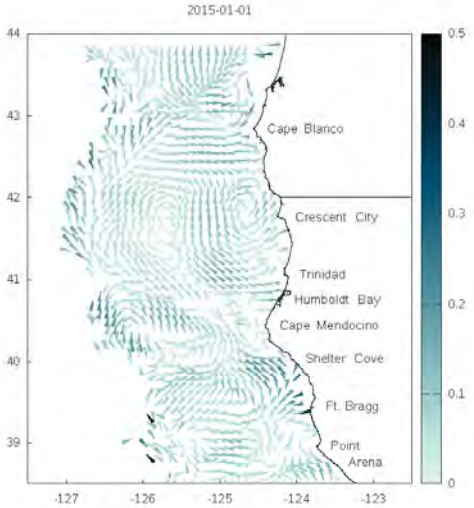
2015-01-01
Cape Blanco
Crescent City
Trinidad
Humboldt Bay
Cape Mendocino
Shelter Cove
Ft. Bragg
Point Arena

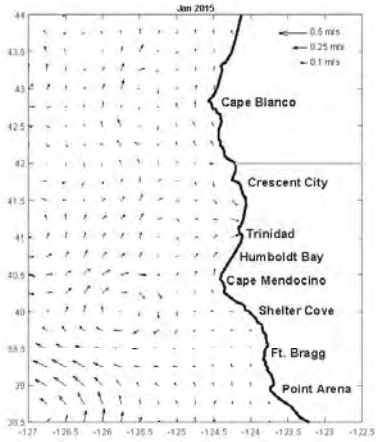
Jan 2015
0.5 m/s
0.25 m/s
0.1 m/s
Cape Blanco
Crescent City
Trinidad
Humboldt Bay
Cape Mendocino
Shelter Cove
Ft. Bragg
Point Arena

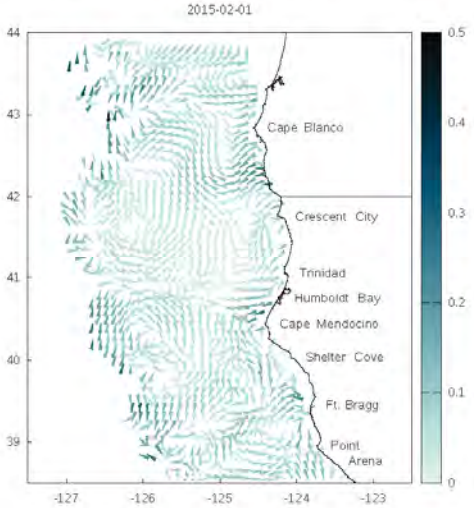
2015-02-01
Cape Blanco
Crescent City
Trinidad
Humboldt Bay
Cape Mendocino
Shelter Cove
Ft. Bragg
Point Arena

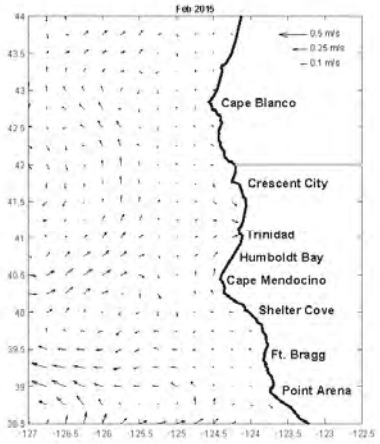
Feb 2015
0.5 m/s
0.25 m/s
0.1 m/s
Cape Blanco
Crescent City
Trinidad
Humboldt Bay
Cape Mendocino
Shelter Cove
Ft. Bragg
Point Arena

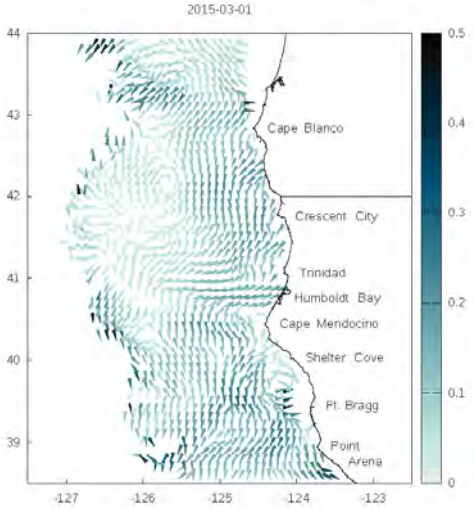
2015-03-01
Cape Blanco
Crescent City
Trinidad
Humboldt Bay
Cape Mendocino
Shelter Cove
Ft. Bragg
Point Arena

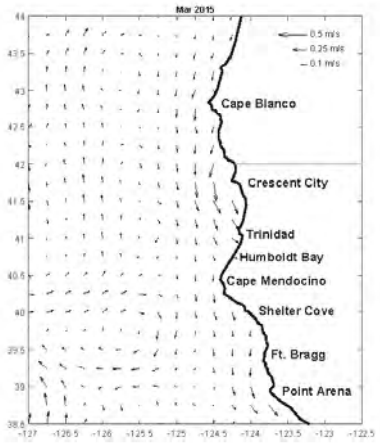
Mar 2015
0.5 m/s
0.25 m/s
0.1 m/s
Cape Blanco
Crescent City
Trinidad
Humboldt Bay
Cape Mendocino
Shelter Cove
Ft. Bragg
Point Arena

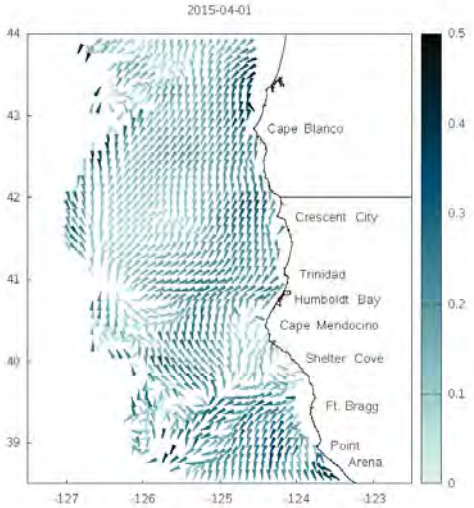
2015-04-01
Cape Blanco
Crescent City
Trinidad
Humboldt Bay
Cape Mendocino
Shelter Cove
Ft. Bragg
Point Arena

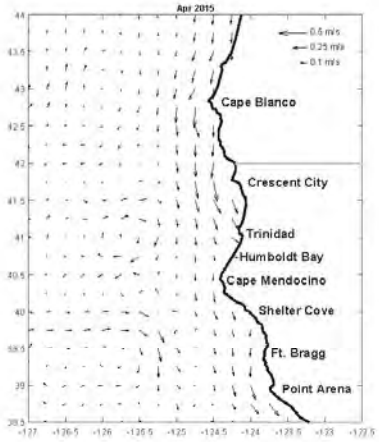
Apr 2015
0.5 m/s
0.25 m/s
0.1 m/s
Cape Blanco
Crescent City
Trinidad
Humboldt Bay
Cape Mendocino
Shelter Cove
Ft. Bragg
Point Arena

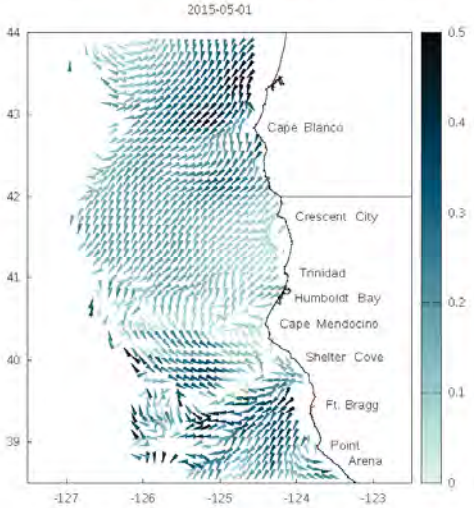
2015-05-01
Cape Blanco
Crescent City
Trinidad
Humboldt Bay
Cape Mendocino
Shelter Cove
Ft. Bragg
Point Arena

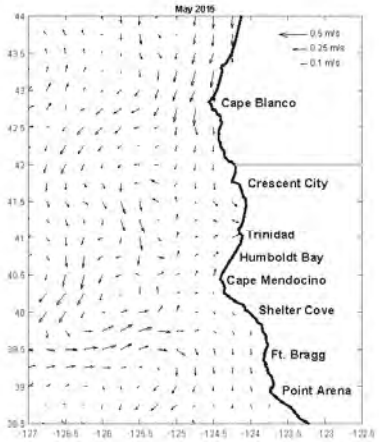
May 2015
0.5 m/s
0.25 m/s
0.1 m/s
Cape Blanco
Crescent City
Trinidad
Humboldt Bay
Cape Mendocino
Shelter Cove
Ft. Bragg
Point Arena

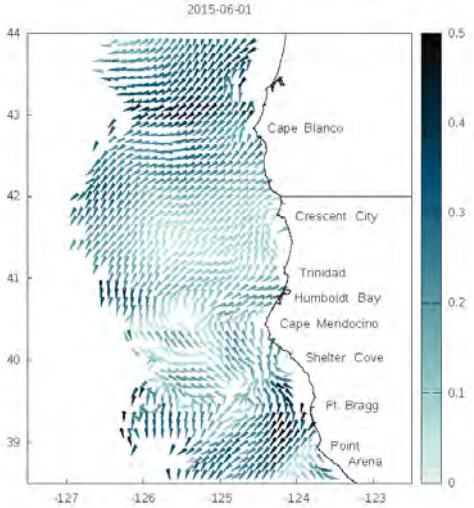
2015-06-01
Cape Blanco
Crescent City
Trinidad
Humboldt Bay
Cape Mendocino
Shelter Cove
Ft. Bragg
Point Arena

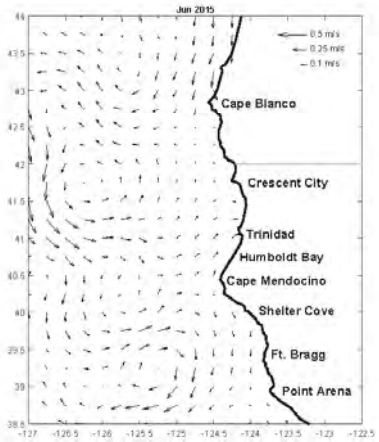
Jun 2015
0.5 m/s
0.25 m/s
0.1 m/s
Cape Blanco
Crescent City
Trinidad
Humboldt Bay
Cape Mendocino
Shelter Cove
Ft. Bragg
Point Arena

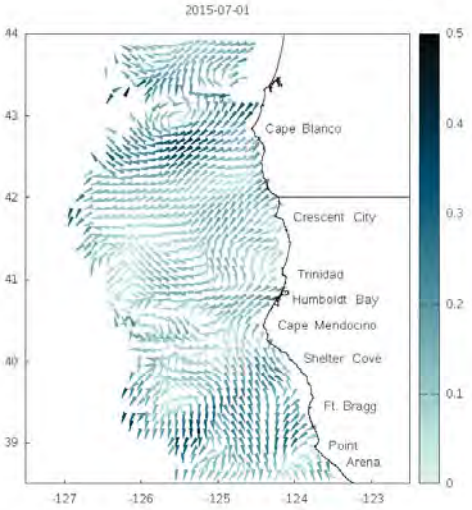
2015-07-01
Cape Blanco
Crescent City
Trinidad
Humboldt Bay
Cape Mendocino
Shelter Cove
Ft. Bragg
Point Arena

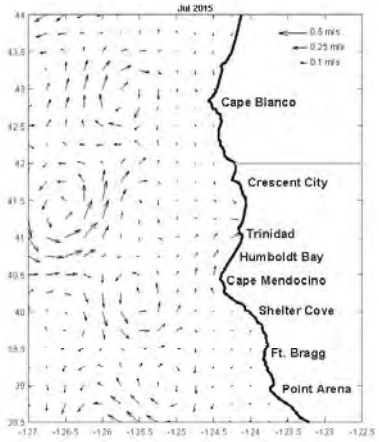
Jul 2015
0.5 m/s
0.25 m/s
0.1 m/s
Cape Blanco
Crescent City
Trinidad
Humboldt Bay
Cape Mendocino
Shelter Cove
Ft. Bragg
Point Arena

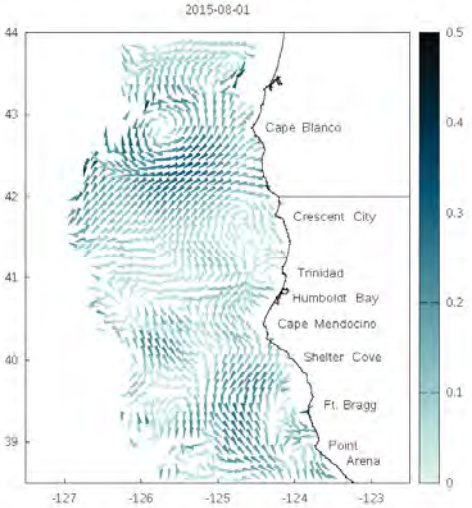
2015-08-01
Cape Blanco
Crescent City
Trinidad
Humboldt Bay
Cape Mendocino
Shelter Cove
Ft. Bragg
Point Arena

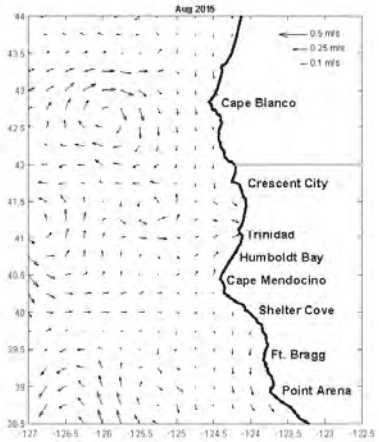
Aug 2015
0.5 m/s
0.25 m/s
0.1 m/s
Cape Blanco
Crescent City
Trinidad
Humboldt Bay
Cape Mendocino
Shelter Cove
Ft. Bragg
Point Arena

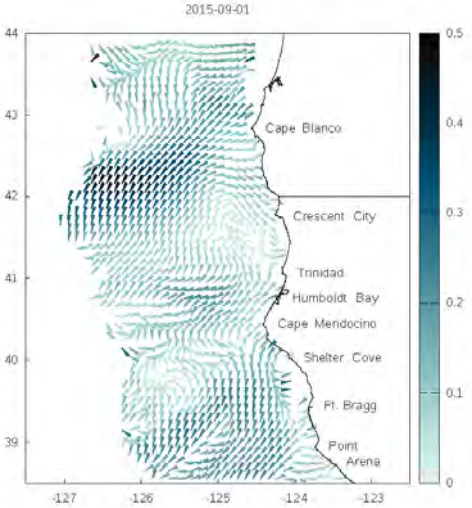
2015-09-01
Cape Blanco
Crescent City
Trinidad
Humboldt Bay
Cape Mendocino
Shelter Cove
Ft. Bragg
Point Arena

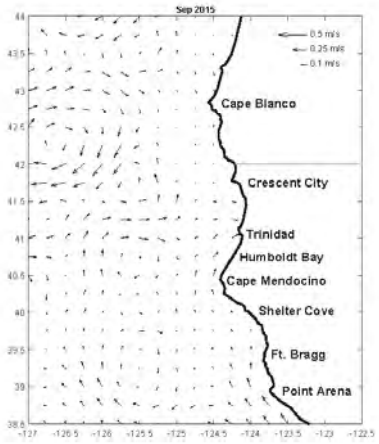
Sep 2015
0.5 m/s
0.25 m/s
0.1 m/s
Cape Blanco
Crescent City
Trinidad
Humboldt Bay
Cape Mendocino
Shelter Cove
Ft. Bragg
Point Arena

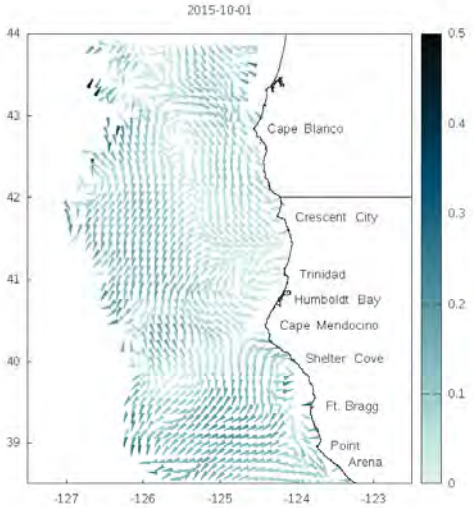
2015-10-01
Cape Blanco
Crescent City
Trinidad
Humboldt Bay
Cape Mendocino
Shelter Cove
Ft. Bragg
Point Arena

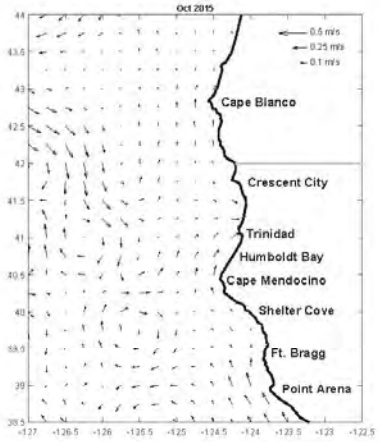
Oct 2015
0.5 m/s
0.25 m/s
0.1 m/s
Cape Blanco
Crescent City
Trinidad
Humboldt Bay
Cape Mendocino
Shelter Cove
Ft. Bragg
Point Arena

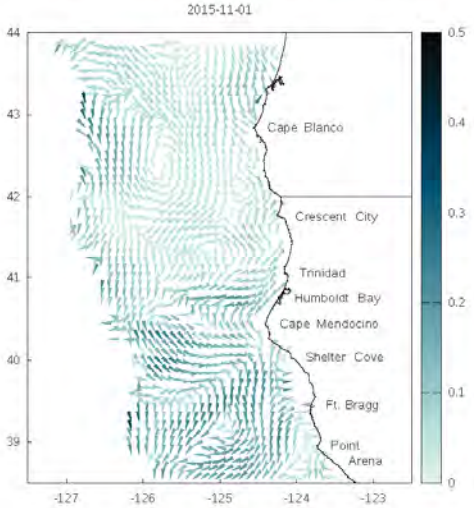
2015-11-01
Cape Blanco
Crescent City
Trinidad
Humboldt Bay
Cape Mendocino
Shelter Cove
Ft. Bragg
Point Arena

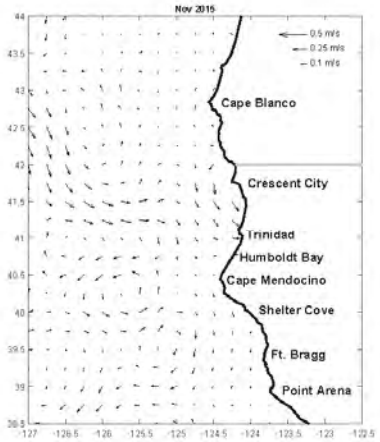
Nov 2015
0.5 m/s
0.25 m/s
0.1 m/s
Cape Blanco
Crescent City
Trinidad
Humboldt Bay
Cape Mendocino
Shelter Cove
Ft. Bragg
Point Arena

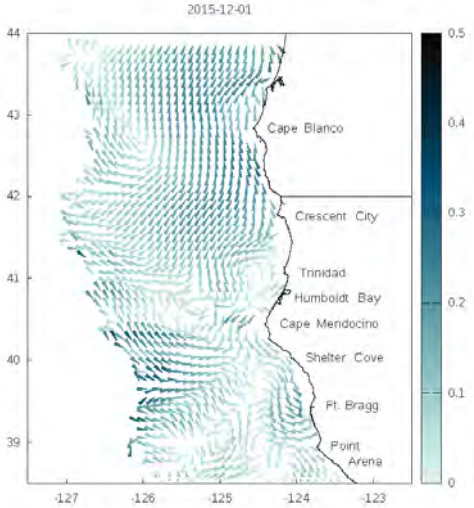
2015-12-01
Cape Blanco
Crescent City
Trinidad
Humboldt Bay
Cape Mendocino
Shelter Cove
Ft. Bragg
Point Arena

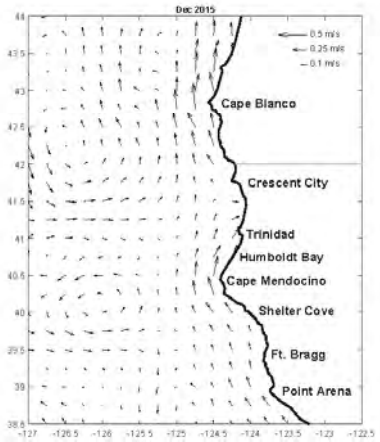
Dec 2015
0.5 m/s
0.25 m/s
0.1 m/s
Cape Blanco
Crescent City
Trinidad
Humboldt Bay
Cape Mendocino
Shelter Cove
Ft. Bragg
Point Arena

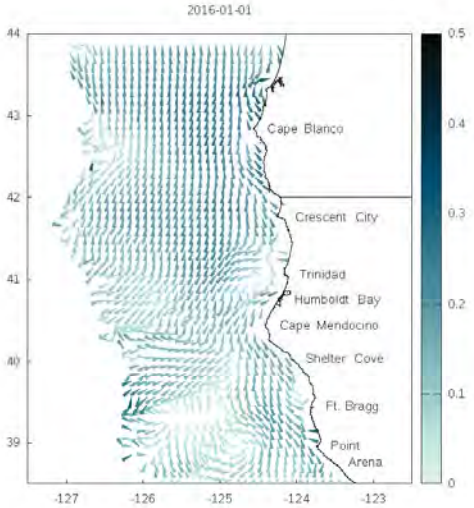
2016-01-01
Cape Blanco
Crescent City
Trinidad
Humboldt Bay
Cape Mendocino
Shelter Cove
Ft. Bragg
Point Arena

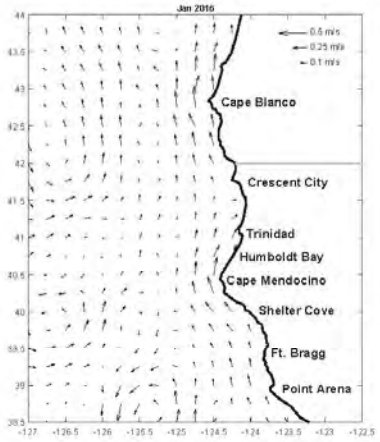
Jan 2016
0.5 m/s
0.25 m/s
0.1 m/s
Cape Blanco
Crescent City
Trinidad
Humboldt Bay
Cape Mendocino
Shelter Cove
Ft. Bragg
Point Arena

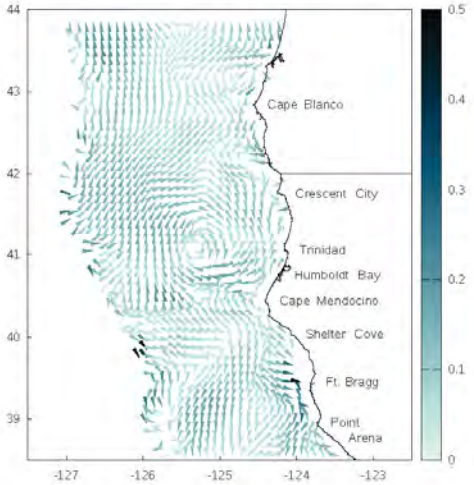
2016-02-01
Cape Blanco
Crescent City
Trinidad
Humboldt Bay
Cape Mendocino
Shelter Cove
Ft. Bragg
Point Arena

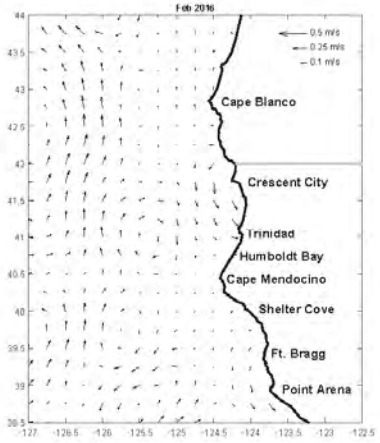
Feb 2016
0.5 m/s
0.25 m/s
0.1 m/s
Cape Blanco
Crescent City
Trinidad
Humboldt Bay
Cape Mendocino
Shelter Cove
Ft. Bragg
Point Arena

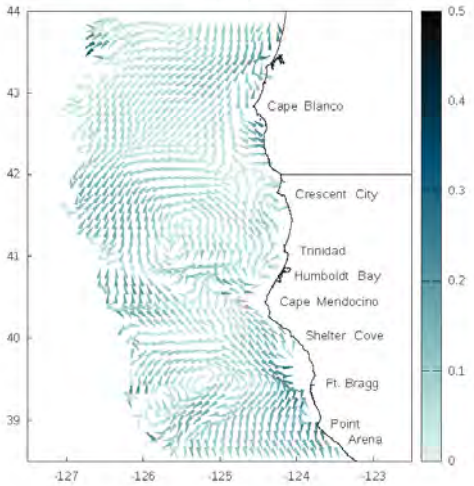
2016-03-01
Cape Blanco
Crescent City
Trinidad
Humboldt Bay
Cape Mendocino
Shelter Cove
Ft. Bragg
Point Arena

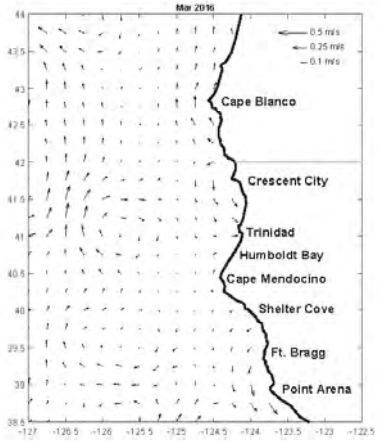
Mar 2016
0.5 m/s
0.25 m/s
0.1 m/s
Cape Blanco
Crescent City
Trinidad
Humboldt Bay
Cape Mendocino
Shelter Cove
Ft. Bragg
Point Arena

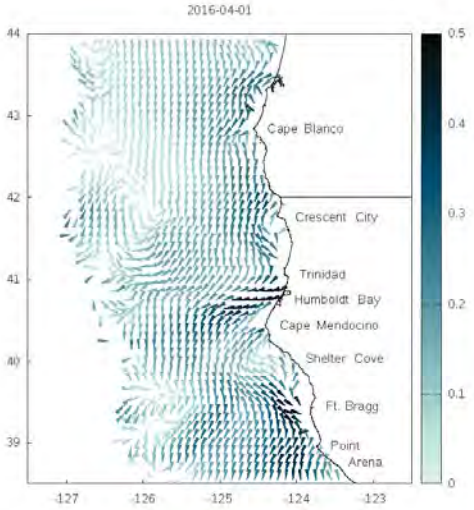
2016-04-01
Cape Blanco
Crescent City
Trinidad
Humboldt Bay
Cape Mendocino
Shelter Cove
Ft. Bragg
Point Arena

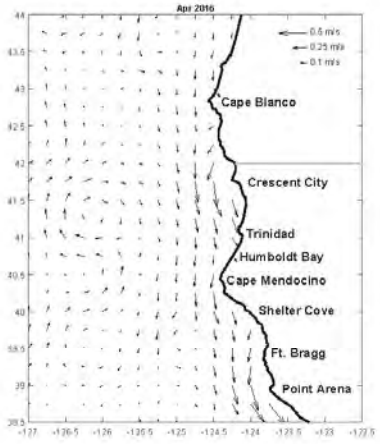
Apr 2016
0.5 m/s
0.25 m/s
0.1 m/s
Cape Blanco
Crescent City
Trinidad
Humboldt Bay
Cape Mendocino
Shelter Cove
Ft. Bragg
Point Arena

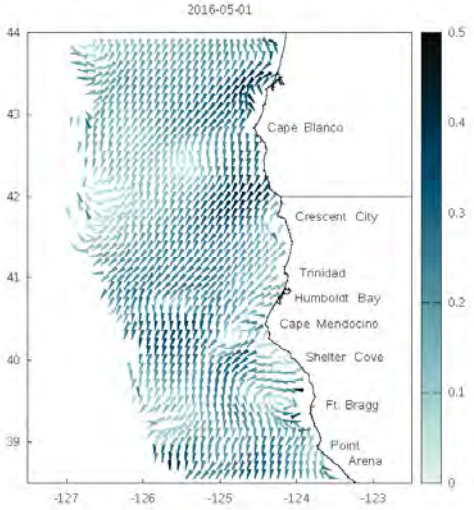
2016-05-01
Cape Blanco
Crescent City
Trinidad
Humboldt Bay
Cape Mendocino
Shelter Cove
Ft. Bragg
Point Arena

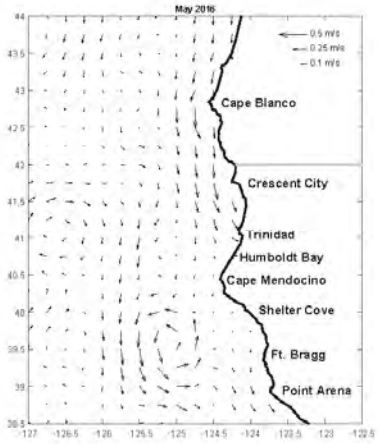
May 2016
0.5 m/s
0.25 m/s
0.1 m/s
Cape Blanco
Crescent City
Trinidad
Humboldt Bay
Cape Mendocino
Shelter Cove
Ft. Bragg
Point Arena

Appendix SO: Satellite observations of coastal SST and chlorophyll a for the NCSR

The following sets of plots are based on data collected by the MODIS-Aqua sensor, and include sea-surface temperature, indices of spatial structure in the coastal ocean (gradient in SST and an SST-based frontal index), and chlorophyll-a concentrations; see main text for definitions and data processing.

Two sets of figures are presented. The first are a series of Hovmoller (time by space) diagrams (and related plots) that summarize mean monthly conditions in a cross-shelf band (from 0.0125°-0.125° offshore) by latitude. The first of these present a climatological average taken over all years in the record leading up to the Baseline Study Period (BSP, 2003-2013), followed by paired plots for each year of the BSP showing observed monthly means (top panels) and anomalies from the climatology (bottom panels). The second set of figures shows mean cross-shelf structure from which the Hovmoller plots are extracted, as a means of showing greater spatial detail and context.

These maps and figures are intended to provide broad context in terms of conditions leading up to and during observations made during ecological surveys, and as a resource for formulating more specific queries of the underlying data sets as part of analyses designed to explore connections between oceanographic and ecological data. Several of these plots are best viewed on-screen under some magnification.

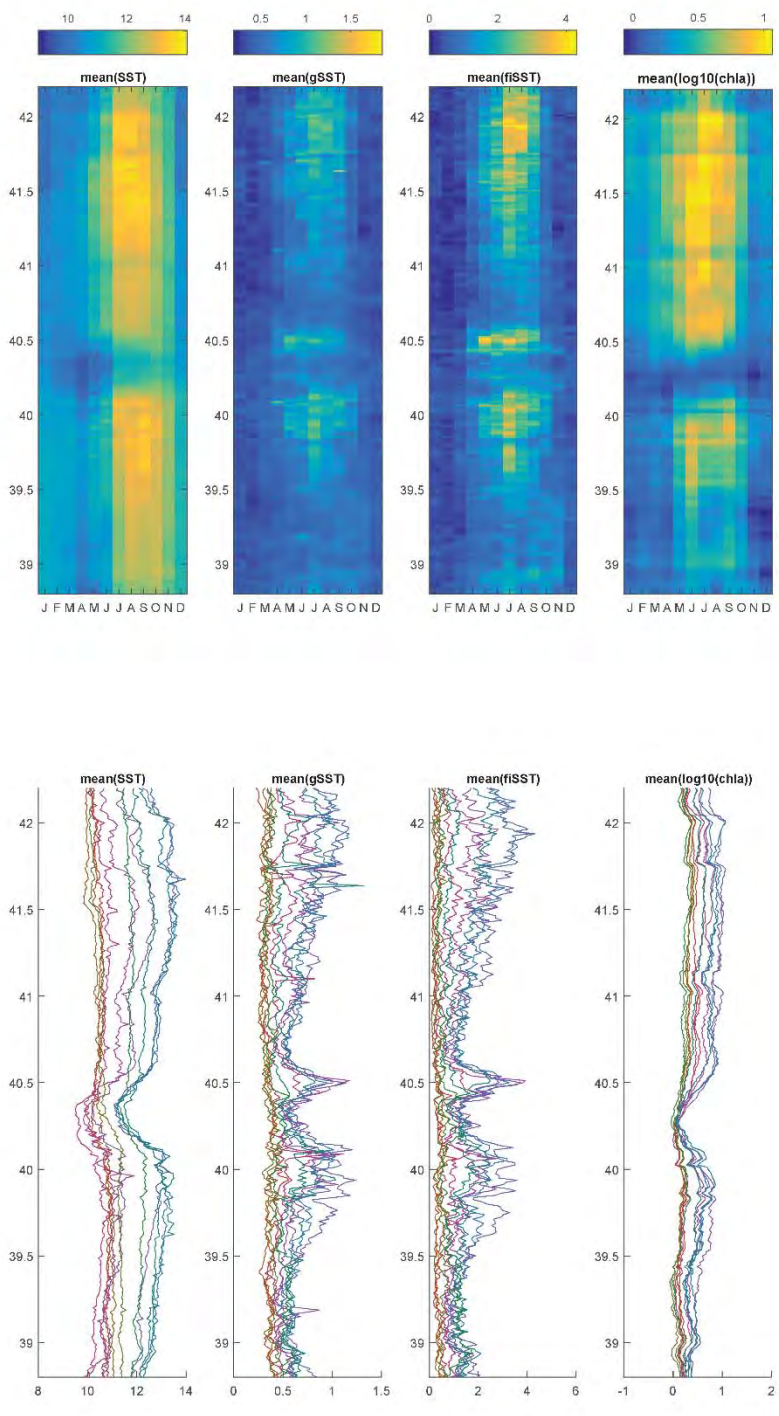

Figure A-SO-1: Two views of variability in monthly mean coastal oceanography averaged by latitude across a cross-shelf band extending 0.0125-0.125° from the coast based on MODIS-Aqua observations over the course of the annual cycle. Upper panel: Hovmöller diagram (latitude by month) of SST, gradient in SST, front index , and log-scaled chlorophyll a concentration. Lower panel: same data as in upper panel, with seasonal progression indicated by browns (winter) via purples (spring) to blues (summer) and back through greens (fall).

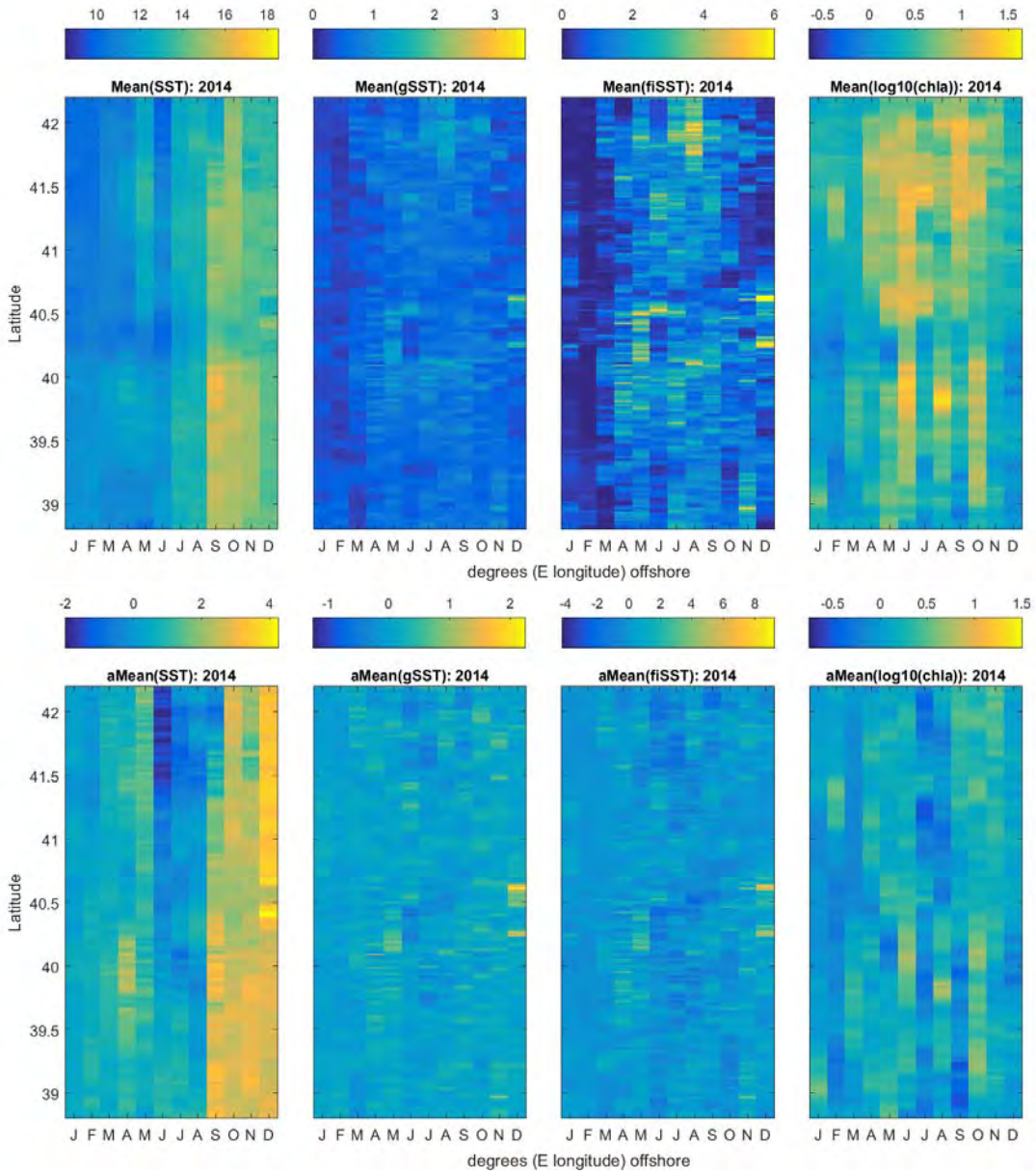

Figure A-SO-2. Top panel: Hovmöller (latitude by month) diagram of monthly mean SST, gradient in SST, SST Front Index and $\log_{10}$ chl (mg/m^3) averaged by latitude across a cross-shelf band extending 0.0125-0.125° from the coast based on MODIS-Aqua observations over the course of the annual cycle for 2014. Bottom panel: Hovmöller (latitude by month) diagram of the anomaly in monthly mean SST, gradient in SST, SST Front Index and $\log_{10}$ chl a (mg/m^3) averaged by latitude across a cross-shelf band extending 0.0125-0.125° from the coast based on MODIS-Aqua observations over the course of the annual cycle for 2014 relative to the 2003-2013 climatological mean.

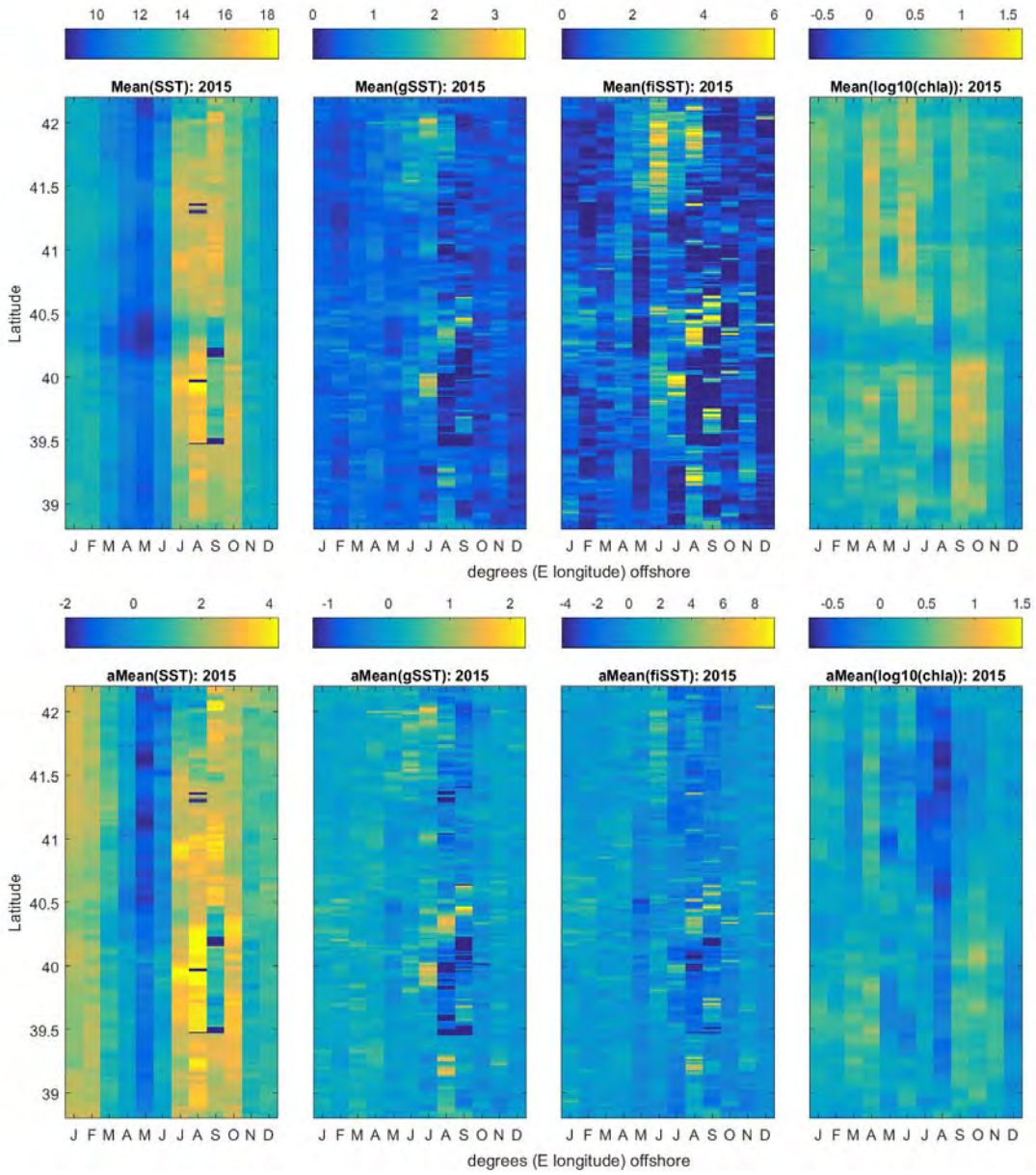

Figure A-SO-3. As for Figure A-SO-2, for 2015.

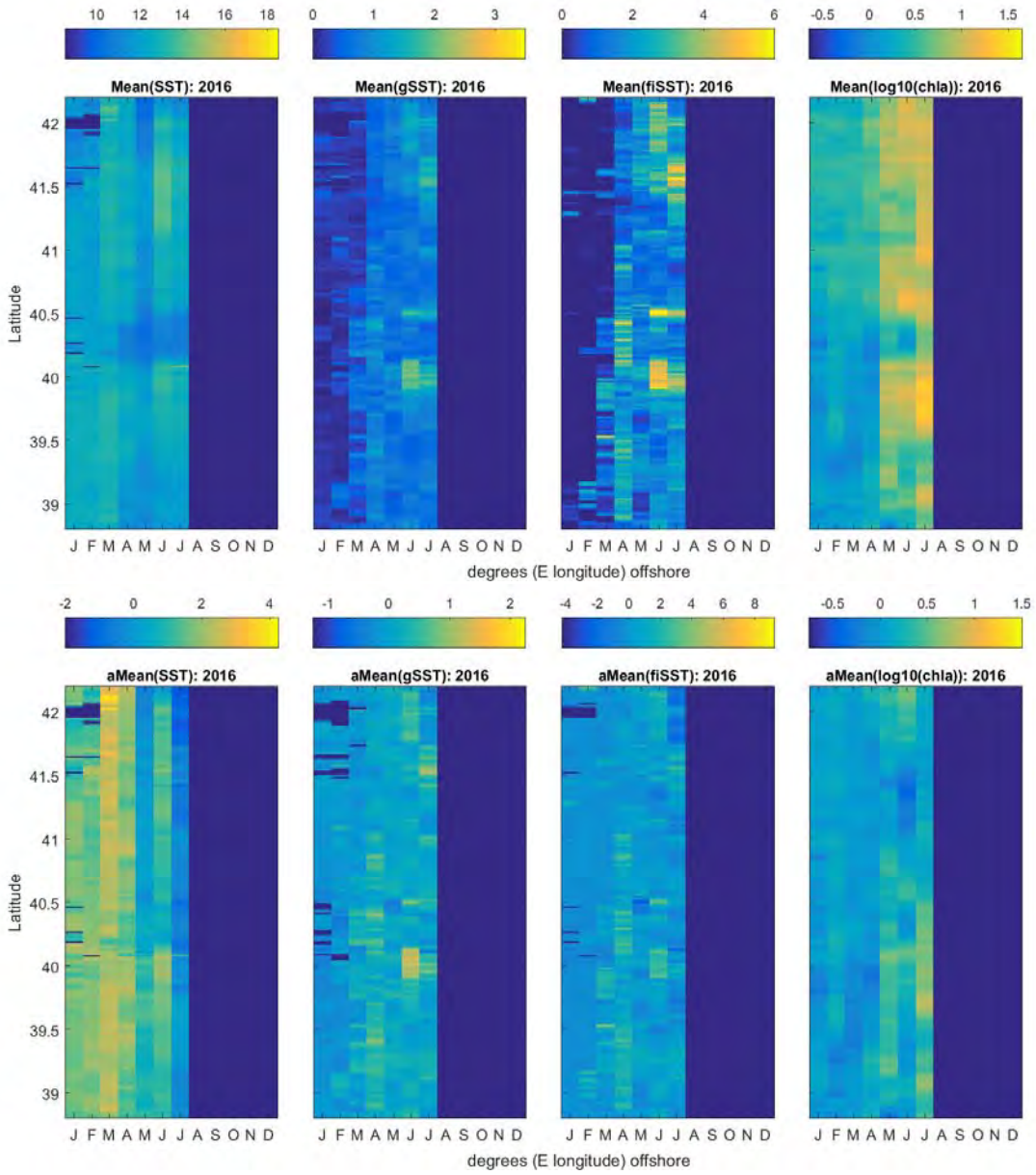

Figure A-SO-4. As for Figure A-SO-2, for 2016.

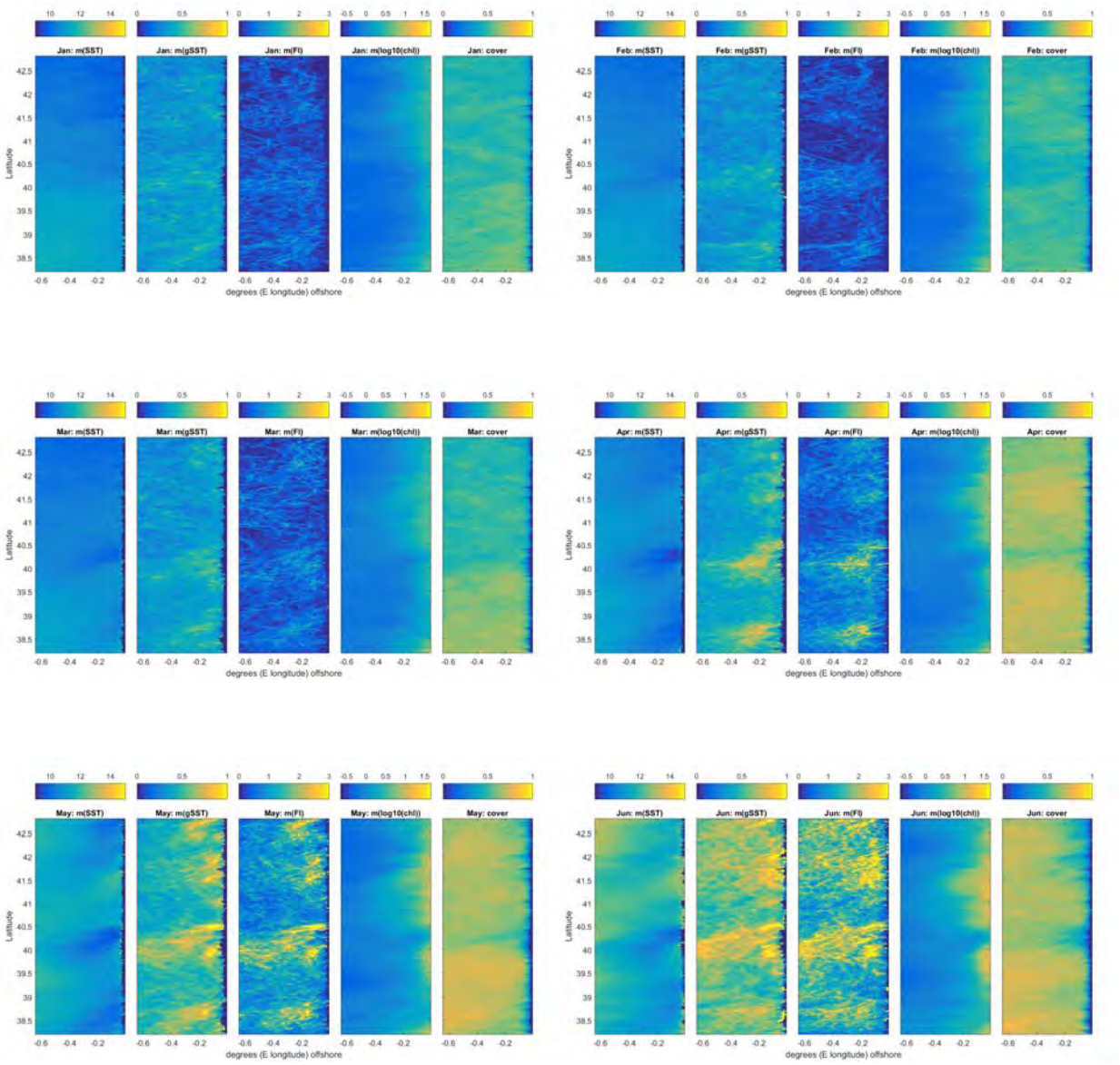

Figure A-SO-5: Climatological mean alongshore and cross-shelf structure, by month, in coastal oceanographic conditions based on MODIS-Aqua observations for 2003-2013. For each month, plots show sea surface temperature (SST), gradient in SST (gSST), SST Front Index (FI), $\log_{10}$ chl a (mg/m^3) , and pixel coverage (%).

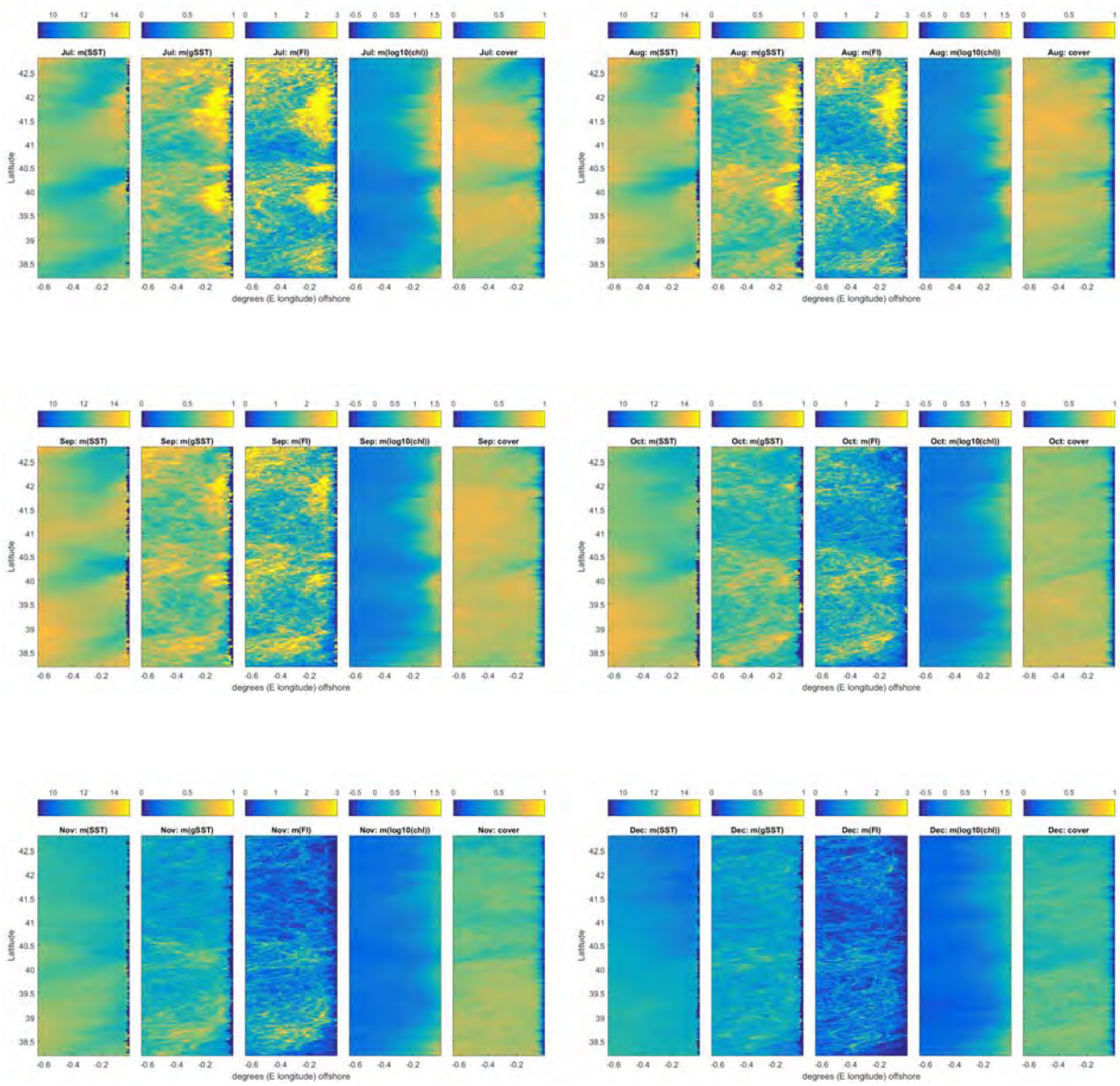

Figure A-SO-5 (continued).

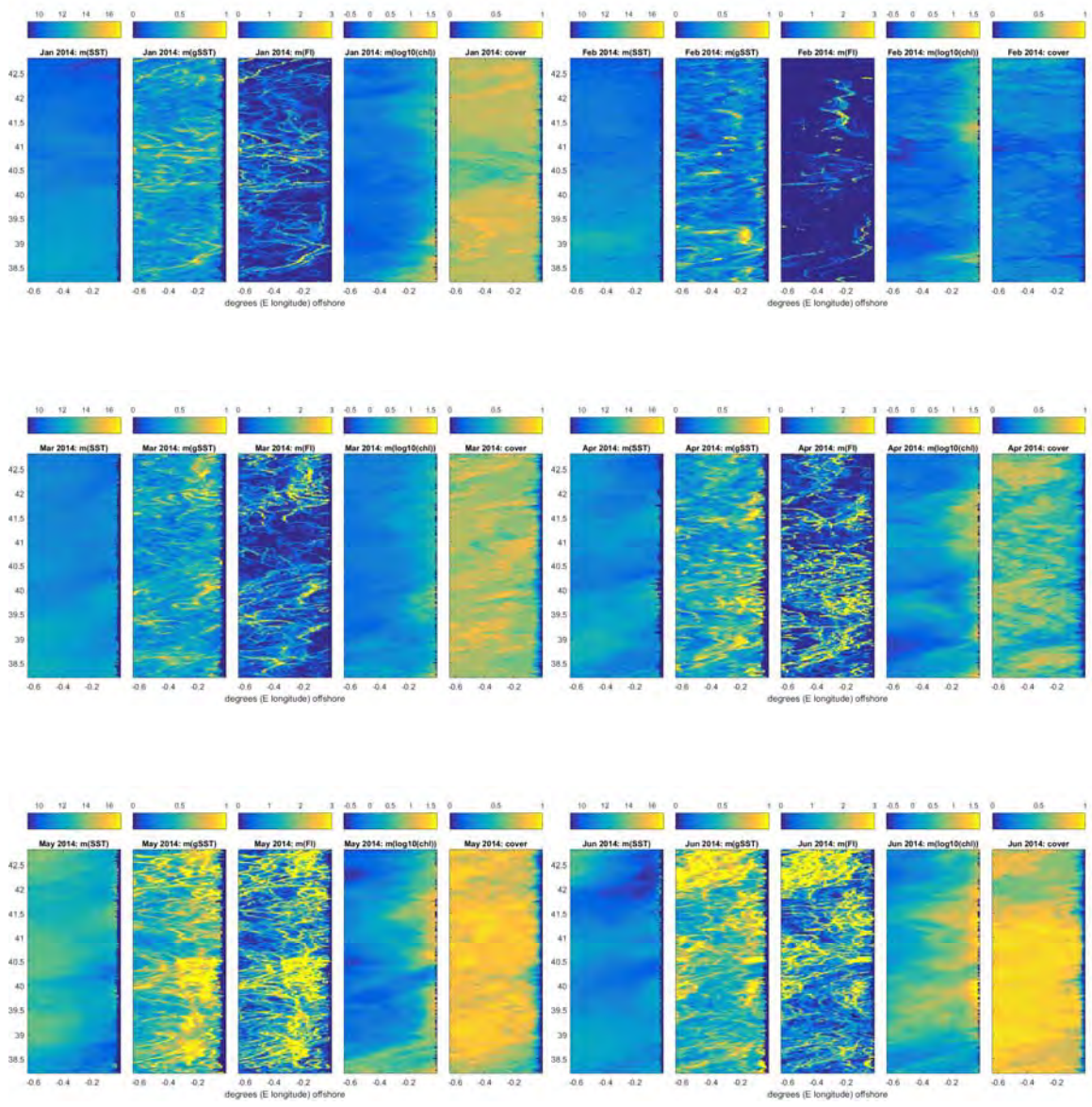

Figure A-SO-6: Monthly mean alongshore and cross-shelf structure, by month, in coastal oceanographic conditions based on MODIS-Aqua observations for 2014. For each month, plots show sea surface temperature (SST), gradient in SST (gSST), SST Front Index (FI), $\log_{10}$ chl a (mg/m^3), and pixel coverage (%).

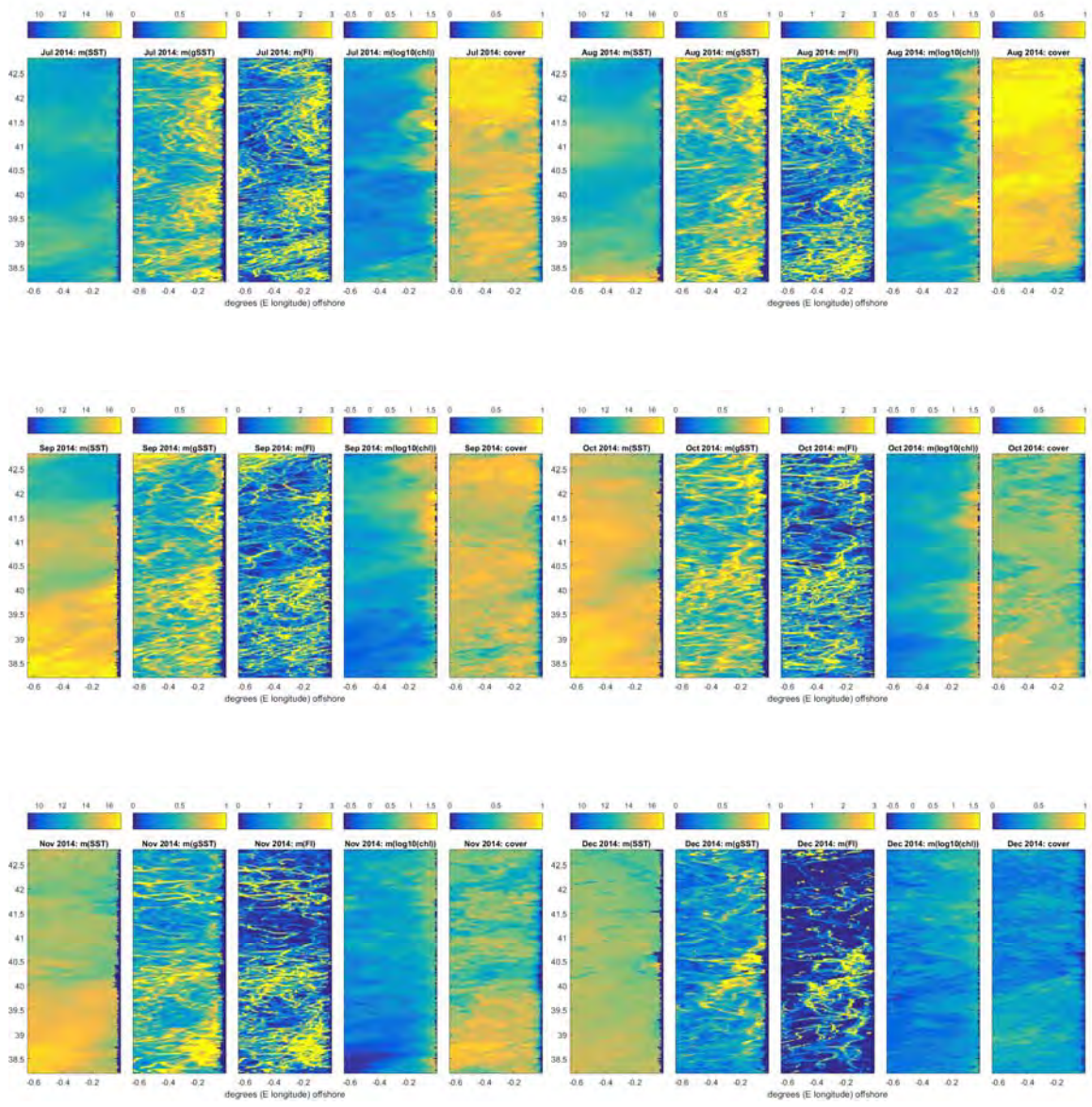

Figure A-SO-6: (continued).

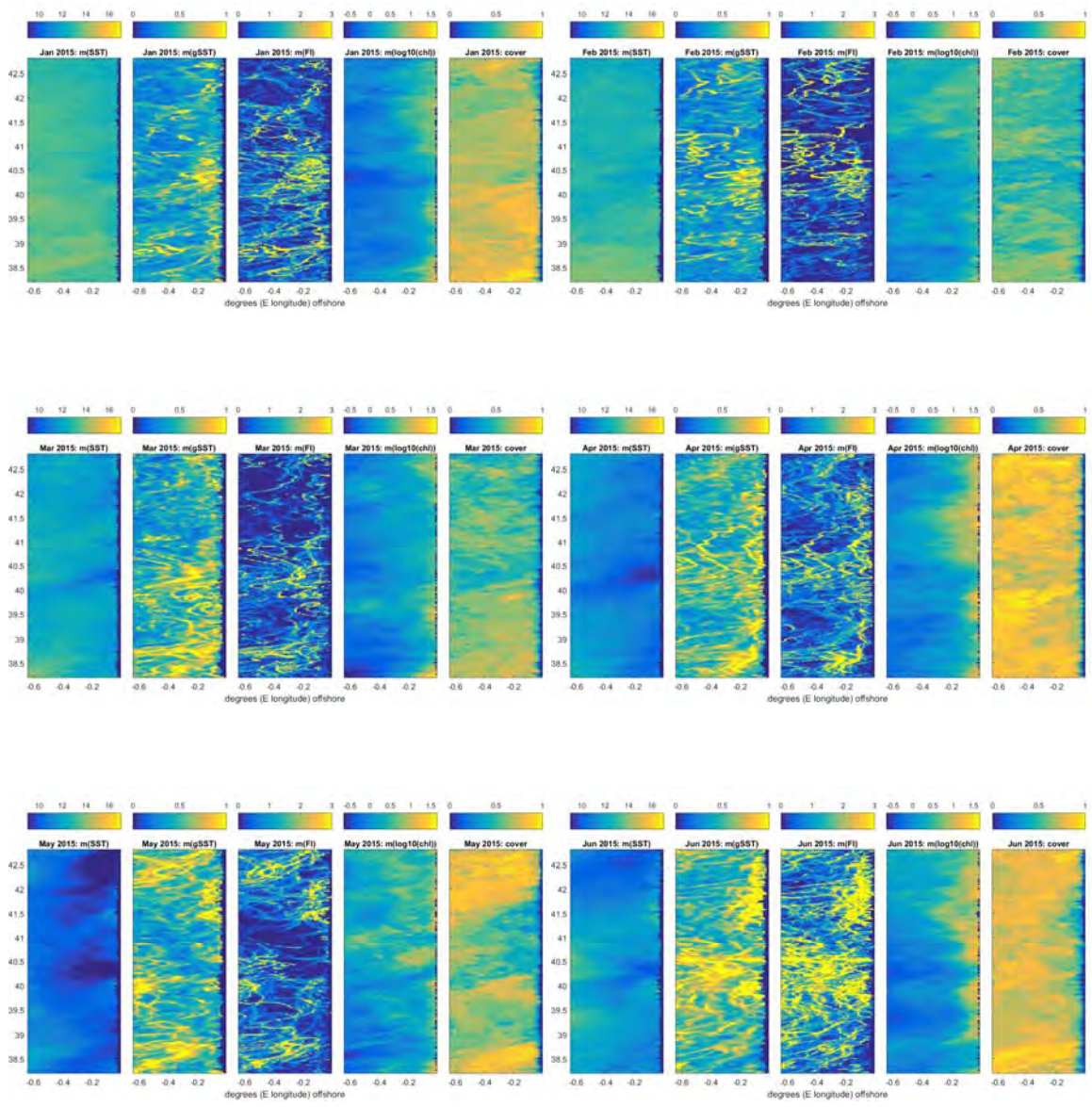

Figure A-SO-7: Monthly mean alongshore and cross-shelf structure, by month, in coastal oceanographic conditions based on MODIS-Aqua observations for 2015. For each month, plots show sea surface temperature (SST), gradient in SST (gSST), SST Front Index (FI), $\log_{10}$ chl a (mg/m^3), and pixel coverage (%).

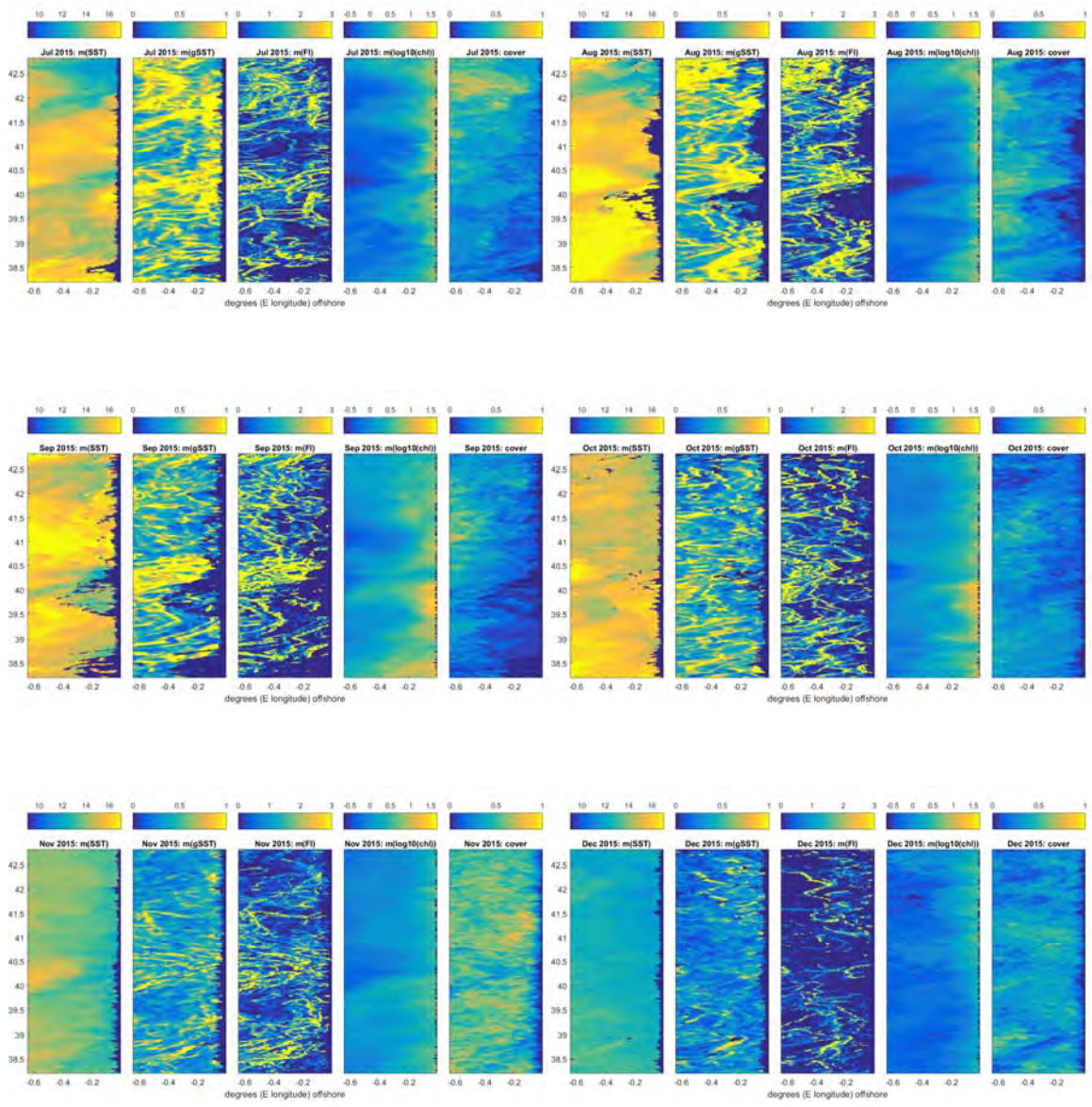

Figure A-SO-7: (continued).

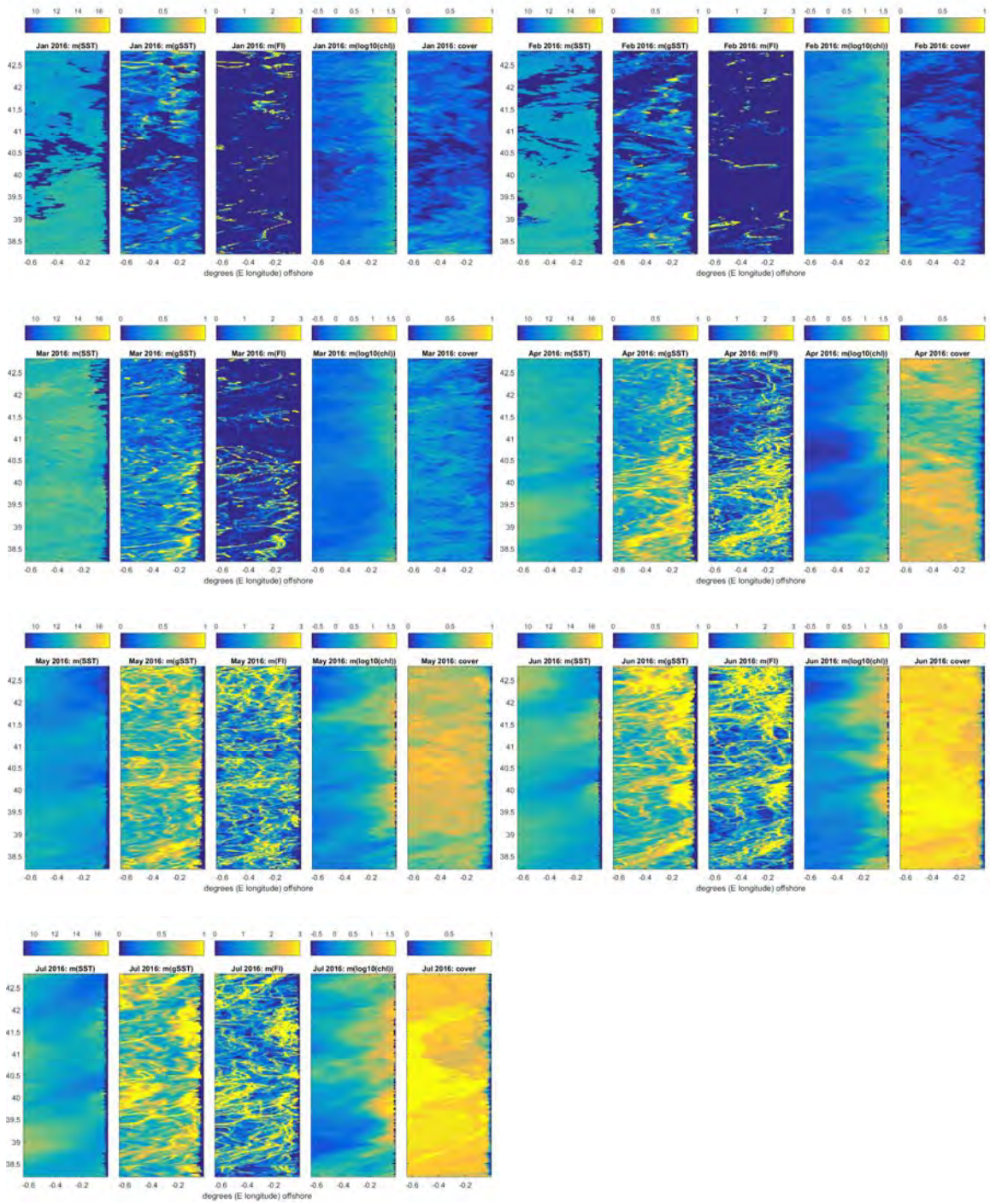

Figure A-SO-8: Monthly mean alongshore and cross-shelf structure, by month, in coastal oceanographic conditions based on MODIS-Aqua observations for early 2016. For each month, plots show sea surface temperature (SST), gradient in SST (gSST), SST Front Index (FI), $\log_{10}$ chl a (mg/m^3), and pixel coverage (%).

Appendix FW: Freshwater discharge to the NCSR

This appendix summarizes monthly mean flows from gauged river systems draining to the NCSR coast, based on data reported by the USGS (http://waterdata.usgs.gov/nwis/monthly). For each selected watershed, we highlight flow during the Baseline Study Period in the context of recent flow patterns, as well as recent time series of monthly mean flows. These figures are intended to provide broad context in terms of conditions leading up to and during observations made during ecological surveys, and as a resource for formulating more specific queries of the underlying data sets as part of analyses designed to explore connections between oceanographic and ecological data.

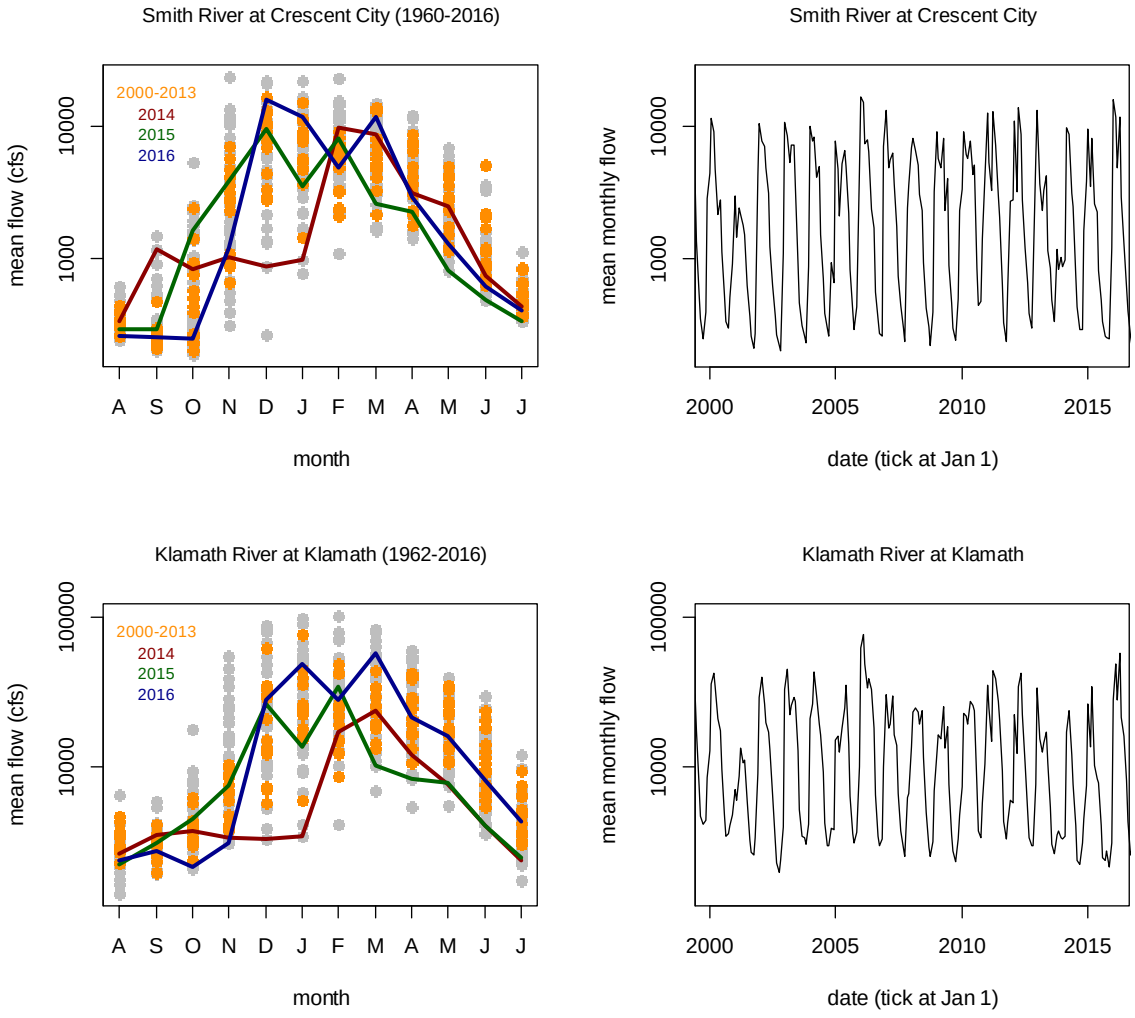

Figure A-FW-1: Mean monthly flows for a shifted water year (1 August of the preceding year through 31 July), highlighting the distribution of flows from 2000-2013, and flow patterns for each year of the Baseline Study Period (left hand panels) and a time series of monthly mean flow for the period from 2000-2016 (right hand panels).

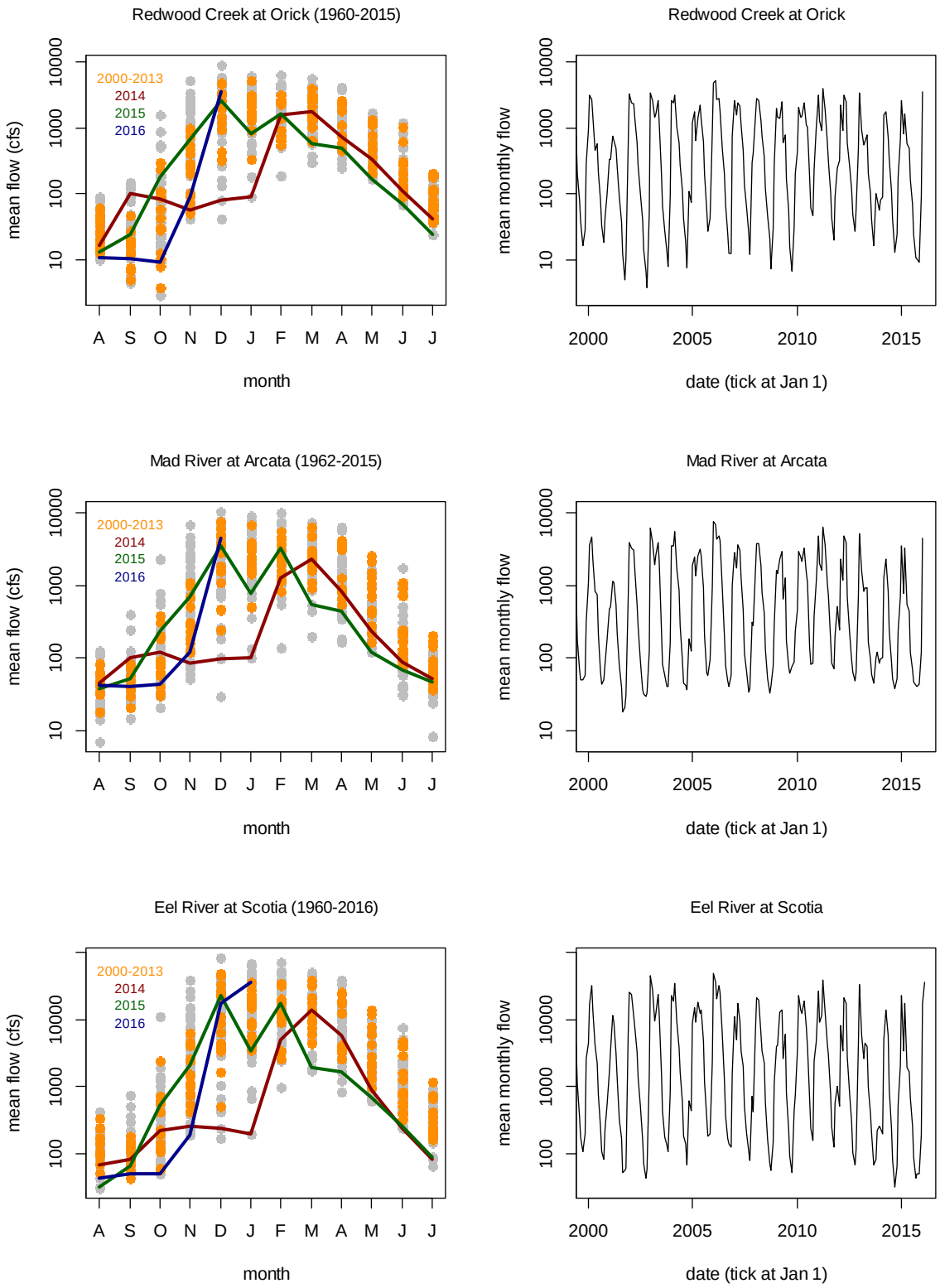

Figure A-FW-1: (continued.)

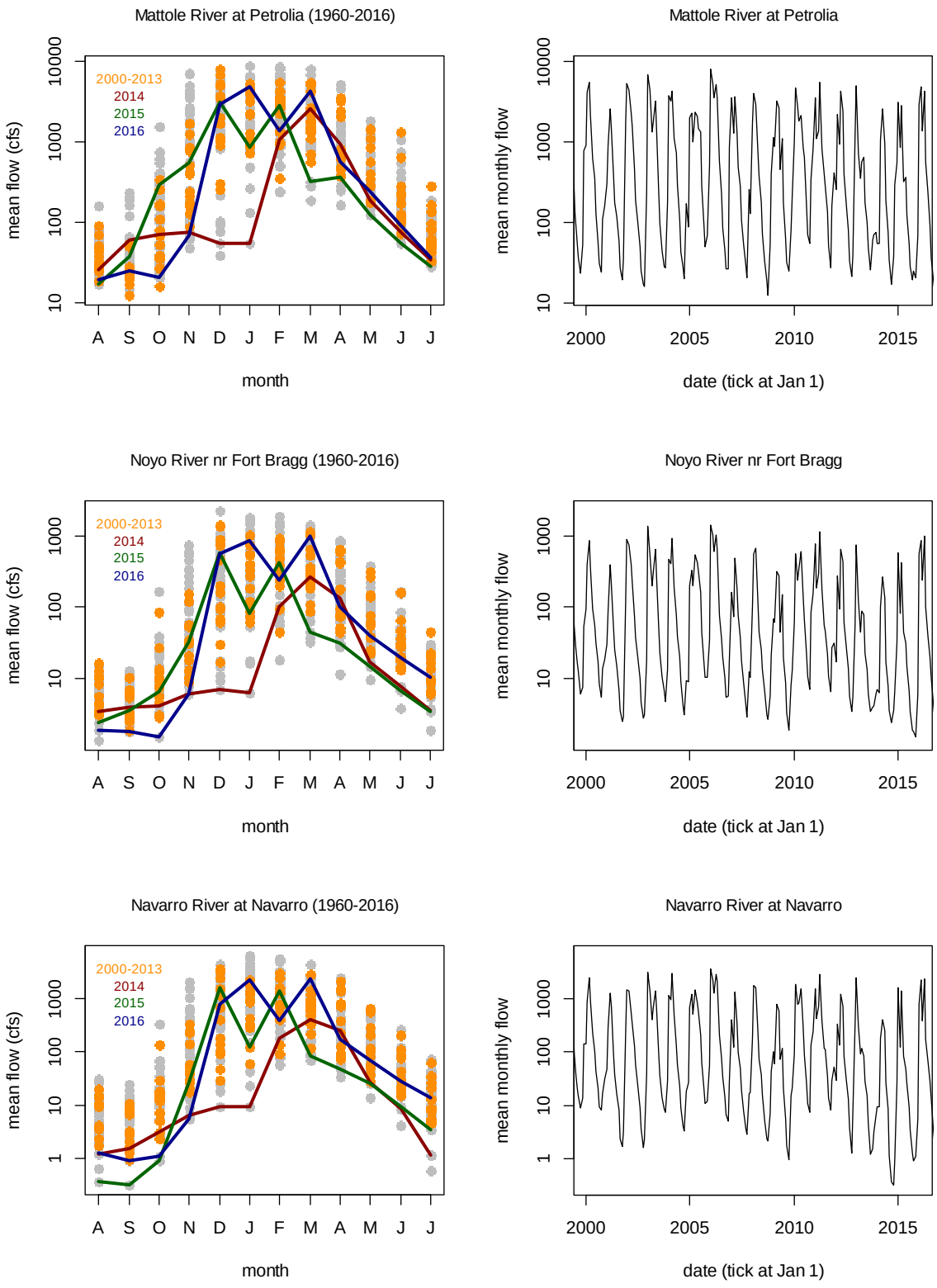

Figure A-FW-1: (continued.)

Appendix KM: k-means clustering analysis of coastal oceanographic conditions

This appendix presents results from k-means clustering applied to coastal oceanographic conditions as an approach to investigating structure along the coast that might inform comparisons among MPAs and among MPAs and reference sites. Several sets of results are shown. First a comparison of analyses applied to data that include or exclude latitude are shown to illustrate insensitivity of analysis to the inclusion of latitude as a structuring factor. Second, a series of analyses illustrating clustering for k = 2 to k = 10 applied to monthly means of coastal oceanographic data illustrates general consistency in distributions of (normalized) oceanographic conditions over the course of the year, which supports similar consistency in the location of breaks between groups. Third, analyses of annual means for a 2014 and 2015 (the BSP years most strongly affected by the North Pacific Marine Heatwave, and for which we have complete oceanographic data) is compared to analysis for a climatology based on 2003-2013 to demonstrate consistency of structure, despite changes in mean values of some conditions (e.g., temperature).

These figures are intended to provide broad context in terms of conditions leading up to and during observations made during ecological surveys, and as a resource for formulating more specific queries of the underlying data sets as part of analyses designed to explore connections between oceanographic and ecological data. Note that color carries no meaning from one case to another in these plots; the relevant information is in the location of breaks within the plots. Note also that the breaks indicated do not necessarily indicate a sharp transition in oceanographic conditions, at least with respect to all parameters included in the analysis.

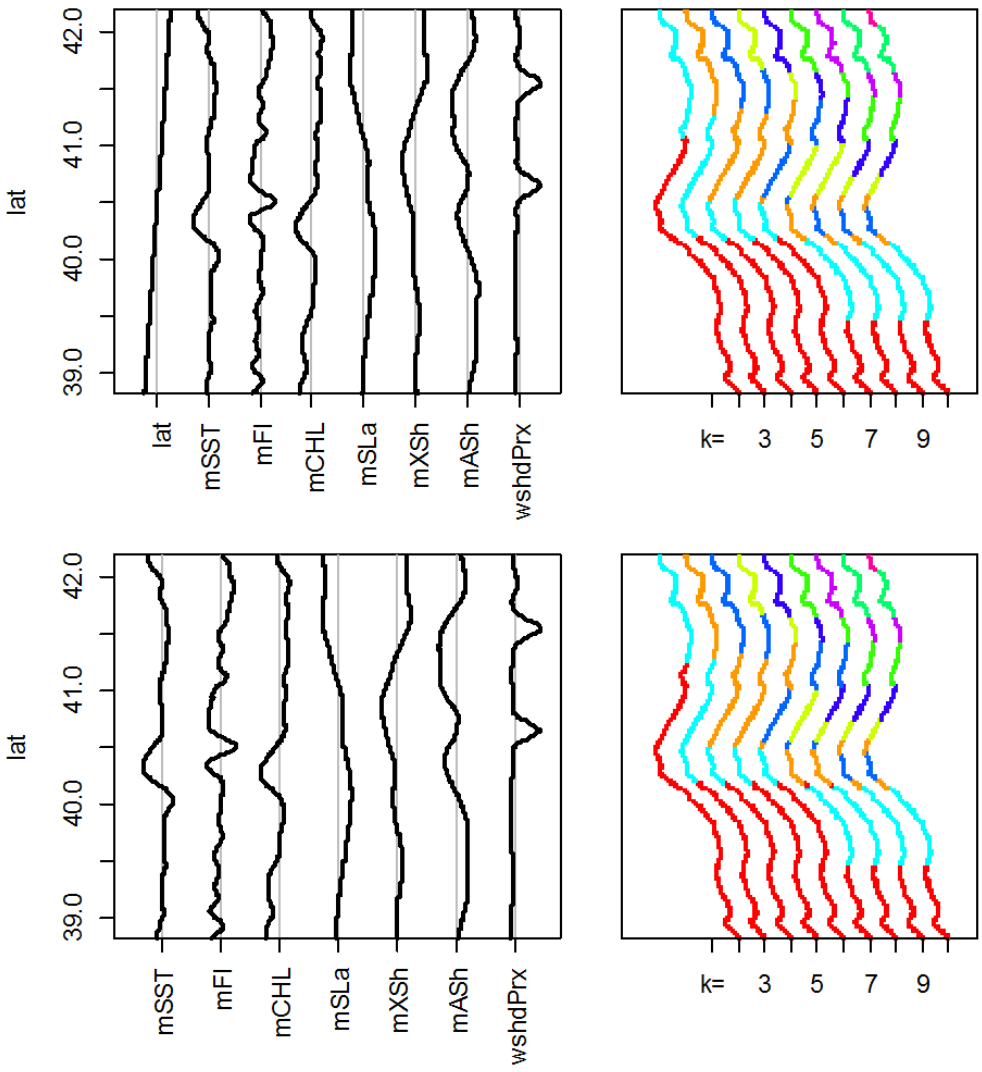

Figure A-KM-1: Comparison of results from k-means clustering applied to annual mean coastal oceanographic conditions averaged over 2003-2013 that include (upper panels) or exclude (lower panels) latitude as a structuring value. Black lines in left panels indicate structure in normalized metrics along the coast; the grey lines indicate a value of zero (i.e., mean conditions). Colors in right-hand panels indicate groupings, but do not imply similarity from one clustering analysis to the next.

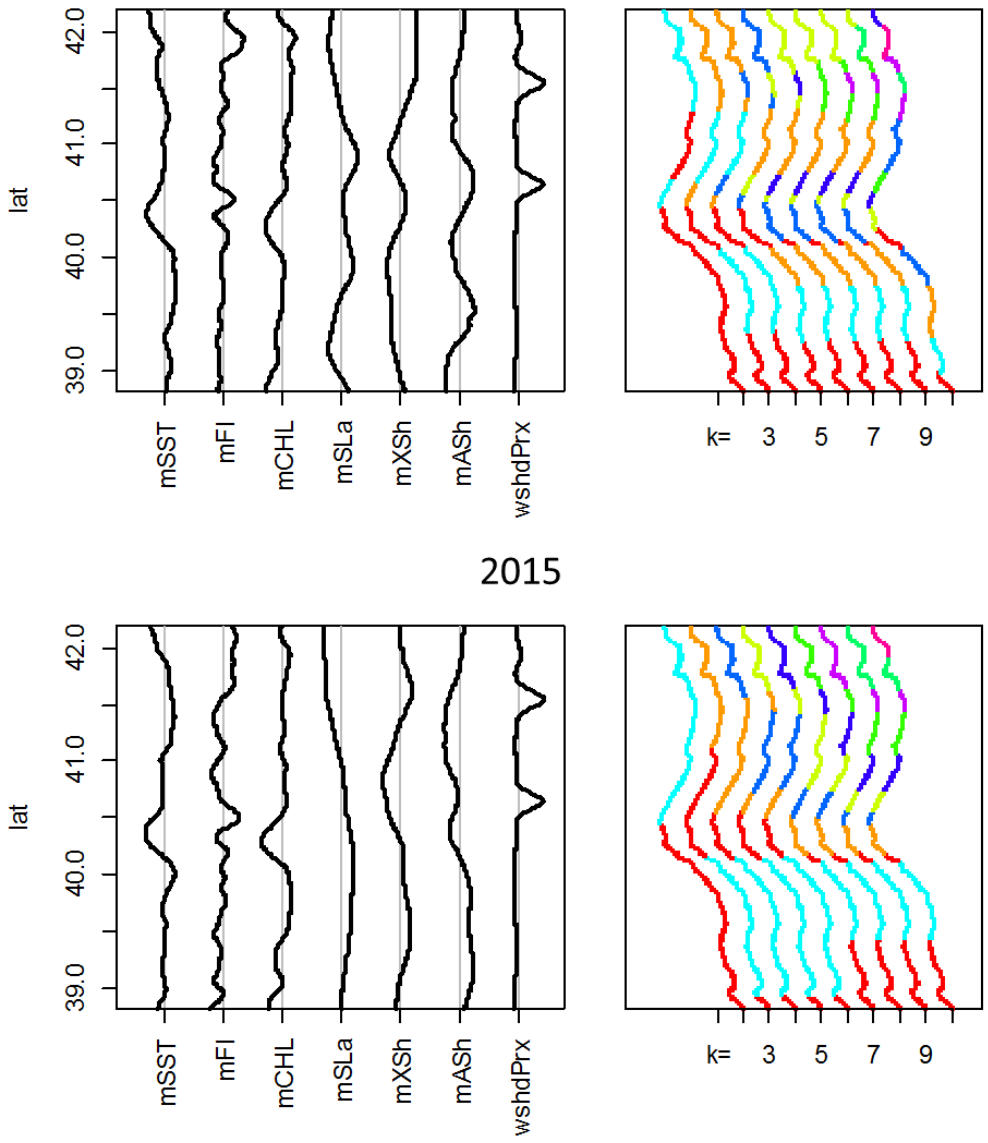

Figure A-KM-2: Comparison of results from k-means clustering for k = 2 to k = 10 applied to annual mean coastal oceanographic conditions for 2014 (upper panels) and 2015 (lower panels). For comparison refer to lower panels in Figure A-KM-1. All else as in Figure A-KM-1.

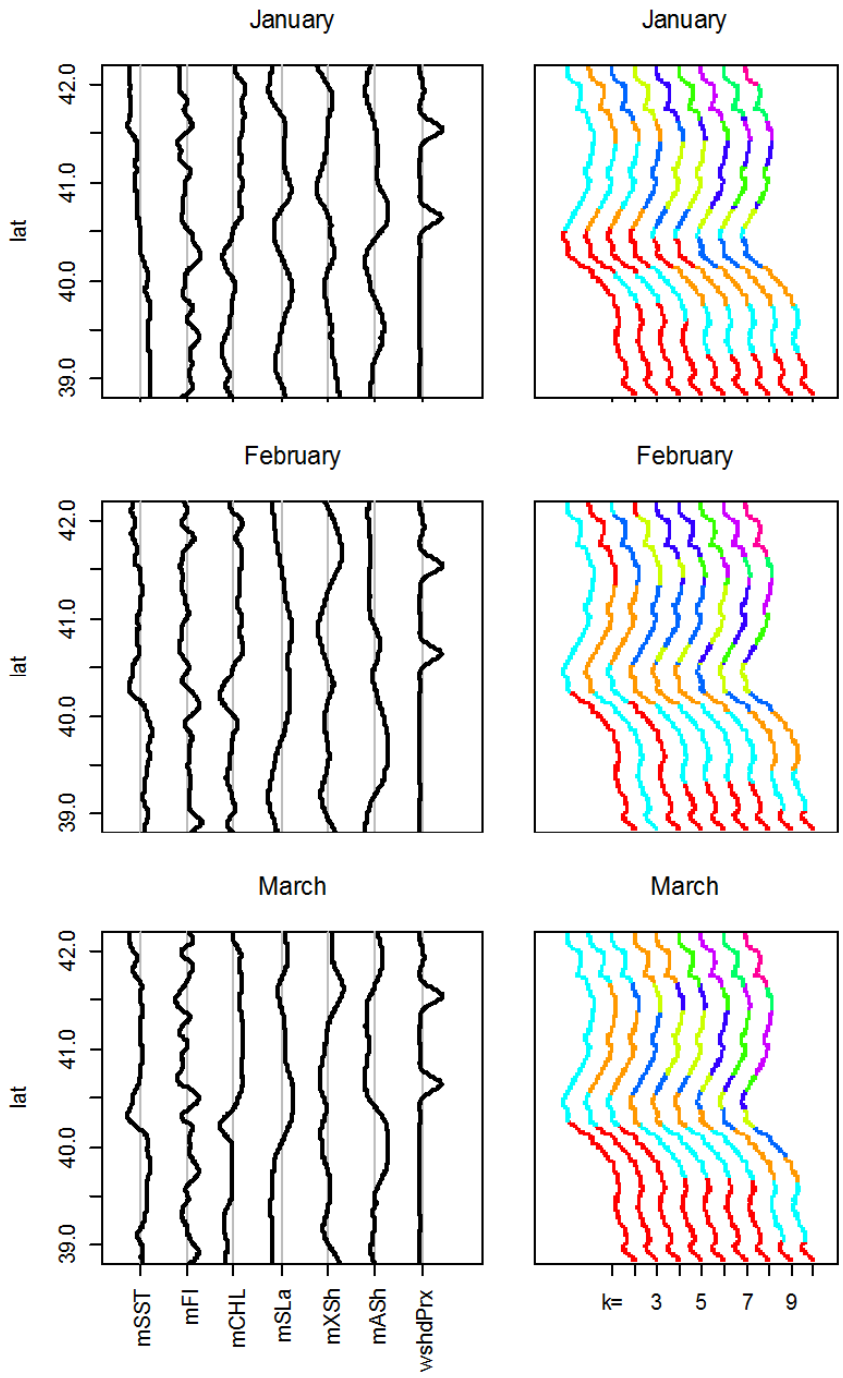

Figure A-KM-3. (1/4) Comparison of results from k-means clustering applied to monthly mean coastal oceanographic conditions averaged across years (2002-2016). All else as in Figure A-KM-1.

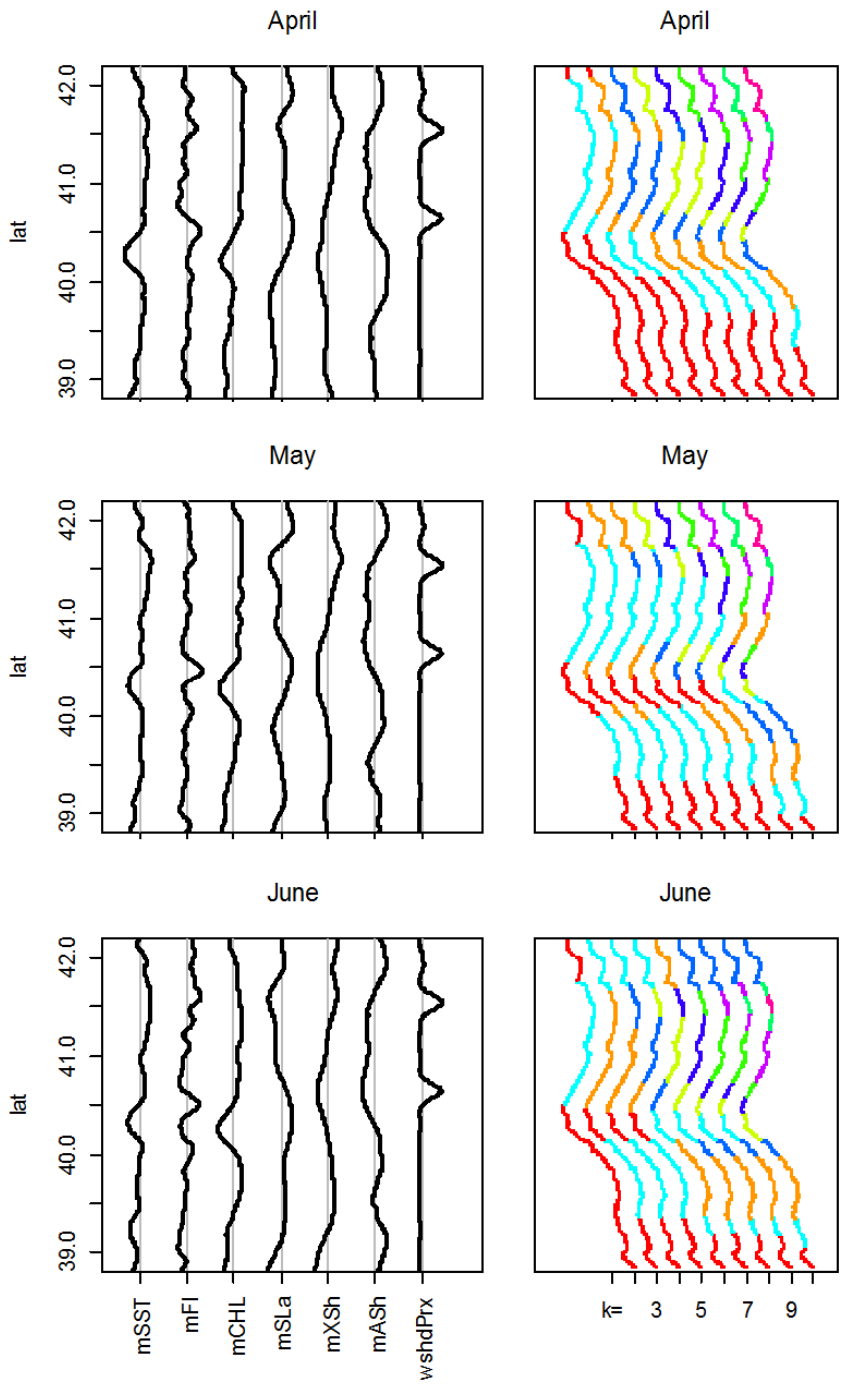

Figure A-KM-3. (2/4) Continued.

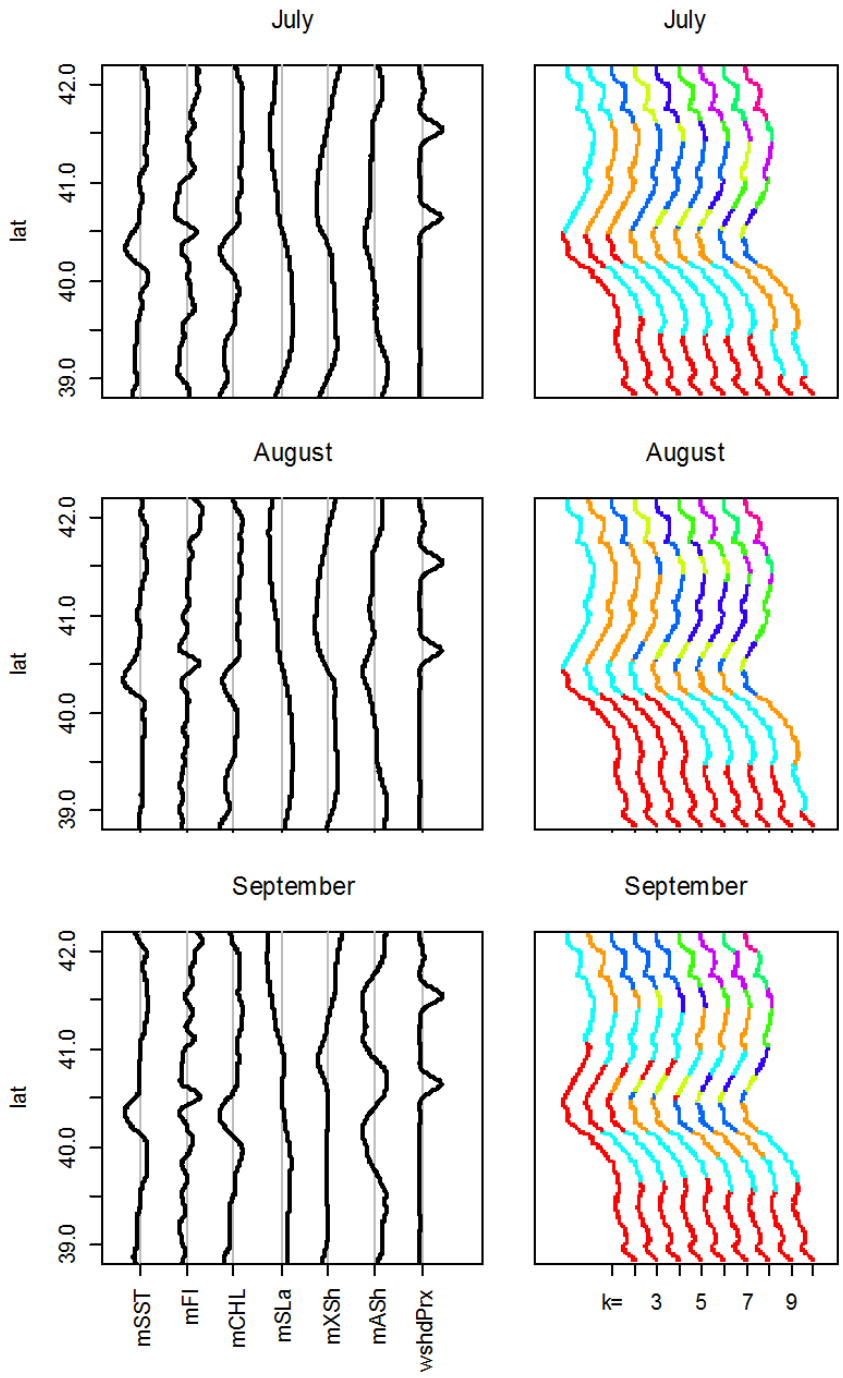

Figure A-KM-3. (3/4) Continued.

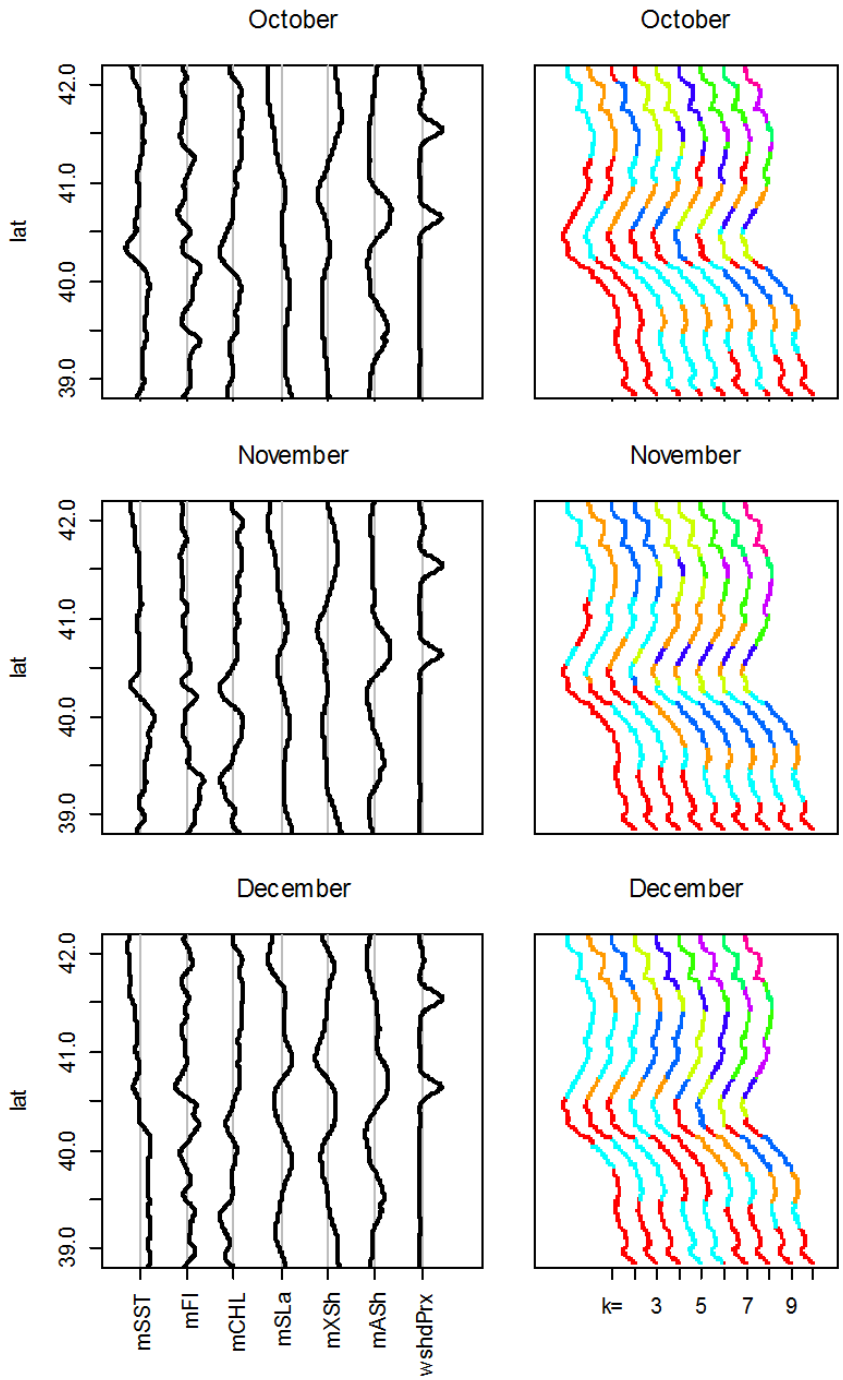

Figure A-KM-3. (4/4) Continued.

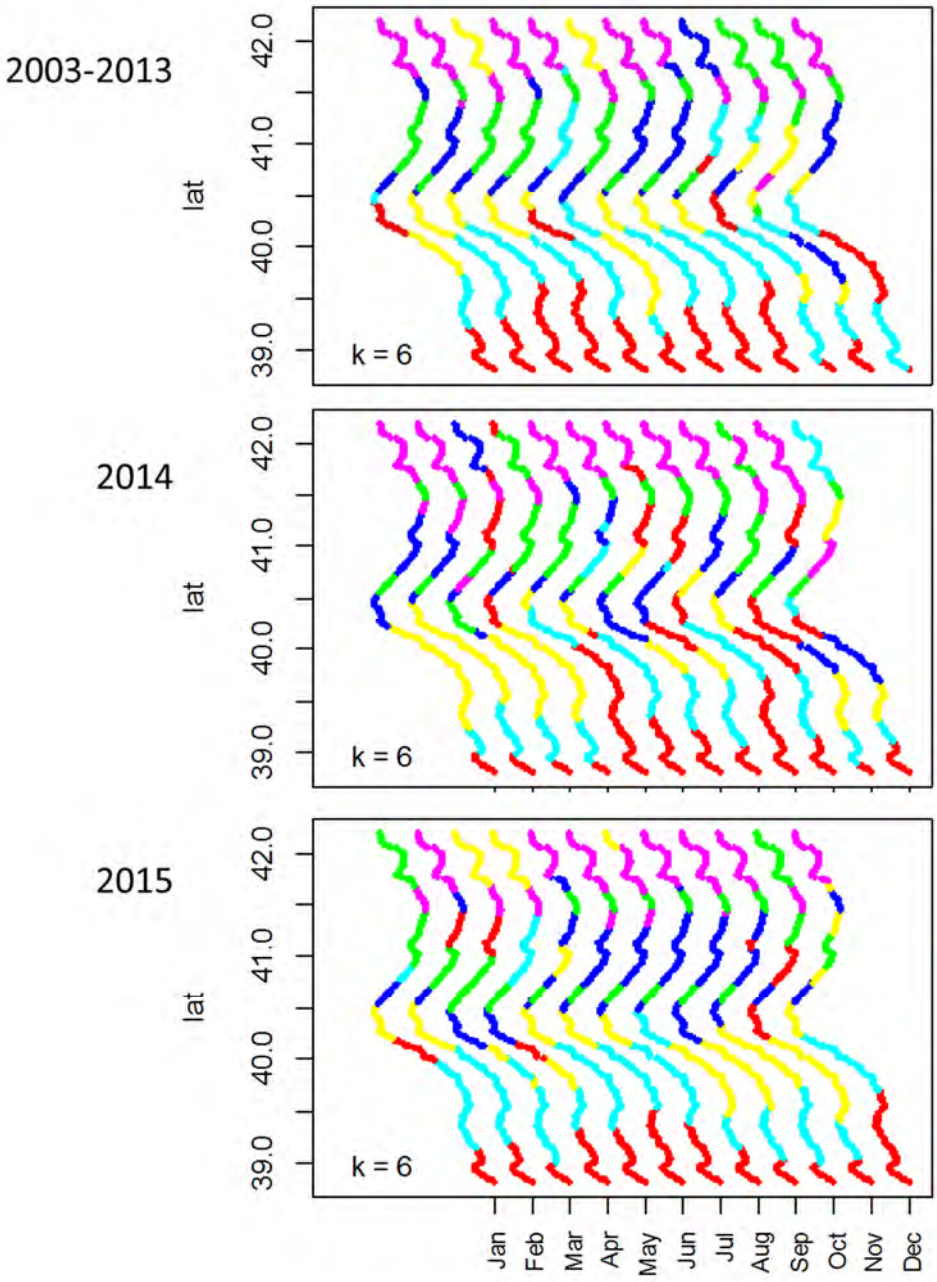

Figure A-KM-4. Comparison of k-means clustering (k=6) applied to monthly mean coastal oceanographic conditions for climatological (2003-2013) means, and separately for 2014 and 2015.